THE GEOLOGY AND ALTERATION/MINERALIZATION OF THE VAN ROOI'S VLEY W/Sn DEPOSIT, NAMAQUA METAMORPHIC COMPLEX, SOUTH AFRICA

by

R.H. Smithies

Submitted as partial requirement for the degree of Master of Science (Economic Geology) at Rhodes University, Grahamstown.

July 1987

All arguments and interpretations
presented in this thesis are my own,
except where referenced.

R.H. SMITHIES

ABSTRACT

Scheelite, wolframite and cassiterite mineralization is hosted within numerous quartz-tourmaline-feldspar-fluorite veins at Van Rooi's Vley, N.W. Cape Province. Mineralization and hydrothermal alteration within, and around, these veins is highly complex and reflects the intricate interaction of hydrothermal activity upon a structurally deformed sequence of Proterozoic medium to high-grade gneisses.

Four distinct stages of alteration and mineralization occurred, including a late 'epithermal stage'. Although the location of mineralization was strongly controlled by structure, the concentration of mineralization was controlled by physicochemical variables, of which host-rock geochemistry was particularly important.

Further W/Sn mineralization occurs on a local scale, some of which is spatially related to minor leucogranite dykes. Leucogranite bodies are not uncommon within the region and some are enriched in W and Sn.

By comparing F/B ratios, W/Sn ratios, the alteration mineralogy, the ore mineralogy and the Fe-content of tourmaline, the deposits within the Van Rooi's Vley area can be placed into a 'proximal' to 'distal' classification, with respect to a common source of mineralizing hydrothermal fluids. The Van Rooi's Vley deposit, whilst affiliated to greisen-style deposits, represents a 'distal' quartz-vein lode deposit.

LIST OF FIGURES

		PAGE
1.1	Location of the Van Rooi's Vley deposit.	1
2.1	Tectonic subprovinces of the Namaqua Province.	5
2.2	Tectonic terranes in the Gordonia and Kheis Belts.	7
2.3	Mineral occurrences throughout the Namaqua Province.	9
2.4	The geodynamic evolution of the Namaqua Province.	13
3.1	Geology of the Van Rooi's Vley area.	18
3.2	Geology of the Van Rooi's Vley deposit.	20
3.3	Longitudinal section - Geology Zone 4.	21
3.4	Geology of the Upington - Kakamas Terranes.	23
3.5	Location of late to post-tectonic microgranites.	30
3.6	Paleosetting of the Van Rooi's Vley deposit.	35
4.1	Construction of a Conally contour diagram.	38
4.2	Longitudinal sections - Conolly, strike, dip and thickness - Zone 4.	39
4.3	Longitudinal sections - Conolly, strike, dip and thickness - Zone 5.	41
4.4	Stereogram - Zone 4.	42
4.5	Stereogram - Zone 5.	43
4.6	Mechanism of fissure opening.	44
4.7	Longitudinal section, low-pressure zones - Zone 4.	46
4.8	Longitudinal section, low-pressure zones - Zone 4.	47
4.9	Longitudinal section, low-pressure zones - Zone 5.	48
5.1	Longitudinal section, Sn-grade - Zone 4.	50
5.2	Zone 4 cassiterite grain size histograms.	51
5.3	Longitudinal section, Sn-grade - Zone 5.	52
5.4	Longitudinal section, W-grade - Zone 4.	54
5.5	Longitudinal section, W-grade - Zone 5.	55
5.6	Distribution of W, Sn, Mo and Cu across a vein zone.	56
7.1	Section through a 'typical' vein-zone, showing alterations.	66
8.1	F_2O_{-1} vs CO_2 diagram for the system Ca-Fe-W-C-O-F.	88
9.1	Geology of the Witkop deposit.	93
9.2	Log fS_2 vs Log fO_2 diagram.	98

10.1 Fe vs. MgO diagram showing tourmaline compositions. 107
10.2 Fe vs. MgO diagram showing tourmaline compositions. 109
11.1 Genetic model for mineralization within the Van Rooi's Vley area. 115

LIST OF PLATES

		PAGE
3.1	Tourmalinite at Kakamas.	19
3.2	Contorted quartz vein - Zone 4.	23
3.3	Dark Gneiss.	25
3.4	Crenulated Pink Gneiss.	26
3.5	Tourmaline pod from the Cnydas granite.	29
3.6	Syn-tectonic dykes.	30
3.7	Mineralized leucogranite.	32
6.1	Mineralized tourmaline-rich assemblage.	59
6.2	Wolframite replacing scheelite.	60
6.3	Scheelite + fluorite clusters.	61
7.1	Potassic alteration after tourmalinization.	69
7.2	T1 and T2 generations of tourmaline.	70
7.3	T1 and T2 generations of tourmaline.	71
7.4	Magnetite veining in Pink Gneiss.	72
7.5	Magnetite breccia.	73
7.6	Chloritized clast.	74
7.7	Greisenous assemblage.	75
7.8	Epithermal alteration.	78
9.1	Pelitic micaceous gneiss - Witkop.	94
9.2	Scheelite + wolframite - Witkop.	95
9.3	Sulphide assemblage - Witkop.	95
9.4	Greisenization - Witkop.	96

LIST OF TABLES

		PAGE
3.1	Lithostratigraphy of the Korannaland Sequence.	16
3.2	Lithostratigraphy of the Bushmanland Sequence.	34
6.1	Paragenesis of ore minerals.	58
7.1	Paragenesis of alteration minerals.	65
10.1	Partial chemical analyses of tourmaline.	104-106
11.1	Comparison of local W/Sn deposits.	114

TABLE OF CONTENTS

		Page
1.	INTRODUCTION.	1
2.	GEOTECTONIC FRAMEWORK OF THE NAMAQUA PROVINCE AND A METALLOGENIC APPROACH TO TECTONIC MODELLING.	2
	2.1 Introduction.	2
	2.2 Past models for Namaqua tectonogenesis.	2
	2.3 Geotectonic Framework.	3
	2.4 Metallogenic Framework.	8
	2.5 Constraints on a model.	11
	2.6 A Geodynamic-metallogenic model for the Namaqua Province.	12
3.	LOCAL GEOLOGICAL SETTING.	16
	3.1 Geology.	16
	3.1.a Stratigraphy.	16
	3.1.b Structure.	19
	3.1.c Mineralization.	22
	3.2 Host lithologies.	24
	3.2.a Dark Gneiss (Biesjepoort Formation).	24
	3.2.b Pink Gneiss (Riemvasmaak Formation).	26
	3.3 Local granitic rock-types.	27
	3.3.a Introduction.	27
	3.3.b The Colston granite.	27
	3.3.c The Cnydas granite complex.	27
	3.3.d Syn-tectonic granitic dykes.	28
	3.3.e Late to post-tectonic granitic dykes.	29
	3.4 Paleosetting of the Van Rooi's Vley area.	33
	3.5 The McTaggarts Camp - Dyasons Klip deposits.	34
4.	STRUCTURE OF THE MINERALIZED ZONES.	37
	4.1 Introduction.	37
	4.2 Conolly contour diagrams.	37
	4.2.a Construction.	37
	4.2.b Interpretation.	37
	4.3 Determination of shear movement.	40

4.4 The formation of open space or low-pressure zones. 44

5. STRUCTURAL CONTROLS ON THE DISTRIBUTION OF MINERALIZATION. 49
5.1 Introduction. 49
5.2 Distribution of Sn. 49
5.2.a Zone 4. 49
5.2.b Zone 5. 52
5.3 Distribution of W. 53
5.3.a Zone 4. 53
5.3.b Zone 5. 55
5.4 Distribution of other ore elements. 56
5.5 Conclusions. 57

6. ORE MINERALOGY 58
6.1 Introduction. 58
6.2 Cassiterite. 58
6.3 Scheelite 60
6.4 Wolframite. 62
6.5 Fe-oxides. 62
6.6 Sulphides. 62

7. WALL-ROCK ALTERATION 64
7.1 Introduction. 64
7.2 Pre-ore Stage (A1). 67
7.3 Mineralization Stage (A2). 69
7.4 Post-ore stage (A3). 76
7.5 Epithermal Stage (A4). 77
7.6 Van Rooi's Vley - a greisen deposit? 77

8. CONTROLS ON MINERALIZATION. 81
8.1 Introduction. 81
8.2 Geochemistry of tungsten and tin. 81
8.2.a Geochemistry of W and Sn. 81
8.2.b Concentration of W and Sn. 82
8.2.c Transport and deposition of W. 83
8.2.d Transport and deposition of Sn. 84
8.3 Ore mineral relationships at Van Rooi's Vley - Chemical

controls on mineralization. 85
8.3.a Scheelite - Wolframite. 85
8.3.b Cassiterite. 87

9. THE WITKOP W/Sn DEPOSIT - A COMPARISON WITH VAN ROOI'S VLEY. 92
9.1 Introduction. 92
9.2 Local Geology. 92
9.3 Ore Mineralogy. 92
9.4 Wall-rock Alteration. 94
9.5 Comparison with Van Rooi's Vley. 97

10. PREVIOUS GENETIC MODELS FOR MINERALIZATION AT VAN ROOI'S VLEY. 99
10.1 Introduction. 99
10.2 Two contrasting models for the genesis of the Van Rooi's Vley deposit. 99
10.3 The geochemistry of tourmaline - A clue to the origin of mineralization. 102
10.3.a The tourmaline system. 102
10.3.b The nature of tourmaline at Van Rooi's Vley and McTaggart's Camp. 102
10.3.c Discussion. 108
10.4 Conclusions. 110

11. CONCLUSION :- THE GENESIS OF THE VAN ROOI'S VLEY DEPOSIT, AND RELATED MINERAL OCCURRENCES. 111

12. ACKNOWLEDGEMENTS. 117

13. REFERENCES. 118

APPENDICES.

1. INTRODUCTION

The Van Rooi's Vley W/Sn deposit is situated on the farm Van Rooi's Vley, 45km WSW of Upington, NW Cape Province (Fig. 1.1). The area studied forms part of the Namaqua metamorphic complex (or province) a tectonically distinct region that developed adjacent to the Kaapvaal Craton, approximally between 2.0 and 1.0 Ga.

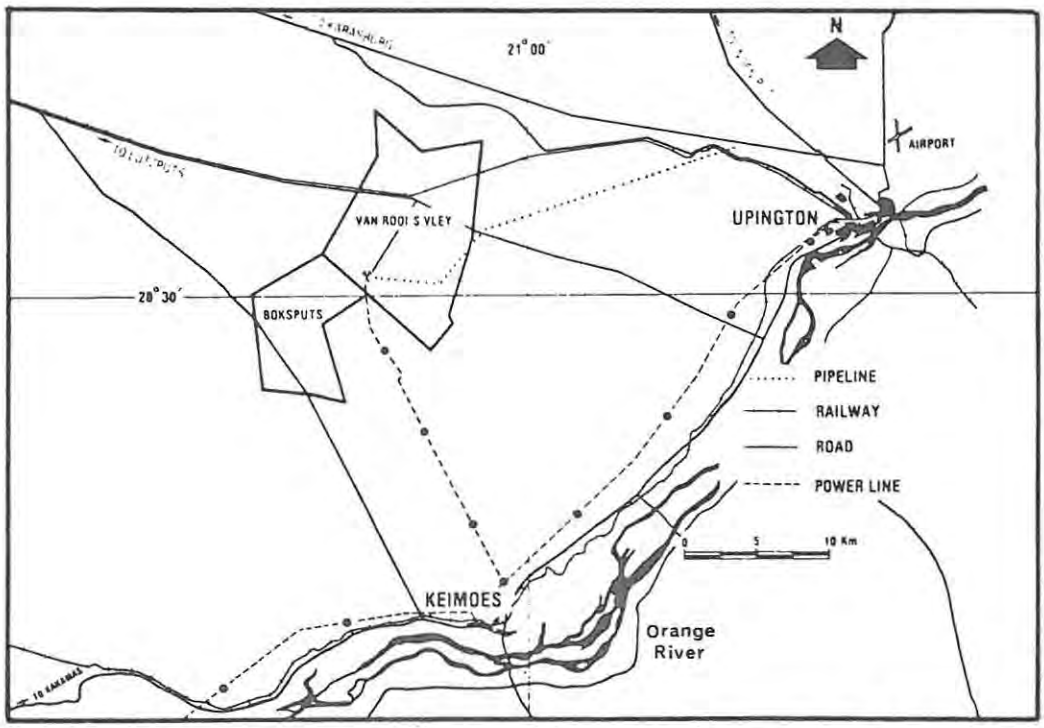

Figure 1.1. Location of the Van Rooi's Vley deposit, N.E. Cape Province.

Lying marginal to the SW edge of the Kalahari desert, the Van Rooi's Vley region is covered by thick layer of calcrete and Kalahari sand. Consequently, outcrop is poor. The generally low relief of the region is, however, occasionally punctuated by small hills that usually define domal structures. The Van Rooi's Vley deposit lies on the sheared edge of one such structure.

Mineralization was discovered at Van Rooi's Vley in 1943, and was periodically extracted up to 1958. The currently dormant deposit, is now owned by Shell South Africa Metals Division, in a joint venture with Phelps Dodge Mining.

Von Backstrom (1964) first researched the Van Rooi's Vley deposit, and provided a detailed description of numerous important geological features. Wheatley and De Beer (1986), provided an account of more recent ideas as to the genesis of mineralization. The main object of the current study was to identify and describe the numerous and complex alteration/mineralization systems that occur at Van Rooi's Vley and to provide an explanation for the presence, intensity and distribution of this alteration and mineralization. In identifying, explaining and characterizing the processes that led to mineralization the genesis of the deposit, and spatially related W/Sn mineralization, may be better understood. Mineralization at Van Rooi's Vley may then be placed into context with more regional geological features.

2. GEOTECTONIC FRAMEWORK OF THE NAMAQUA PROVINCE AND A METALLOGENIC APPROACH TO TECTONIC MODELLING

2.1 Introduction

A metallogenic approach to tectonic modelling has been somewhat neglected in the past. Pioneering work by Hutchinson (1983), Sawkins (1984) and Mitchell and Garson (1981), has documented deposit types with specific or general tectonic settings. Developments in this field are now such that a metallogenic approach can be used to constrain tectonic modelling. However, metallogeny is only part of a full picture, and must be considered in conjunction with other geological and structural data.

The following section combines the work and ideas of the 1986 Rhodes MSc. Exploration Geology class (including the present author), and is the result of a two week field trip to the Namaqua Province, and a subsequent literature survey. Although the tectonic model that follows is based heavily on geological and tectonic information from the work of Hartnady et al. (1985), attention is drawn to the technique employed below, of using mineral deposits to constrain tectonic models.

2.2 Past models for Namaqua tectonogenesis

Past opinion concerning Proterozoic crustal evolution is divided between two schools, the uniformitarian school (eg. Windley 1984), that invokes Phanerozoic-type plate tectonics, and the non-uniformitarian school (eg. Kruner 1981), that favour ensialic processes. Both schools have applied their ideas to the development of the Namaqua Province (see reviews by Albat 1984). However; neither has been entirely successful, mainly because many such attempts refer only to specific parts of the Namaqua Province.

It is now generally agreed that the Namaqua Province, as a whole, is the product of a continental collision (the "**Namaqua event**") which occurred about 1200 - 1000 Ma ago and produced the major metamorphic overprint throughout the region. Many geological manifestations of this collision,

and of the preceding **'Orange River event'**, are closely reminiscent of Phanerozoic plate tectonic processes. Certainly, the mineral deposits of the Namaqua Province show characteristics of deposits related to such processes, and give good reason to infer that Phanerozoic-type tectonism was active in the Proterozoic of Southern Africa.

2.3 Geotectonic Framework

Hartnady et al. (1985) recognized three subprovinces within the Namaqua Province (Fig. 2.1), vis; the Richtersveld, Bushmanland and Gordonia Subprovinces. Each subprovince is characterized by a combination of lithology, structure, metamorphic grade and predominant radiometric age. Hartnady et al (op. cit.) exclude the Kheis Belt from the Namaqua Province, on the basis of a major age discrepancy, although, the Richtersveld Subprovince developed during the same period as the Kheis Belt, some 500 Ma prior to the main Namaqua tectonic event. The Kheis Belt is thus included here as a marginal subprovince of the Namaqua Province.

The Kheis Belt is bounded to the east by the Kaapvaal Craton, and to the west by the Gordonia Subprovince, and consists of a low grade (high pressure) metamorphic sequence dominated by quartzites, phyllites and amphibolite of the Matsap Group. Through correlation with the supracrustal Olifantshoek sequence, on the Kaapvaal Craton, the Matsap Group is dated at between 2068 $\pm$ 70 and 1800 Ma (Barton and Burger 1983). In the north of Kheis Belt, at least five major easterly directed thrust sheets, and numerous east-vergent recumbent folds are recognized (Hartnady et al 1985). To the south, Coward and Potgieter (1983) recognize two dominant movement vectors, a southerly direction of overthrusting and a later northerly direction. The proposition that the Kheis Belt was initially a broad pericratonic shelf, coupled with the observed cratonward fold vergence and thrusting, implies that this belt was developed on a stable sialic (Kaapvaal) basement that became increasingly mobile westward (Stowe et al. 1984).

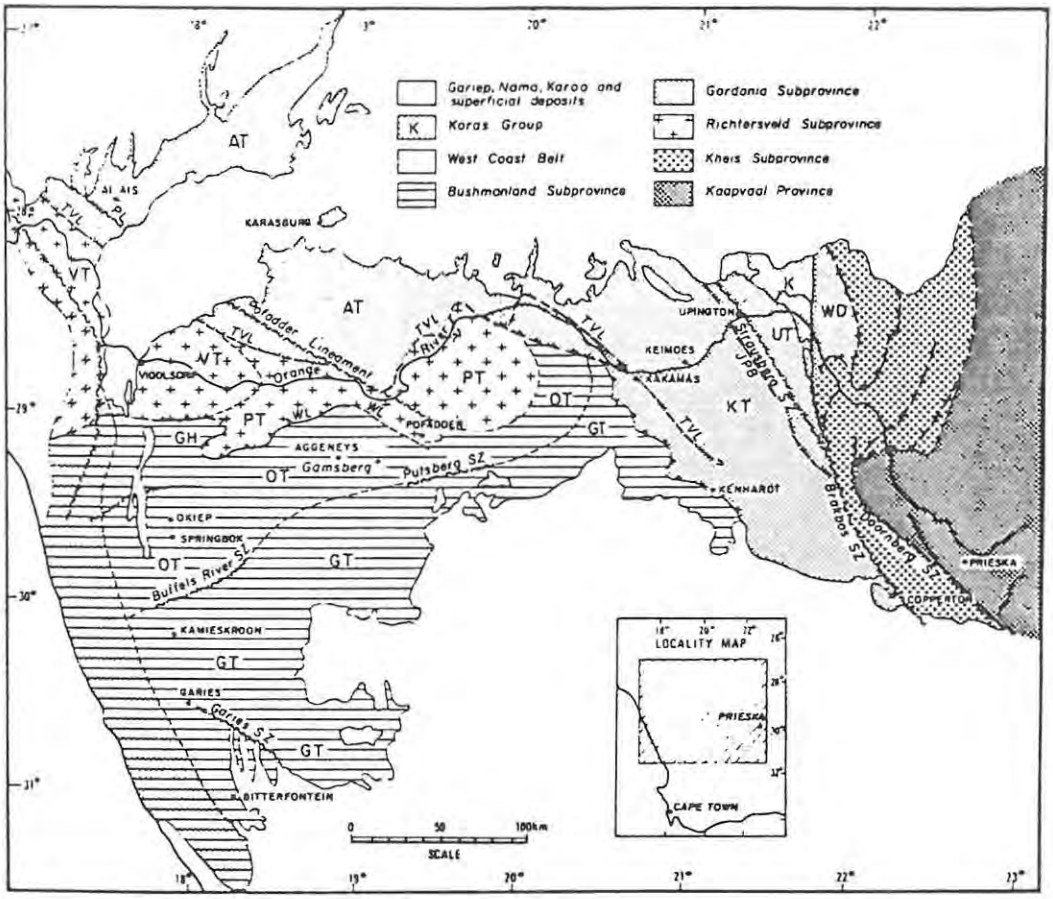

Figure 2.1. Map of the tectonic subprovinces, belts and terranes, Namaqua Province. AT - Aus Terrane ; GT - Garies Terrane ; JPL - Jannelsepan Line ; KT - Kakamas Terrane ; OT - Okiep Terrane; PT - Pella Terrane ; TVL - Tantalite Valley Line ; UT - Upington Terrane ; VT - Vioolsdrif Terrane; WL - Wortel Line ; WD - Wilgenhoutsdrif Formation. (after Hartnady et al 1985).

The Richtersveld Subprovince comprises a 2.0 Ga succession of calc-alkaline volcanics and interbedded sediments (the Orange River Group), intruded by 1.9 to 1.7 Ga I-type granitoids of the Vioolsdrif Suite (Blignault et al 1983). Hartnady et al (1985) suggest that the Richtersveld Subprovince developed through the reworking, along an active continental margin, of a 2.0 Ga island-arc complex. The Richtersveld Subprovince may be divided into the Pella Terrane, to the east, and the Vioolsdrif Terrane, to the west. During the Namaqua event, rocks of the Pella Terrane were metamorphosed to

amphibolite facies and were deformed. Rare-element bearing pegmatites intruded granitoids of the Vioolsdrif suite, along the southern margin of the subprovince.

The northern boundary of the Richtersveld Subprovince is taken as the 'Tantalite Valley Belt' (Fig. 2.1) , a wide zone of mylonitization, whilst the southern boundary is taken as the 'Wortel Belt'. The latter is a narrow zone of biotite gneiss that contains numerous mafic intrusives, dated at 2.2 Ga (Joubert 1984). Blignault et al (1983), suggest that the Wortel Belt is the sole of a thrust that pushed rocks of the Richtersveld subprovince southwards, onto the Bushmanland Subprovince.

The Bushmanland Subprovince is bounded to the east by the Gordonia Subprovince (Fig. 2.1) and to the north by the Richtersveld Subprovince. Although metamorphic grades decrease northwards towards the Wortel Belt, the Bushmanland Subprovince is dominantly composed of high-grade supracrustals. Paragenesis, orthogneises, granulites and granitoids indicate a metamorphic - plutonic history that spans between 1200 and 900 Ma. The supracrustal Bushmanland and Okiep Groups are characterized by a quartzite-schist-banded-iron-formation association, and overlie a distinctive "Pink-Gneis" which has been variously interpreted as originating from an arkosic, rhyolitic or granitic protolith (Tankard et al 1982). The igneous history of the Bushmanland Subprovince began, to the north, at about 1.8 Ga (Joubert 1984) with the intrusion of the Gladkop Suite of S-type granites (Reid and Barton 1983). The late-tectonic (~1.2 - 1.1 Ga) I(?) - type (D. Gadd-Claxton, pers. comm.) Spektakel Suite was followed, within the Okiep district (Fig. 2.1), by the Koperberg Suite of anorthosites to hypersthenites. Four major phases of folding have been described in Bushmanland (Joubert 1971 ; 1981). The main period of deformation resulted in prominent E-W trending, south-vergent isoclinal folds (F_2). These were refolded about a NE-trending axis (F_3), prior to deflection by later shearing. The F_3 and F_4 deformations, and the later shearing, are almost certainly due to the main Namaqua event.

The Gordonia Subprovince lies between the Kheis Belt and the Bushmanland Subprovince (Fig. 2.1) and, like the latter, is predominantly composed of supracrustal paragneisses, orthogenesis and granitoids, related to a 1200 - 900 Ma thermal event. The subprovince was first a zone of convergent

thrusting and folding, followed by extensive dextral shearing along numerous NW-trending shear zones (Hartnady et al 1985). One such shear zone, the Brakbos fault (Fig. 2.2), divides the Gordonia Subprovince into the Upington Terrane, to the east, and the Kakamas Terrane, to the west. The Upington Terrane consists of 2.0 Ga quartz-pelite equivalents of the Kheis Belt and is rapidly transitional, in both metamorphic grade and structure, from the Kheis Belt to the high-grade Kakamas Terrane. To the extreme west of the Upington Terrane, volcanic-plutonic amphibolites of the Jannelsepan Formation crop out and comprise calc-alkaline basalts and andesites, as well as calcareous and argillaceous sediments. These rocks - may have formed within a magmatic-arc, between 1300 and 1100 Ma (Barton and Burger 1983). In the NE of the Upington Terrane, pillow basalts and associated volcanoclastics of the Wilgenhoutdrif Formation crop out (Fig.2.2) and are dated at 1340 Ma (Stowe 1983). A continental rift origin is indicated by

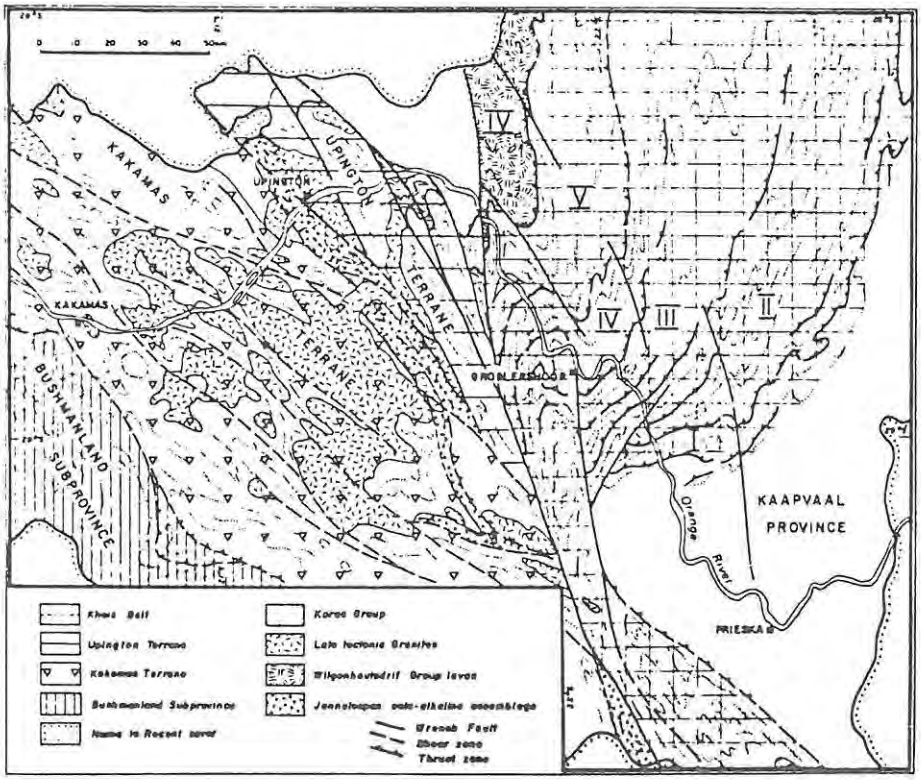

Figure 2.2. Regional pattern of tectonic terranes in the Gordonia and Kheis Belts (after Hartnady et al. 1985).

trace element ratios (Stowe 1983), and Hartnady et al (1985) suggest that these rocks were deposited within a back-arc-basin, behind the Jannelsepan arc. The Kakamas Terrane comprises a highly deformed zone of high-grade supracrustals (The Korannaland Sequence), including calc-silicates and cordierite-sillimanite gneisses. This terrane was also the focus of granitic intrusions. Granitoids that are syn-tectonic with respect to the Namaqua event are well foliated I-types. Of particular interest is the Straussberg Suite of syn-tectonic granits, which shows a progressive enrichment in potassium eastward. Post-tectonic granitoids are non-foliated, have recognizable contact aureoles, and include leucocratic and pegmatitic phases. The Keimoes Suite of granitoids contains highly evolved post-tectonic phases (eg, within the Cnydas granites) which, according to Jankowitz (1986) are similar to the collision-related "hercynotype" granitoids of Pitcher (1982).

2.4 Metallogenic Framework

A diversity of mineral deposits occur within the Namaqua Province (Fig. 2.3), Six of the major deposits are briefly discussed below, with particularly reference to their geotectonic implications.

The Haib River low grade porphyry Cu $\pm$ Mo deposit occurs 20km NE of Vioolsdrif (Fig. 2.3) within the Vioolsdrif Terrane of the Richtersveld Subprovince, and represents one of the world's oldest known porphyry system. At Haib River, 2020 to 1970 Ma (Reid 1977) dacitic, andesitic and rhyolitic volcanics of the Orange River Group are intruded by a cogenetic suite of granodiorites to leucogranites (Vioolsdrif Suite). The latter suite intruded between 1960 to 1710 Ma (Reid 1977) and includes the metal bearing quartz-feldspar porphyry, which forms the Haib porphyry stock (Minnitt 1986). The porphyry Cu (Mo) mineralization is related to the Orange River event and closely resembles porphyry systems found in Andean-type magmatic arcs.

The Aggeneys, Black Mt. and Gamsberg polymetallic sulphide deposits occur within the supracrustal Bushmanland Group of the Bushmanland Subprovince (Fig. 2.3). The base-metal sulphides are associated with banded-iron-

formations, and according to Ryan et al (1986) are stratabound exhalative sedimentary deposits. Rozendaal (1980) draws an analogy between the syngenetic Aggeneys - Gamsberg deposits and sulphidic sediments presently forming on the floor of the Red Sea; implying a continental rift environment for the former. Indeed, sedimentary facies analyses of the Bushmanland paragneisses (Moore 1980) defines a large elongate E-W trending ("rift"?) basin, that includes the Aggeneys - Gamsberg area.

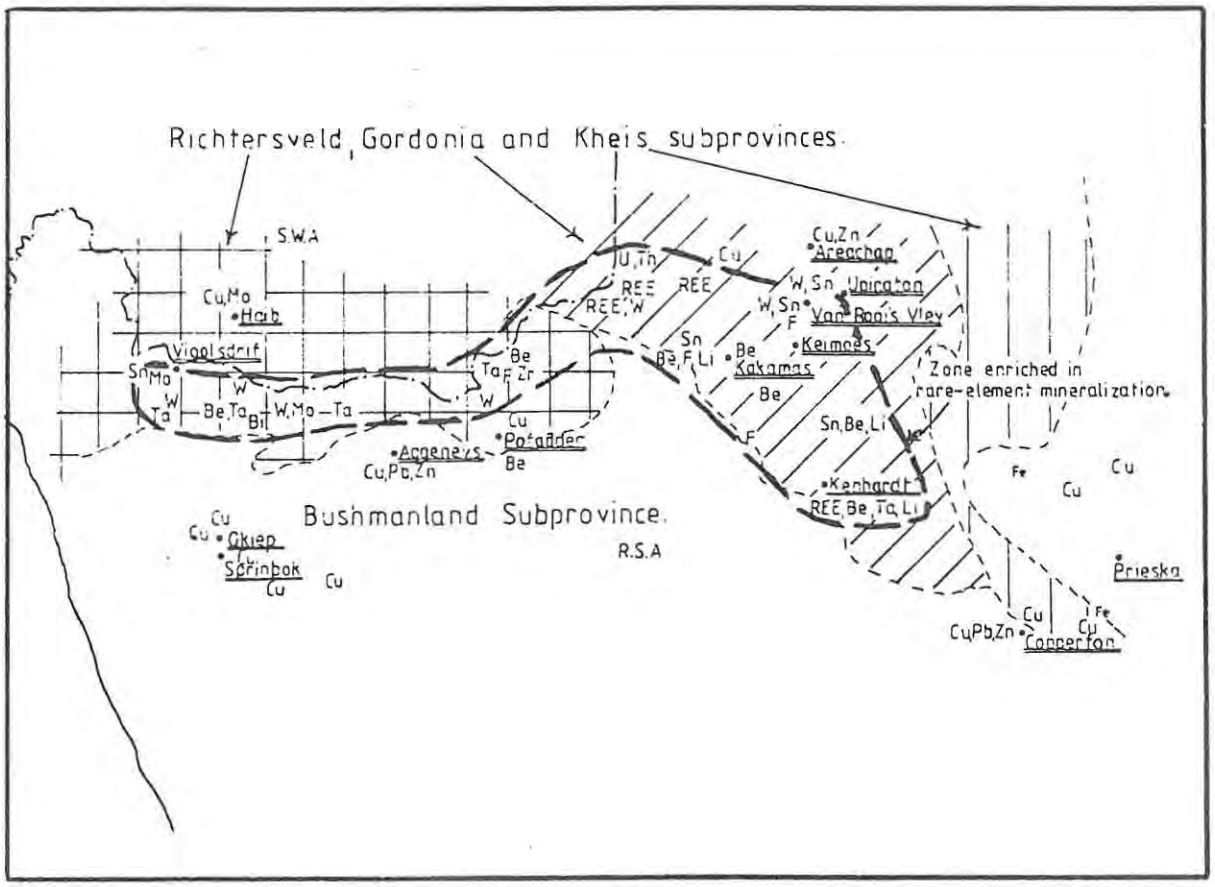

Figure 2.3. Distribution of various mineral occurrences throughout the Namaqua Province. Also shown is a broad zone of rare-element occurrences that possibly relates to a 0.9 Ga to 1.1 Ga period of compressional tectonics.

Hartnady et al (1985) place the age of the Bushmanland Group (and thus the syngenetic Aggeneys - Gamsberg deposits) at between 1.7 and 1.6 Ga.

Copper-rich massive sulphide deposits occur within the Upington Terrane, of the Gordonia Subprovince, at Areachap, Boksputs and Copperton (Fig. 2.3). They lie as metamorphosed chemical sediments, conformably enclosed within massive amphibolite units of the Jannelsepan Formation. According to Geringer et al (1986), mineralization at Boksputs closely resembles that of the Besshi-type bedded Cu-sulphide deposits of Japan. Such deposits are related to early island-arc volcanics, adjacent to continents (Garson and Mitchell 1977). Furthermore, the amphibolites associated with the Boksputs deposit are geochemically similar to island-arc volcanics (Geringer et al 1986).

Koppel (1986) established the age of mineralization at Copperton to be 1305 ± 100 Ma, in accord with the 1300 to 1100 Ma (Barton and Burger 1983) formation history of the Jannelsepan Formation.

Numerous high-grade Cu deposits occur within the Okiep district in the NW corner of the Bushmanland Subprovince (Fig. 2.3). The mineralization is primary (Lombaard et al. 1986) and is confined to the more mafic members of the Koperberg Suite, which intruded the granulite-facies terrane at 1072 ± 20 Ma (Clifford et al 1975). Lombaard and Schreuder (1978) envisage the intrusion of the Koperberg Suite, and the formation of related piercement - type folds, as a result of compressional tectonics, during which a deep crustal magma chamber was drained of Cu-rich magmas.

The Van Rooi's Vley W/Sn deposit occurs to the west of Upington, within the Kakamas Terrane of the Gordonia Subprovince (Fig. 2.3). Mineralization lies within a series of quartz-tourmaline veins hosted by pelitic gneisses of the Korannaland sequence. It is thought, to best relate to the intrusion of highly evolved and volatile-rich post-tectonic granitoids (see sections 10 and 11) probably belonging to the Keimoes Suite. These granitoids intruded at about 1.1 Ga (after the Namaqua event) and probably relate to a continental collision type tectonic setting.

Numerous rare-element bearing pegmatites occur to the south and west of the Van Rooi's Vley deposit, and are also a manifestation of post-tectonic granitic magmatism. In fact, the occurrence of pegmatitic rare-element (eg. Nb, Ta, REE, Sn etc) deposits may be traced, almost continously, from just

SE of Kenhardt, northward through Kakamas, and then westward to Vioolsdrif (Fig. 2.3). Mineralization near Vioolsdrif includes the Blesberg Pegmatitic Be, Bi, Ta-Nb, Li deposit which is dated at 1.1 - 0.95 Ga (F. Pirajno pers. comm.).

It is possible that the abovementioned "belt" of pegmatites defines a broad continental collisional zone, extending from Vioolsdrif to Kenhardt (at least), that was active some 100 to 200 Ma after the peak of the Namaqua event.

2.5 Constraints on a model

Although the broad scale lithological, geochemical and structural nature of each subprovince (and divisions thereof) place obvious constraints on an evolutionary model for the Namaqua Province, such relationships are invariably difficult to interpret and are commonly ambiguous. However, as implied above, by analysing the mineral occurrences of a group of related tectonic entities, genetic constraints may become apparent. vis ;

- the Richtersveld Subprovince, in the north of the Namaqua Province, may represent an Andean-type magmatic arc, that developed between 2.0 to 1.7 Ga, producing porphyry Cu (Mo) mineralization at Haib River ;

- the Aggeneys-Gamsberg region of the Bushmanland Subprovince may have been an area of intra-continental rifting, during the period 1.7 to 1.6 Ga (at least), in which numerous polymetallic sulphide deposits were formed;

- the Areachap, Boksputs, Copperton area, within the Upington Terrane of the Gordonia Subprovince, is interpreted as an island-arc that developed adjacent to a continent, during the period 1.3 to 1.1 Ga;

- Two areas of continental collision and compressional tectonics may be indicated, in the Okiep area (NW Bushmanland Subprovince), and by a broad zone that stretches from Kenhardt to Vioolsdrif (including the area around Van Rooi's Vley). These collisional events occurred during

the period 1.1 to 0.9 Ga.

2.6 A Geodynamic-metallogenic model for the Namaqua Province

An evolutionary model, proposed to account for the metallogenic and tectonic development of the Namaqua Province, is presented below. The model draws heavily from the work of Mallinson (in prep) and is divided into six evolutionary stages, depicted in Fig. 2.4 (a to f). Four continental plates are involved, the Kaapvaal Craton, the Kgalagadi Province (on which the Richtersveld Subprovince developed), the proto-Namaqua Province, and a 'southern continent'.

Stage 1 (-2.1 Ga) Continental attenuation and breakup (Fig. 2.4.a). A triple junction forms as the proto-Namaqua Province, the Kgalagadi Province and the Kaapvaal Craton separate from each other.

Stage 2 (2.1 - 2.) Ga). Whereas ocean opening isolated the proto-Namaqua Province, to the south, separation between the Kgalagadi Province and the Kaapvaal Craton proceeded no further than an incipient rifting stage (Fig. 2.4.b). A prograding clastic wedge (the Olifantshoek sequence) filled the Kgalagadi-Kaapvaal rift basin, with the major sediment supply comming from the Kaapvaal Craton.

Stage 3 (2.0 - 1.5 Ga). The Kgalagadi -Kaapvaal aulacogene closed, forming the Kheis Belt as the Olifantshoek Sequence was folded and thrust onto the Kaapvaal Craton (Fig. 2.4.c).

Subduction occurred along the edge of the Kgalagadi and proto-Namaqua Provinces. A steady state between spreading and subduction was achieved and was maintained for a long period of time. Subduction along the Kaapvaal Craton was inhibited by the thickness of the Kaapvaal lithosphere. The Orange River Group volcanics (and sediments), and the Vioolsdrif intrusive suite, developed on the edge of the Kgalagadi Province whereas the Gladkop intrusive suite, and volcanic equivalents, developed along the edge of the proto-Namaqua Province. Recycled sediments and/or microplate collisions mark a later, more felsic phase of calc-alkaline magmatism, during which the Haib porphyry copper deposit was developed.

d.

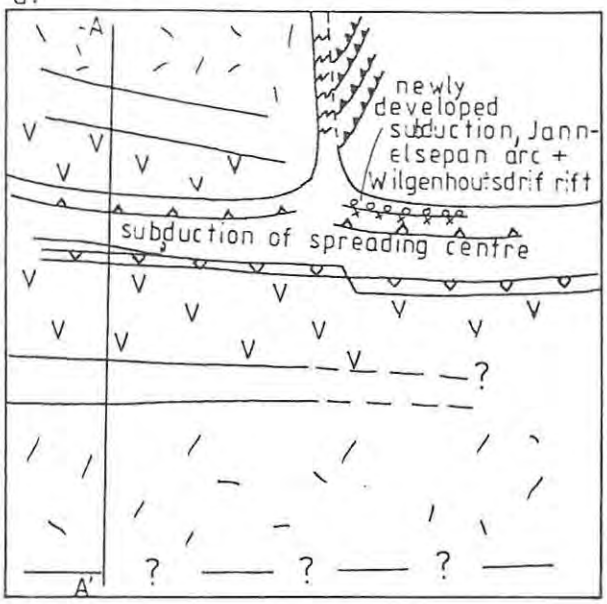
A
newly developed subduction, Jannelsepan arc + Wilgenhoutsdrif rift
subduction of spreading centre
A'

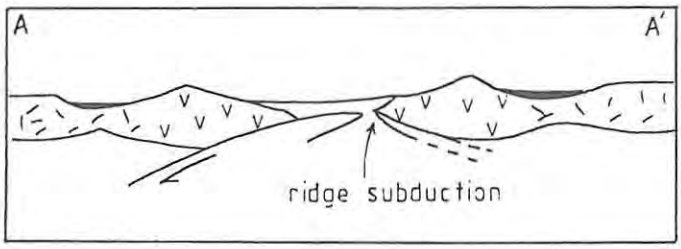
A
A'
ridge subduction

e.

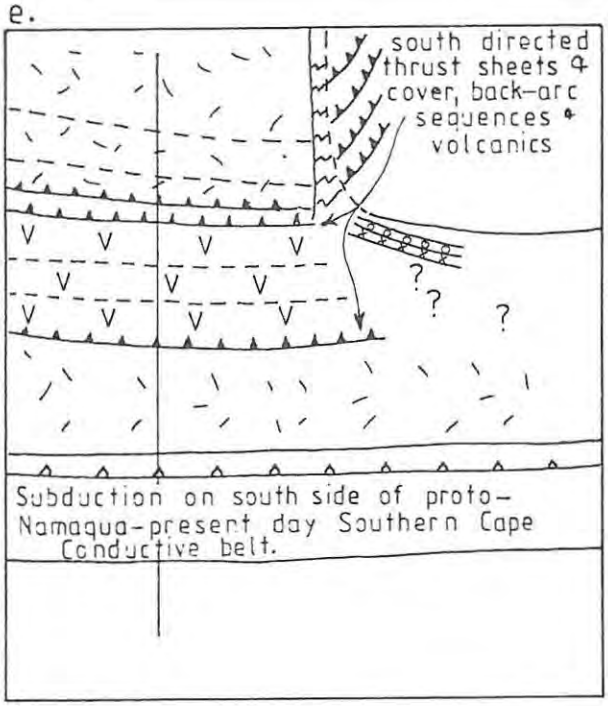
south directed thrust sheets of cover, back-arc sequences & volcanics
Subduction on south side of proto-Namaqua-present day Southern Cape Conductive belt.

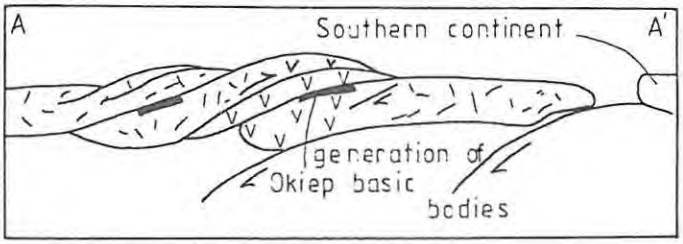
A
Southern continent
A'
generation of Okiep basic bodies

f.

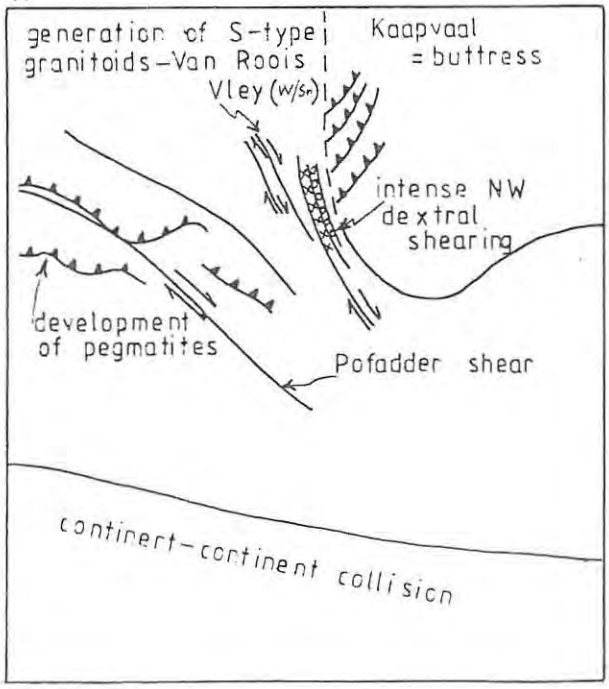
generation of S-type granitoids-Van Roois
Vley (w/sr)
Kaapvaal = buttress
intense NW dextral shearing
development of pegmatites
Pofadder shear
continent-continent collision

A back arc extensional rift developed in the proto-Namaqua Province, where the Bushmanland Sequence and the Aggeneys-Gamsberg massive sulphide deposits developed.

Stage 4 (1.5 - 1.3 Ga). Subduction was initiated off-shore of the Kaapvaal Craton as the 'Namaqua ocean' closed (Fig. 2.4.d). The Jannelsepan magmatic arc, associated Besshi-type sulphide deposits (ie Boksputs - Areachap - Copperton) and the Wilgenhoutsdrif rift sediments (and volcanics) developed. The spreading ridge met up with the proto-Namaqua Province and terminated subduction along the edge of that province.

Stage 5 (1.3 - 1.05 Ga). The proto-Namaqua and Kgalagadi Provinces collided, with partial subduction of the former, beneath the latter. Major south-moving thrust wedges developed (Fig. 4.2.e) and supracrustals caught between the wedges were isoclinally folded and sheared. During this period the F_1, F_2, and F_3 folds and fabrics of the Namaqua Province developed and metamorphism peaked (The Namaqua event). Within the Springbok-Okiep area, silicic granitoids intruded along thrust fabrics, and were followed by intrusion of the Cu-rich Koperberg suite. The latter may have resulted from multi-stage partial melting of an asthenospheric wedge that was brought into the crust on the sole of a thrust slice. The Springbok area is radiometrically enriched and it is considered that the Proterozoic geothermal gradient within the area, was high.

During Stage 5, the central portion of the Richtersveld Subprovince was not substantially thickened by thrusting, as were the regions immediately north and south of that portion. This central portion would have subsided in sympathy with subsidence of the adjacent thickened areas and thereby be protected from erosion. As the adjacent areas eroded, so the whole region lifted, leaving a central low-grade portion of the Richtersveld, flanked by two high grade regions.

At about this stage, subduction along the southern margin of proto-Namaqua Province was initiated. Remnants of this subduction zone are inferred, today, as the reason for the Southern Cape Conductive Belt, a 1200 km long geomagnetic anomaly, to the south of the Namaqua Province.

Stage 6 (1,05 - 1,0 Ga). A continent-continent collision is envisaged to have occurred between the now Namaqua Province and a southern continent. The collision marks the assembly of Gondwanaland. Crustal shortening was achieved by oblique sideways movement of large portions of the Namaqua Province along mostly dextral slip lines or wrench systems (Fig. 4.2.f). The Kaapvaal Province acted as a rigid buttress. In the Prieska region, original thrust faults that had been turned on end by back-folding were reactivated as dextral wrench faults. The Jannelsepan/Wilgenhoutsdrif arc/back-arc couplet was shunted along the Kaapvaal-Kheis boundary and juxtaposed with slivers of Namaqua and Kheis material, in the Gordonia subprovince.

During this final phase of the Namaqua Orogeny, various anatectic "S"-type granitoids were generated and intruded along NE shears. Tin/tungsten mineralization at Van Rooi's Vley is of this age. Large belts of pegmatites were also developed along the lines of collision between the Bushmanland and Richtersveld/Gordonia Subprovinces. Individual pegmatite emplacement was often controlled by NW trending shear fabrics.

3. LOCAL GEOLOGICAL SETTING

3.1 Geology

3.1.a Stratigraphy

The Van Rooi's Vley deposit lies within the Kakamas Terrane of the Gordonia Subprovince (Fig. 2.2) and is hosted by the pretectonic **Korannaland Sequence** of supracrustals. The stratigraphy of the Korannaland Sequence is presented in table 3.1 and is represented by a series of upper-amphibolite to granulite facies schists and gneisses. Lithologies outcropping at the Van Rooi's Vley deposit are detailed within Section 3.2.

TABLE 3.1

LITHOSTRATIGRAPHY OF THE KORANNALAND SEQUENCE

Rooidam Formation	Banded, garnetiferous, quartz-feldspar-biotite gneiss, with biotite schist, amphibolite and quartzofeldspathic layers.
Toeslaan Formation	Dark garnet-sillimanite-cordierite-biotite gneiss, with disseminated magnetite and quartzofeldspathic intercalations.
Goedehoop Formation	Thin-bedded sericitic quartzite.
Biesjepoort Formation	Banded biotite-cordierite gneiss with thin magnetite-rich tourmaline or feldspathis quartzite layers and calc-silicate rock, marble and hornblende gneiss with ferruginous quartzite intercalations.
Riemvasmaak Formation	Pink, banded, quartzofeidspathic, biotite gneiss, locally porphyroblastic and granitoid in part. Discontinuous quartz-magnetite-hematite lenses, biotite-sillimanite-cordierite gneiss and local tourmaline enrichment in the upper part.

(after Wheatley and De Beer 1986)

A distinctive quartz-feldspar gneiss (**Riemvasmaak Formation**), locally termed the "**Pink Gneiss**" because of its abundance of pink feldspar, forms the base of the Korannaland Sequence. The Pink Gneiss is overlain by the **Biesjepoort Formation**, which is dominated, at the base, by marbles, calc-silicates and hornblende-feldspar gneiss, but is progressive upwards into pelitic units. These rocks are locally termed "**Dark Gneiss**". The Biesjepoort Formation crops out at, and to the west of, the Van Rooi's Vley deposit but is apparently absent from the stratigraphy to the east of the deposit (Fig. 3.1). Furthermore, only the pelitic units of the Biesjepoort Formation are present at Van Rooi's Vley, and here they lie directly upon the Pink Gneiss.

Locally, thin and discontinuous layers of tourmaline ($\pm$ magnetite) quartzites occur near the top of the Biesjepoort Formation (Fig. 3.1). Tourmaline quartzites also occur within the upper-most unit of the Riemvasmaak Formation (Plate 3.1), near Kakamas to the west, and approximately 2km NE of the Van Rooi's Vley deposit, within the lower units of the Toeslaan Formation. Slack (1982) uses the term "**tourmalinite**" to describe essentially bimineralic tourmaline quartzites (with modal tourmaline $>15\%$), and ascribes their origin to the subaqueous exhalation of boron-rich fluids. A similar origin may be suggested for at least some tourmalinites within the Korannaland Sequence (i.e. the Kakamas tourmalinite). Some of these tourmaline layers are spatially related to the Van Rooi's Vley deposit and their significance is assessed in Sections 3.4 and 10.

The **Goede Hoop Formation**, of sericitic quartzites, is missing from the stratigraphy at Van Rooi's Vley. Instead, the **Toeslaan Formation** transgresses from the Biesjepoort Formation, in the west, down to the Riemvasmaak Formation to the NE (Fig. 3.1), although most contact relationships are hidden by the Quarternary Kalahari sand cover. The Toeslaan Formation dominantly consists of coarse grained garnet + sillimanite + cordierite + biotite gneisses and granulites.

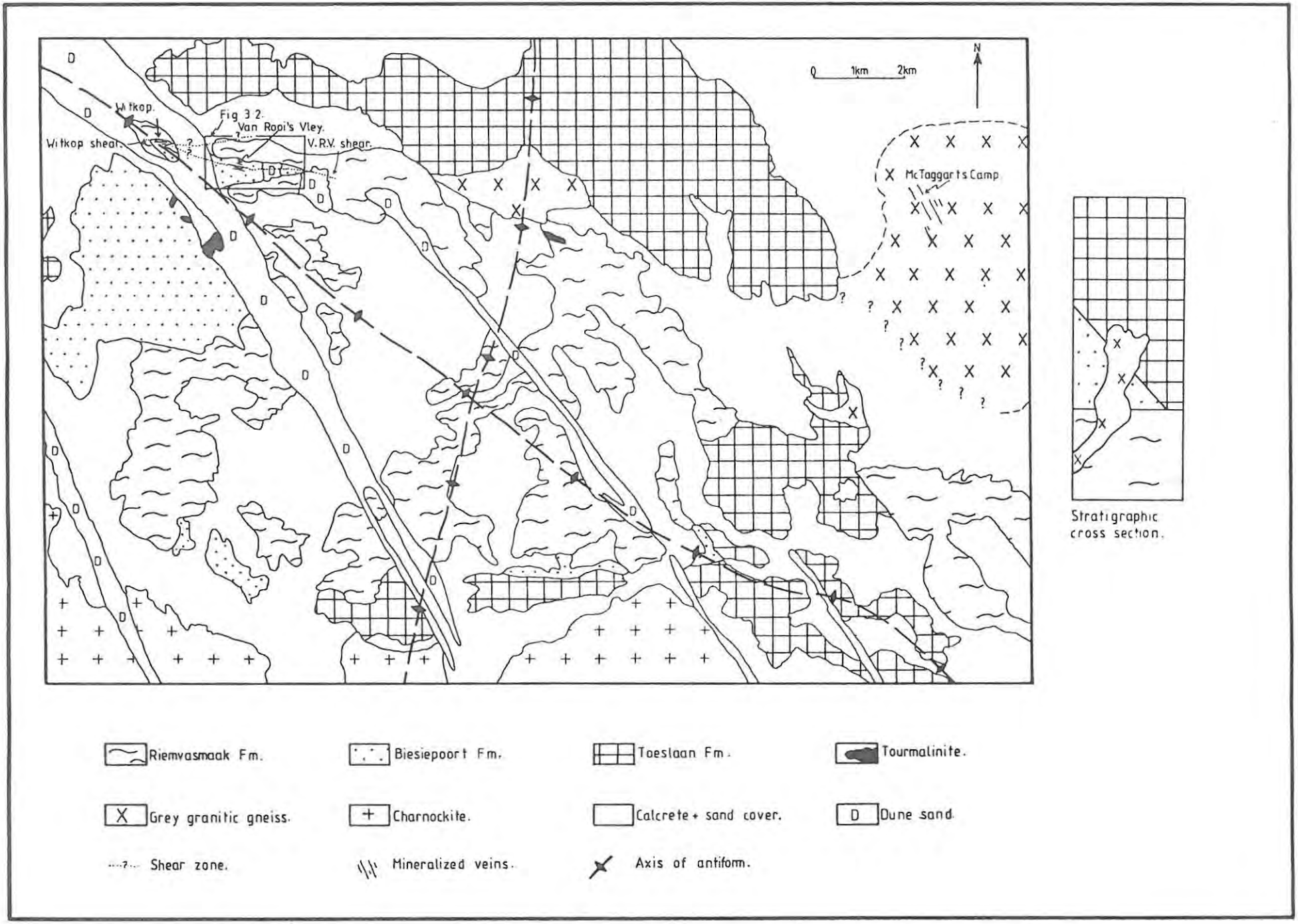

Figure 3.1. Geology of the Van Rooi's Vley area, including a schematic cross-section through the local stratigraphy succession.

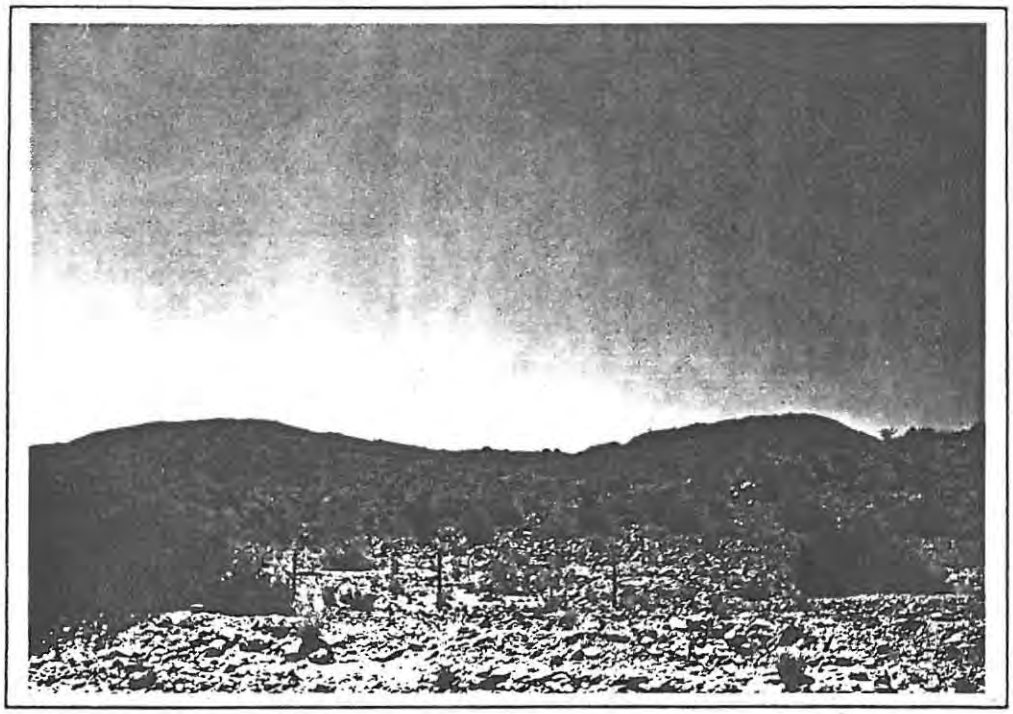

Plate 3.1. Well-bedded tourmalinite layers (dark) at the top of the Riemvasmaak Fm, near Kakamas.

The Korannaland Sequence is intruded by numerous syn- to post-tectonic granitoids. Although no granitoids crop-out at Van Rooi's Vley, they are encountered within drill core and do crop-out to the north of the deposit (see Fig. 3.4 and Section 3.3).

3.1.b Structure

Mineralization at Van Rooi's Vley occurs within five major E-W trending en-echelon quartz-tourmaline vein zones. These vein zones lie within a steep (78° to 85°) northerly dipping and E-W trending shear zone, here termed the **Van Rooi's Vley shear** (Figs. 3.1 and 3.2a). The mineralized shear zone is transgressive to bedding and cuts a tight westerly plunging synform developed on the northern edge of a domal structure. 'Dome and basin' tectonics is typical of the region (Von Backstrom 1964) and represents interference folding at the intersection of the F_2 and F_3 fold axis of the Namaqua Province (Fig. 3.1).

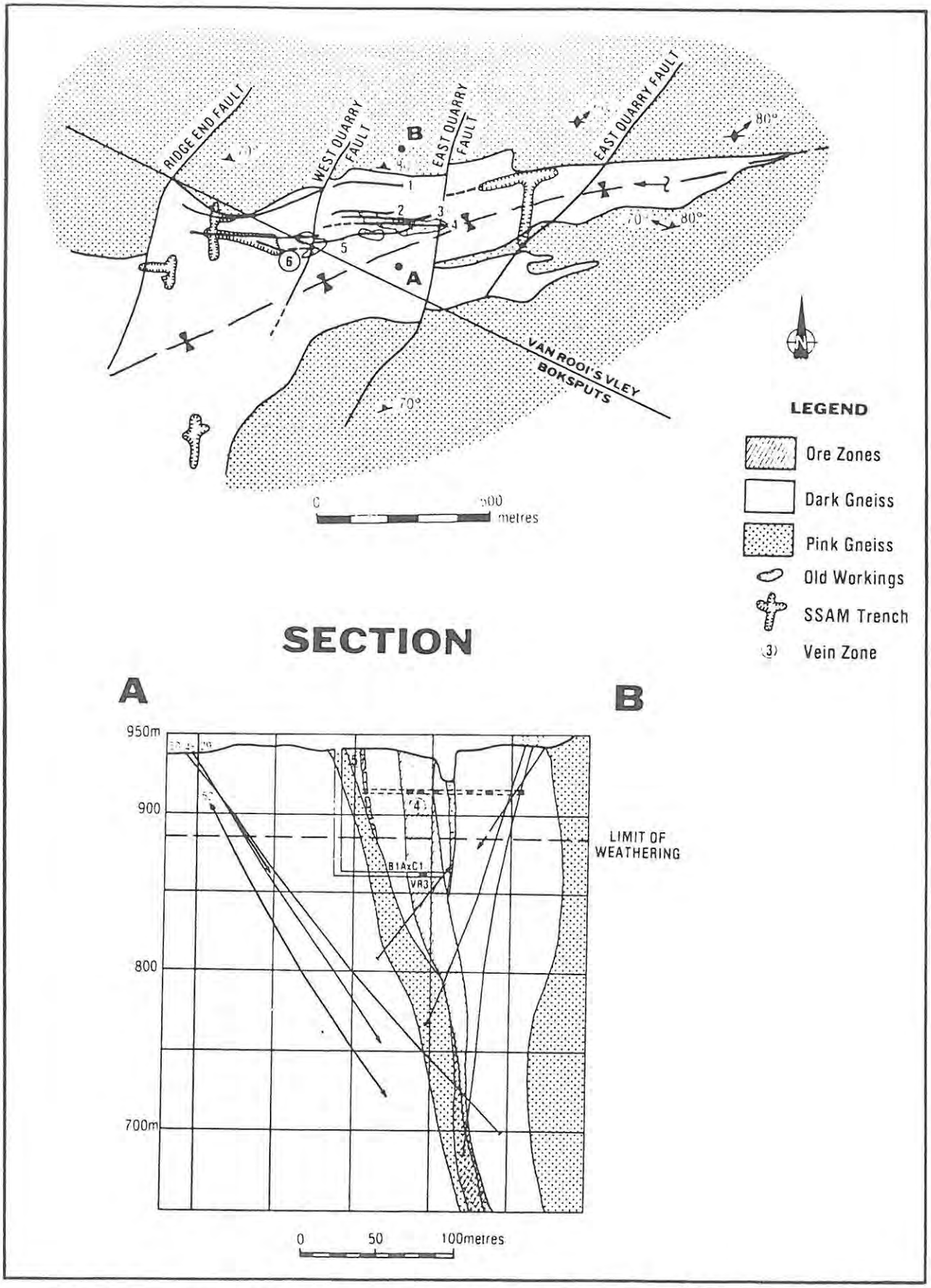

Figure 3.2. Local geology of the Van Rooi's Vley deposit and cross-section through the mineralized shear zone (after Wheatley and De Beer 1986).

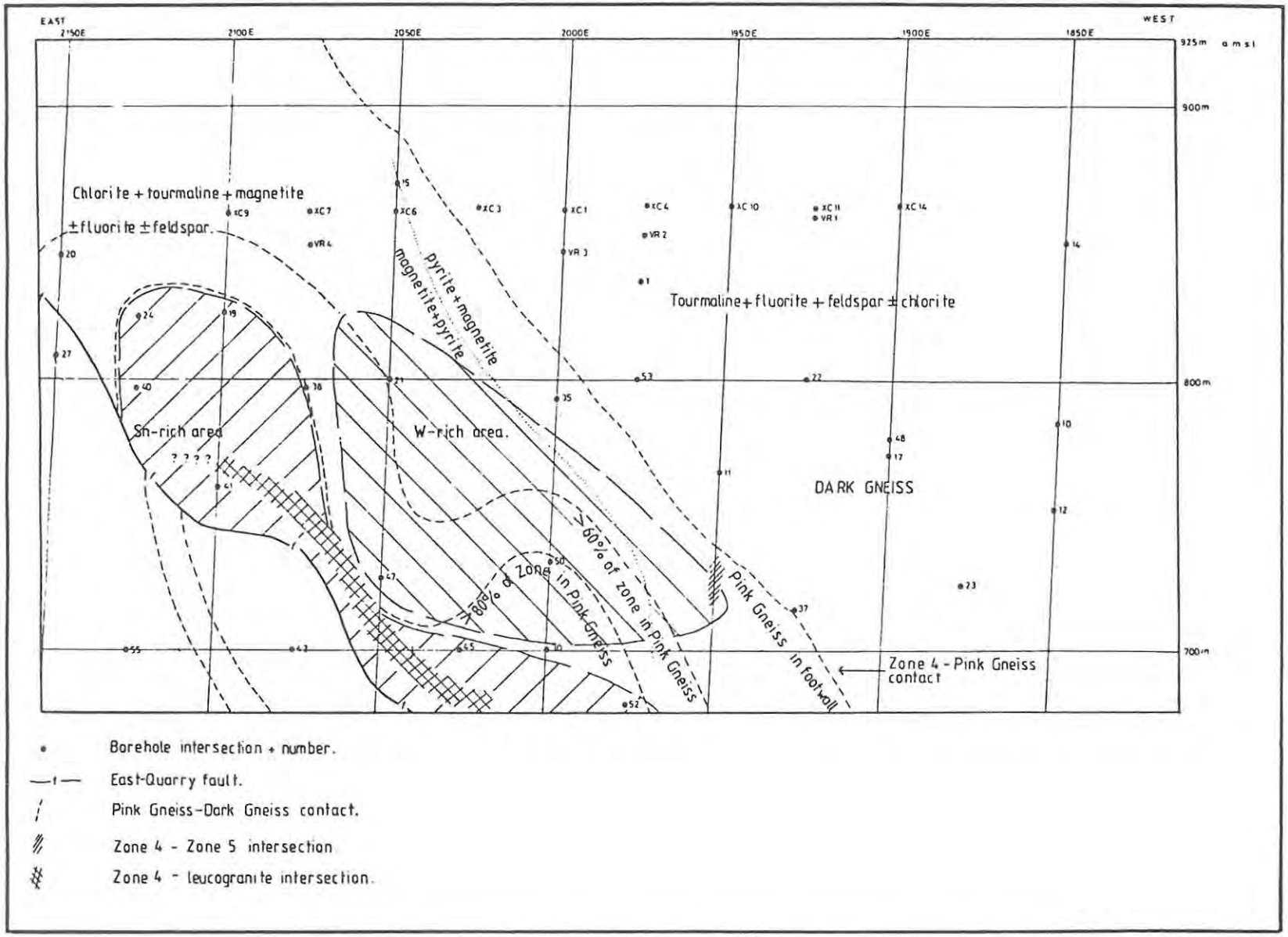

Figure 3.3. Longitudinal section of zone 4, showing areas of high grade mineralization, and general geological features. Note : all longtudinal sections produced within this thesis are drawn looking to the south ; the E-W axis is therefore reversed.

The ore-bodies occur within the upper pelitic units of the Biesjepoort Formation, and within a tectonically dislocated sliver of Pink Gneiss (Fig.3.2.b). The ore-bodies, and the Pink Gneiss sliver, plunge to the west (Fig. 3.3) in common with the synform in which they lie. Major NE trending faults (e.g. the **East Quarry Fault**), offset the ore-bodies and dominantly display a sinistral reverse displacement (Fig. 3.2.a).

Further W/Sn mineralization occurs at Witkop, approximately 1km NW of the Van Rooi's Vley deposit, again near the Pink Gneiss-Dark Gneiss contact. The area between the two deposits is covered by Kalahari sands and although the Witkop deposit roughly aligns with the direction of shearing along the Van Rooi's Vley shear, geophysics has failed to identify any connecting shear zone (P. Friggens pers. comm). Possibly, such a connection has been complicated by movement along the NE trending series of faults. Alternatively, the Witkop deposit represents part of a less well defined shear zone **(the Witkop shear)** that trends slightly east of the Van Rooi's Vley shear (Fig. 3.1).

The Van Rooi's Vley and Witkop shears lie close to, and are probably offshoots of, the prominent NE trending **Cnydas shear** (Fig. 3.4). According to Tankard et al. (1982), movement along the Cnydas shear was sinistral, in contrast to the dominantly dextral shearing within the Gordonia subprovince. Shearing was active during at least part of the mineralizing event at Van Rooi's Vley as evidenced by occassional contorted veins (Plate 3.2). The intrusion of the late-tectonic Cnydas granite suite, to the north of Van Rooi's Vley, was facilitated by the Cnydas shear.

3.1.c Mineralization

The five mineralized zones within the Van Rooi's Vley shear are numbered from north to south. Although mineralization and alteration types are essentially the same within all zones, only **zones 4 and 5** intersect the sliver of Pink Gneiss (Fig. 3.2 and 3.3) and carry grades of economic interest. Zone 4 is the most economic zone and has a strike length in excess of 300m and a depth in excess of 250m.

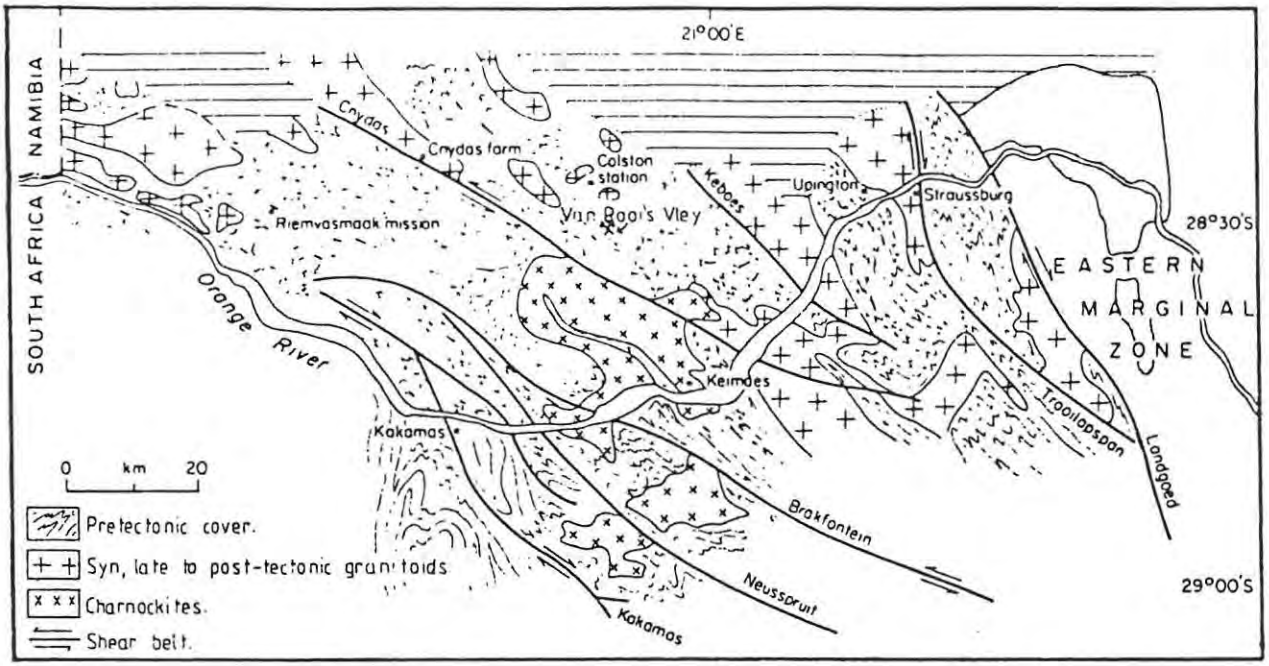

Figure 3.4. Geological map of the Upington and Kakamas Terranes, highlighting the numerous shear zones that occur within the region. Note the position of granitoids (late to post-tectonic) at Colston station (the Colston granite) and at Cnydas farm (the Cnydas granite Complex). The later granitoid body shows a distinct relationship to the Cnydas shear zone.

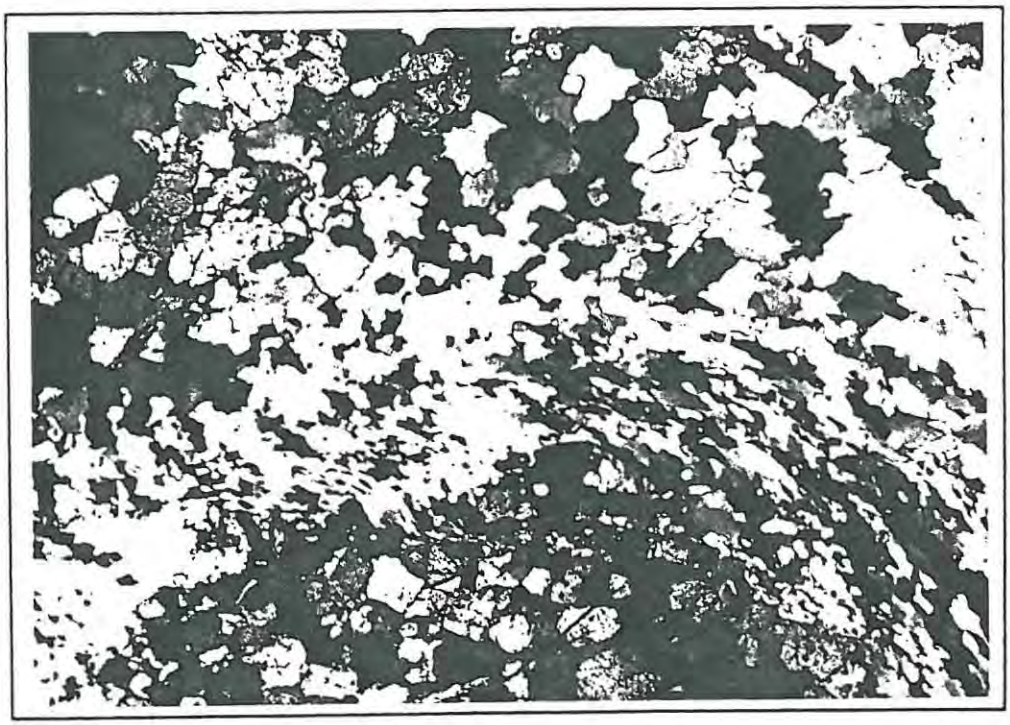

Plate 3.2. Photomicrograph showing a minor quartz vein that has been texturally modified by movement along the Van Rooi's Vley shear (XP, 20).

Mineralization at Van Rooi's Viey is concentrated within veins comprised of quartz, quartz + feldspar, quartz + tourmaline or quartz + tourmaline + fluorite. The mineralized veins are typically 'telescoped' (ie. multi-generation). Scheelite, wolframite and cassiterite are the main ore minerals, with the proportions of scheelite and wolframite being approximately equal, and together exceeding that of cassiterite. Other ore minerals include magnetite, pyrite, molybdenite, hematite and chalcopyrite.

The nature of the surrounding wall-rock alterations depend, to some extent, on the nature of the original lithology. Tourmaline + feldspar $\pm$ fluorite $\pm$ chlorite are the dominant alteration minerals within Dark Gneiss hosted veins, whereas the assemblage chlorite + tourmaline + magnetite $\pm$ fluorite $\pm$ feldspar is characteristic of Pink Gneiss hosted veins (Fig. 3.3). Magnetite is not abundant within the Dark Gneiss hosted veins or wall-rocks, however, minor pyrite is commonly present. Possibly, the pelitic Dark Gneiss represents a more reduced lithology compared to the Pink Gneiss. Highest W/Sn grades commonly occur within, or adjacent to, Pink Gneiss hosted veins. (Fig. 3.3).

3.2 Host lithologies

3.2.a. Dark Gneiss (Biesjepoort Formation)

Only the highest stratigraphic units of the Biesjepoort Formation crop-out at Van Rooi's Vley. These units are characteristically pelitic in composition, and, on the local scale, are moderatly uniform in mineralogy. They are very similar to the overlying pelitic rocks of the Toeslaan Formation.

The Dark Gneiss displays a distinct gneissic foliation and commonly shows small scale, but distinct, dark and light banding (Plate 3.3). Quartz is

the dominant mineral within the lighter bands and is accompanied by plagioclase (An_{10-20}) and perthite. The darker bands are composed of varying proportions of sillimanite, biotite, garnet (andradite), quartz and magnetite, with lesser amounts of plagioclase and cordierite (now mostly pinite). Garnet is erratically distributed, occurring only in certain layers, as porphyroblasts (Plate 3.3) up to 5cm in diameter. Sillimanite is very abundant and is commonly present in both prismatic and fibrous habits. Green spinel (hercynite or gahnite), green-brown tourmaline, zircon, apatite and pyrite are accessory phases within the Dark Gneiss.

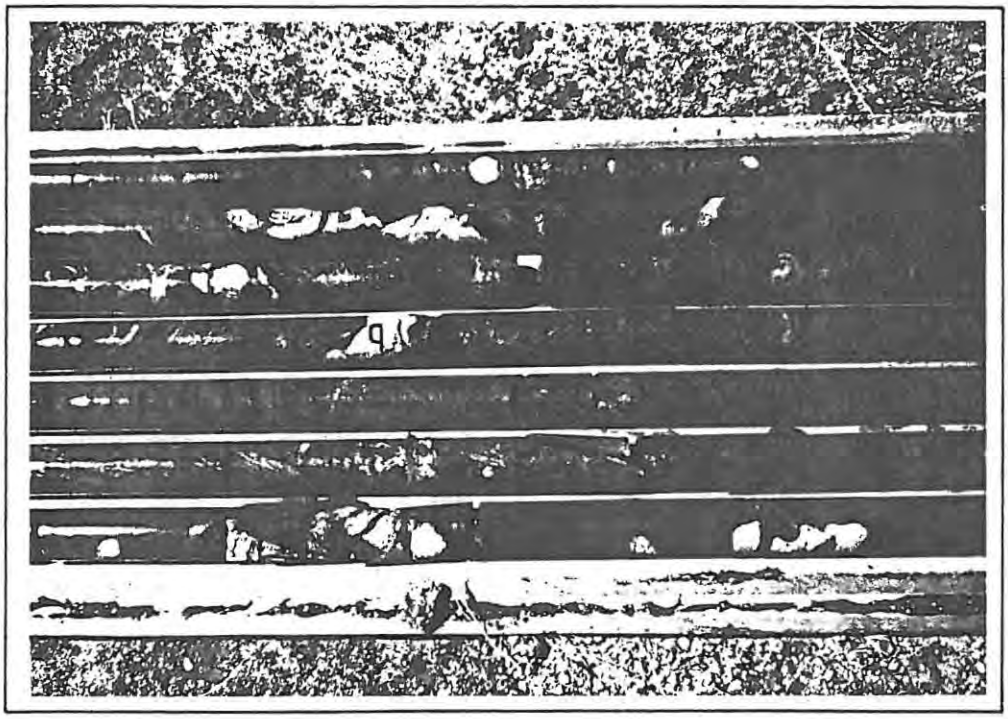

Plate 3.3. Drill-core intersection of the Dark Gneiss. Note the gneissic foliation, banding, garnet porphyroblasts (g) and the presence of large quartz sweat-outs (q) (Lense cap for scale).

Quartz and pegmatitic sweat-outs, of metamorphic (anatectic) origin, are common within the Dark Gneiss (Plate 3.3) and may exceed 10cm in length.

3.2.b Pink Gneiss (Riemvasmaak Formation)

The Pink Gneiss also shows a distinct gneissic lineation, which, in rare cases, is crenulated (Plate 3.4). Commonly the lineation is defined by small scale alternations of quartz (± perthite)-rich bands, with bands rich in perthite, quartz ± plagioclase (An_{10-20}) ± biotite (mostly chloritized). Perthite forms between 40 - 60% (by mode) of the latter bands, and is pink to red in colour. Magnetite commonly forms 1-5% (by mode) of the Pink Gneiss, whilst sillimanite, zircon, tourmaline and apatite are accessory phases. Sillimanite is the only pelitic mineral found, and never exceeds accessory proportions.

The Pink Gneiss of the Upington-Kakamas area has been previously interpreted as a metamorphosed arkose, derived from pre-Kheiss granites to the east (Poldervaart and Von Backstrom, 1949), although a volcanic (rhyolite) origin has also been suggested (Botha et al., 1976).

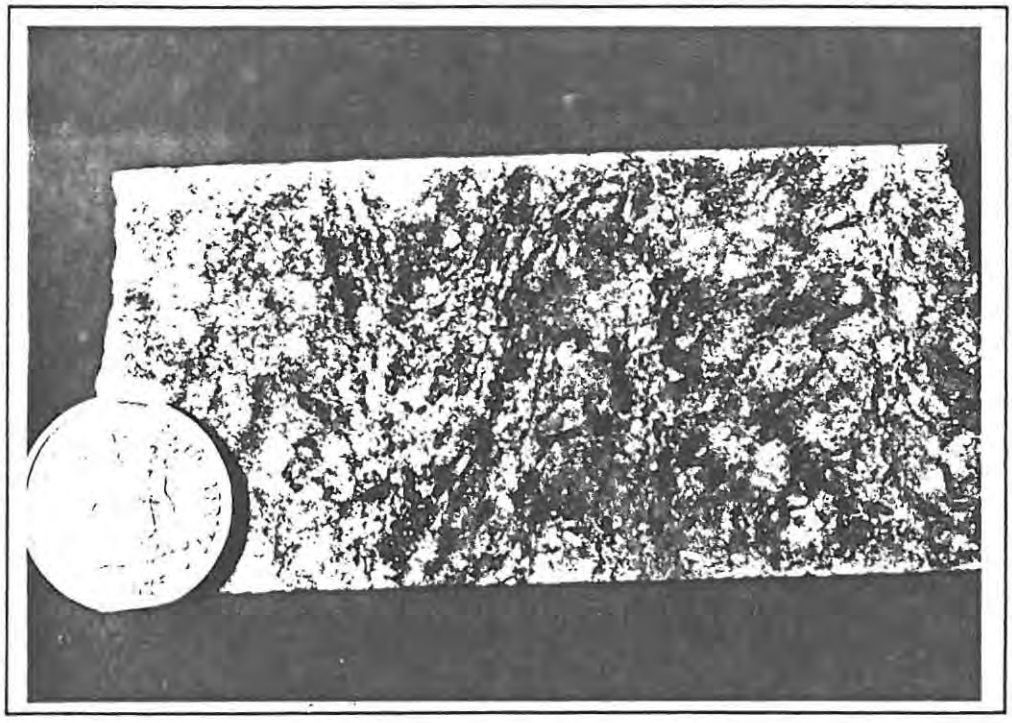

Plate 3.4. Drill-core section of the Pink Gneiss, here showing a distinct crenulated gneissic foliation (DH31).

3.3 Local granitic rock-types

3.3.a Introduction

Four granitic rock-types occur within the Van Rooi's Vley region. The Cnydas granite complex and the Colston granite crop-out to the NW of Van Rooi's Vley (Fig. 3.4), and represent late to post-tectonic rock-types, whilst syn-tectonic and late to post-tectonic granitic dykes are encountered within drill core at Van Rooi's Vley. It is possible that a complex granitic body underlies the deposit.

3.3.b The Colston granite

The major outcrop of Colston granite lies approximately 20km NNW of Van Rooi's Vley, although numerous smaller bodies crop-out as close as 3km from the deposit (Fig. 3.4). The essentially unfoliated nature of the Colston granite suggests a late to post-tectonic (ie. 1.2 Ga) age of intrusion.

Only one sample of the Colston granite was studied (HS8) and was collected from a small outcrop 10km NW of Van Rooi's Vley. This sample is a mesocratic, medium-grained and equigranular granitoid. Quartz, K-feldspar (perthithe microcline) and biotite dominate the mode, with lesser amounts of plagioclase (An_{15-20}). Garnet is often associated with biotite, indicating a peraluminous (possibly S-type) composition for the granitoid. Zircon, apatite, monazite, tourmaline and magnetite? were the accessory phases.

3.3.c The Cnydas granite complex

The Cnydas complex is a composite granitic body that lies 30km WNW of Van Rooi's Vley (Fig. 3.1). The granitoids have a radiometric age similar to other post-tectonic granitoids of the Gordonia subprovince (Jankowitz 1986)

and are unfoliated, except close to the Cnydas shear zone, along which the complex intrudes (Fig. 3.4).

According to Jankowitz (1986), the complex consists of ten different granitic phases, ranging in composition and mineralogy from hornblende + biotite-bearing granodiorites (and a charnockite), to highly differentiated leucogranites. The granitoids are generally calc-alkaline and I-type (Jankowitz 1986) in composition, however the more differentiated phases tend towards more alkaline compositions. Tourmaline is commonly the major dark mineral within the leucogranites, which are essentially comprised of quartz-perthite- and almost pure albite (An_{8-10}) $\pm$ biotite.

Tourmaline becomes a major constituent in some of the leucogranites and may form into discrete tourmaline + quartz (+K-feldspar $\pm$ albite) pods. (Plate 3.5). These pods range up to 25 cm in diameter and may constitute up to approximately 10% of the rock mass. According to F. Pirajno (pers. comm), such pods may represent the initial stages in the development of a magmatic-hydrothermal system. If so, it may be significant that the tourmaline pods contain up to 55ppm W, and the leucogranites themselves may contain up to 735 ppm W and 21 ppm Sn (Jankowitz 1986).

3.3.d Syn-tectonic granitic dykes

A coarse grained dyke was encountrered within a drill-core intersection of Zone 4 (VRD 14), at 75m depth. The dyke intrudes the Dark Gneiss at a high angle to foliation and is approximately 2m thick. No outcrop is known to occur.

Mineralogically the rock consists of quartz - perthite - biotite - sillimanite $\pm$ plagioclase, and is thus quite alkaline, (yet peraluminous), in composition. The rock is well foliated and much of the quartz is brecciated, shows undulose extinction, and now forms a groundmass between 'rolled' perthite crystals. Biotite defines the foliation and is commonly altered to chlorite and sillimanite (Plate 3.6).

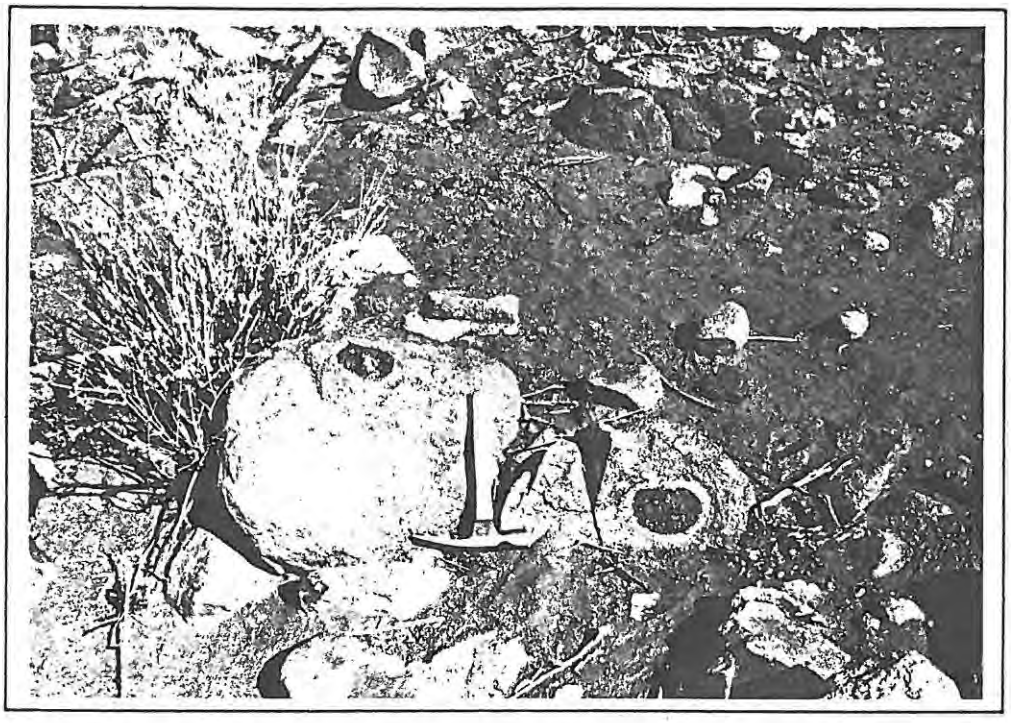

Plate 3.5. Tourmaline pods within the Cnydas leucogranites. Mineralogically, these pods consist of tourmaline + quartz (± K-feldspar ± albite).

The excessive amount of sillimanite (Plate 3.6) is not an igneous feature of this rock and suggests that the dyke is syn-tectonic, intruded prior to, or during, high-grade regional metamorphism. The foliated nature of the granitoid also points to a syn-tectonic age of intrusion.

3.3.e Late to post-tectonic granitic dykes

Numerous fine to medium-grained leucogranite intrusions were encountered within drill-core intersections of the Dark Gneiss, and of Zone 4. Together, these granitic rocks define a large sheet-like dyke (Fig. 3.5) which strikes SW, dips northwards at approximately 60 and varies up to 30cm in width. This sheet does not parallel gneissic foliation or the orientation of the mineralized shear zone, and intersects the Pink Gneiss hosted region of Zone 4 just above the intersection of that zone with the

East Quarry Fault (Figs 3.5 and 3.3). The leucogranites are unfoliated and unmetamorphosed, and thus intruded at a late to post-tectonic stage, with respect to the Namaqua event.

Plate 3.6. Photomicrograph of a syn-tectonic granitic dyke. It can be seen that sillimanite(s) is present in excessive amounts (for a purely igneous rock) and is forming, at least in part, from the break-down of biotite. Note the well foliated nature of the rock and the presence of a brecciated quartz-rich groundmass around 'rolled' perthite crystals. (VRD43, XP, 20).

The composition of the leucogranites differs slightly. All are rich (up to 70% by mode) in alkali-feldspar (perthite alone or perthite + albite), but are peraluminous, as evidenced by the presence of andalusite or, less commonly, of sillimanite and cordierite. Biotite is a common, but minor, constituent and is invariably altered to chlorite, whilst zircon, apatite, opaques and monazite are accessory phases.

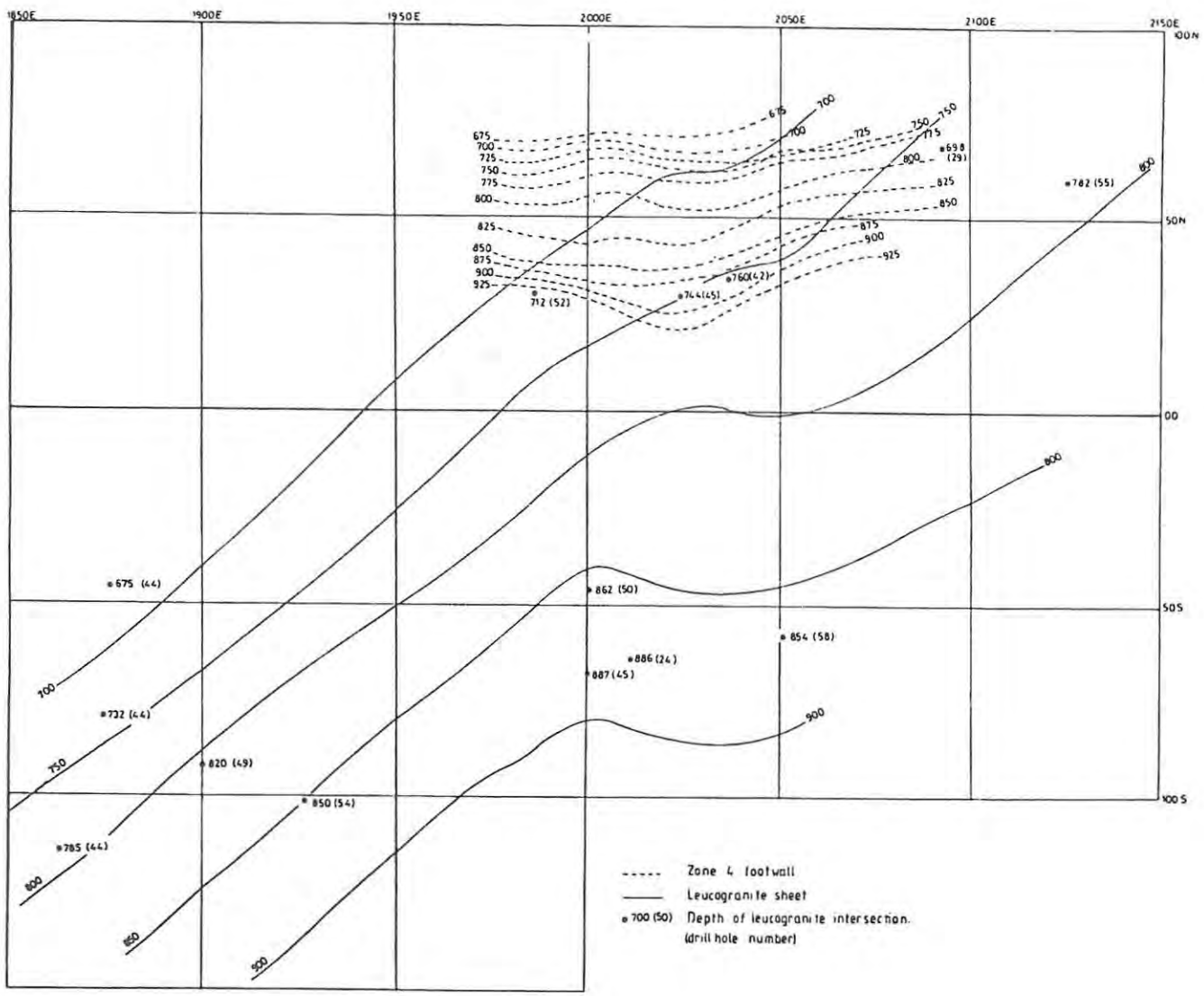

Figure 3.5. Geological plan showing the location and orientation of the late to post-tectonic granitic sheet. The sheet-dyke intersects Zone 4 immediately above the trace of the East-Quarry Fault (Fig. 3.3).

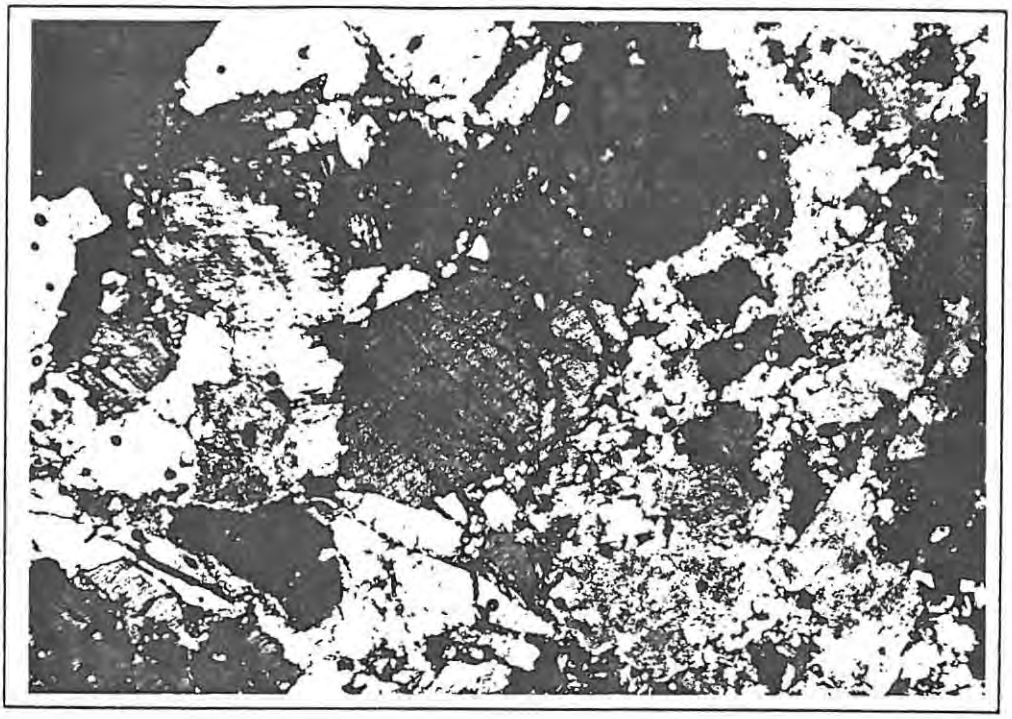

Plate 3.7. Photomicrograph of a late to post-tectonic granitic dyke. This dyke was sampled within Zone 4 and contains cassiterite mineralization (ct). Cassiterite crystals are commonly surrounded by sericitic alteration of feldspars (VR78, XP, X20).

The alteration paragenesis of the Van Rooi's Vley deposit is discussed in Sections 7 and 8, where it is established that sericitic alteration and tourmalinization are closely related to the mineralizing event. Feldspars within the leucogranites are moderately to highly sericitized, secondary tourmaline is present, and indeed, minor cassiterite is encountered where the leucogranites intrude Zone 4 (Plate 3.7). Mineralization at Van Rooi's Vley thus post-dates intrusion of the late to post-tectonic leucogranites.

The feldspar mineralogy of the leucogranites reflects a low temperature of intrusion. Hypersolvus (perthite only) and sub-solvus (perthite + albite) rock-types are present and indicate that the leucogranite sheet intruded at temperatures close to the alkali-feldspar solvus (e.g. 657 C at 1kB - Smith

and Parsons 1974). A low temperature of intrusion is consistent with the presence of andalusite, at low pressures.

3.4 Paleosetting of the Van Rooi's Vley area

As noted in the previous section, the term "Pink Gneiss" is used to describe a pink quartzofeldspathic gneiss that occurs throughout most of the Gordonia and Bushmanland subprovinces and forms the base of the supracrustal sequence. Given the structural complexity of the Namaqua Province, regional correlation of the Pink Gneiss is, however, dubious, particularly across the highly deformed Kakamas Terrane. Nevertheless, the striking similarity of the Pink Gneiss (and of the overlying supracrustal stratigraphy) across the Namaqua Province, invites such a correlation.

The supracrustal sequence within the Bushmanland Subprovince has been well studied (e.g. Rozendaal 1978, Moore 1984). The generalized stratigraphy of the sequence (the Bushmanland Sequence) is presented in table 3.2 and differs only in detail from that of the Korannaland Sequence (c.f. Tables 3.1 and 3.2). The most notable differences are the initially more calcareous compositions of the Biesjepoort Formation (directly overlying the Pink Gneiss of the Korannaland Sequence) and the presence of a B.I.F. sequence (the Aggeneys-Gamsberg-Fe-Formation) above the Pella Quartzite Formation of the Bushmanland Sequence. If regional correlation of the supracrustal sequences is valid, the abovementioned differences could reflect a change in the depositional environment, within a region of general subsidence. To the east, the basal portion of the Biesjepoort Formation was deposited within a shallow carbonate shelf environment, but, due to subsidence, saw an increasing influx of pelitic material. To the west, the entire Namies Formation of pelitic schists was deposited within a deeper water environment.

Locally, at Van Rooi's Vley, the transgressive nature of the pelitic Toeslaan Formation probably represents a sedimentary facies change. The situation depicted in figure 3.6 is envisaged, whereby faulting along the

proto-Van Rooi's Vley shear caused the Toeslaan Formation to transgress over the Biesjespoort Formation and onto the underlying Riemvasmaak Formation. The Van Rooi's Vley deposit occurs within the area of facies change, directly over the proto-Van Rooi's Vley shear. This suture not only controlled local sedimentation, but also provided a pathway for later (late to post-Namaqua event) mineralizing fluids.

TABLE 3.2
LITHOSTRATIGRAPHY OF THE BUSHMANLAND SEQUENCE

Nousees mafic gneiss	Semipelitic quartz-feldspar gneiss, overlain by mafic 'grey' gneiss.
Aggeneys-Gamsberg Fe-Formation	Diverse-Fe-Formation (magnetite, hematite, sulphides, barite etc).
Pella Quartzite	White metaquartzite, usually ferruginous at base.
Namies Schists	Biotite and sillimanite schists.
Haramoep Gneiss Pink	'quartzofeldspathic' gneiss.

(after Rozendaal 1978, SACS 1980)

3.5 The McTaggarts Camp - Dyasons Klip deposits

Further W, Sn and F mineralization occurs on the farms McTaggarts Camp and Dyasons Klip, to the east of Van Rooi's Vley (Fig. 3.1). The country-rock, an augen granite, is pre to syn-tectonic and hosts a series of NNW trending fractures which contain scheelite-wolframite $\pm$ cassiterite $\pm$ arsenopyrite $\pm$

chalcopyrite ± sphalerite ± molybdenite (F. Dooge pers. comm.). A quartz-tourmaline-biotite-muscovite-fluorite-plagioclase alteration assemblage accompanies this mineralization. **Tourmaline bearing leucogranites** also intrude along the fractures, are unfoliated and are very similar to the Cnydas leucogranites. Large E-W trending fluorite veins also occur with the augen granite on the Farm Dyasons Klip.

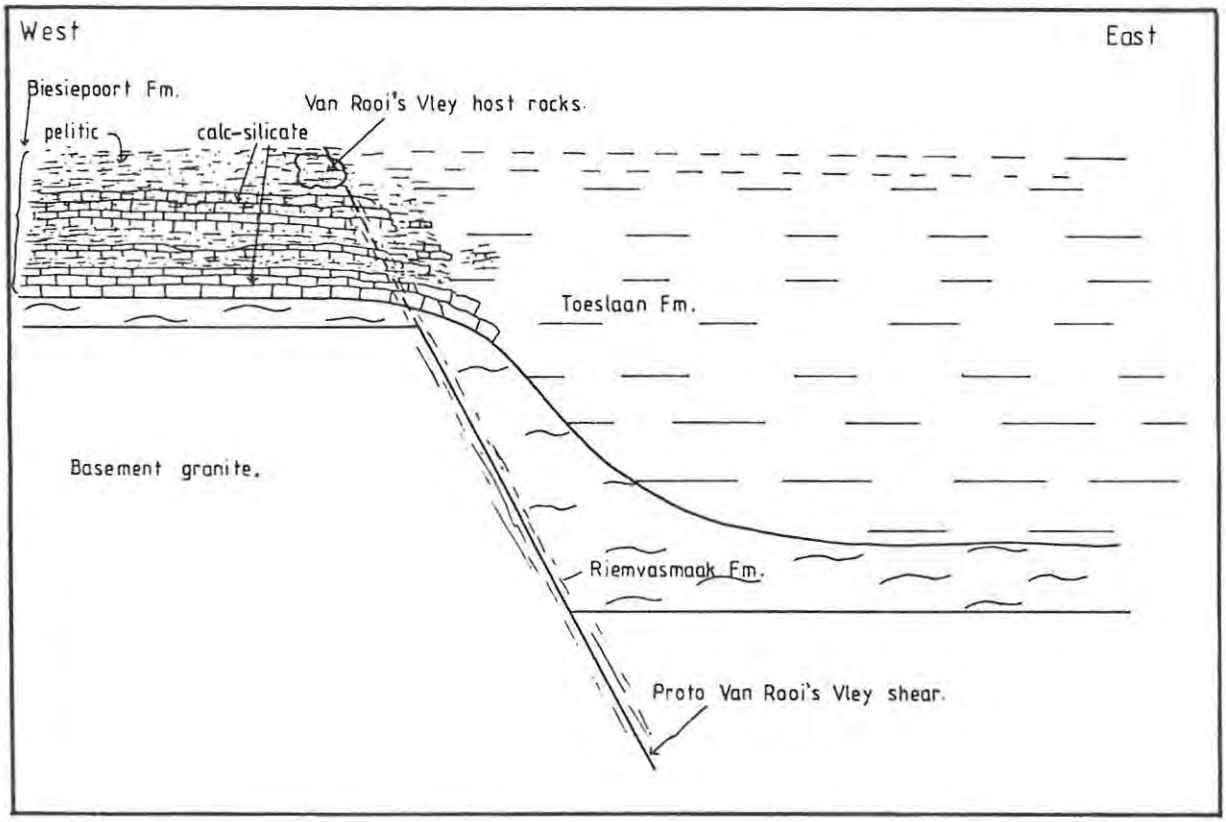

Figure 3.6. Schematic representation of the paleosetting within the Van Rooi's Vley area, before deformation and mineralization. The Van Rooi's Vley shear is envisaged to have once been a large scale normal fault that locally controlled sedimentation, but later provided a pathway for ascending hydrothermal fluids. Note the facies change between the Toeslaan Fm and the Biesjepoort Fm.

Many similarities exist between the Van Rooi's Vley - Witkop group of deposits and the McTaggarts Camp - Dyasons Klip group of deposits, both of which are late to post-tectonic in age and probably relate to the same

mineralizing event. However, the mineralization/alteration assemblages developed at McTaggarts Camp - Dyasons Klip are distinctly more greisen-like, W-rich and F-rich than the tourmaline dominated and quartz-vein hosted, Van Rooi's Vley-Witkop W/Sn deposits. The genetic significance of these differences is discussed in Sections 10 and 11.

4. STRUCTURE OF THE MINERALIZED ZONES

4.1 Introduction

Detailed structural and mineralogical studies of the Van Rooi's Vley deposit were confined to Zones 4 and 5 because these zones contained the highest grades, and because a meaningful analysis of all zones would not have been possible within the time given. Because of the larger number of bore-hole intersections of Zone 4, data pertaining to that zone is much better constrained than that pertaining to Zone 5.

4.2 Conolly-contour diagrams

4.2.a Construction

A Conolly contour diagram (e.g. see Conolly, 1936; Schwartz, 1986) is a longitudinal section on which the horizontal distance from a vein footwall (or hangingwall) to an arbitrary reference plane (the 'Conolly plane') is contoured. This reference plane is chosen such that its attitude approximates the average strike and dip of the vein of interest. The measurements taken between the reference plane and the vein footwall are then transferred to a longitudinal section and are contoured (Fig. 4.1). Completed Conolly contour diagrams for Zones 4 and 5 are presented in figures 4.2.a and 4.3.a respectively. Conolly contour diagrams may be interpreted in the same way as topographic maps, in terms of valleys, hills, etc., with linear features possibly related to faulting. When used in conjunction with longitudinal sections contoured for strike, dip and vein thickness, Conolly contour diagrams may also yield valuable information on the overall structure of a vein.

4.2.b Interpretation

Zone 4 has an average orientation of $80^{\circ}/085^{\circ}$N and, according to figure 4.2.a, is essentially semi-circular in plan. Two low points (or troughs), appear within a general valley shaped feature that runs up-dip, along the

2025° E grid line, and corresponds to an area of rapid lateral strike change (Fig. 4.2.b). The valley feature also roughly corresponds to that area of the vein where the Pink Gneiss becomes the dominant host-rock (cf. Figs. 4.2.a and 3.3). The abovementioned features probably indicate that a competency contrast existed between the two host-rock lithologies, leading to either buckling or faulting of the contact zone during shearing. This westerly plunging contact zone is highly fractured and would be an excellent feeder zone for the mineralizing fluids.

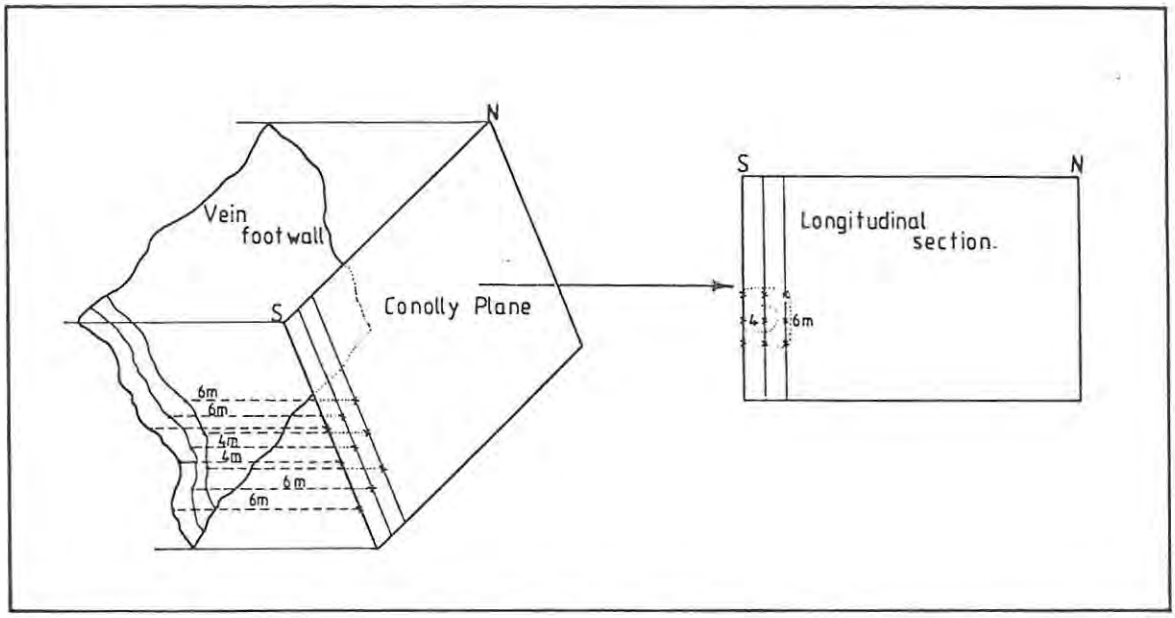

Figure 4.1. Method for constructing a Conolly contour diagram. The 'Conolly Plane' is commonly orientated at the average strike and dip of the vein footwall.

Longitudinal plots of Zone 4 (Fig. 4.2), contoured for zone thickness and for change in dip, also indicate a prominent westerly plunge for that zone. Anomalous changes in dip occur within the central regions of Zone 4 (Fig. 4.2.c), where contours are displaced down plunge. The direction of displacement parallels movement along the East Quarry Fault and is probably caused by two small faults of identical nature (and age) as the latter. These faults off-set (at right-angles) the general step-like, down-plunge, nature of the footwall surface.

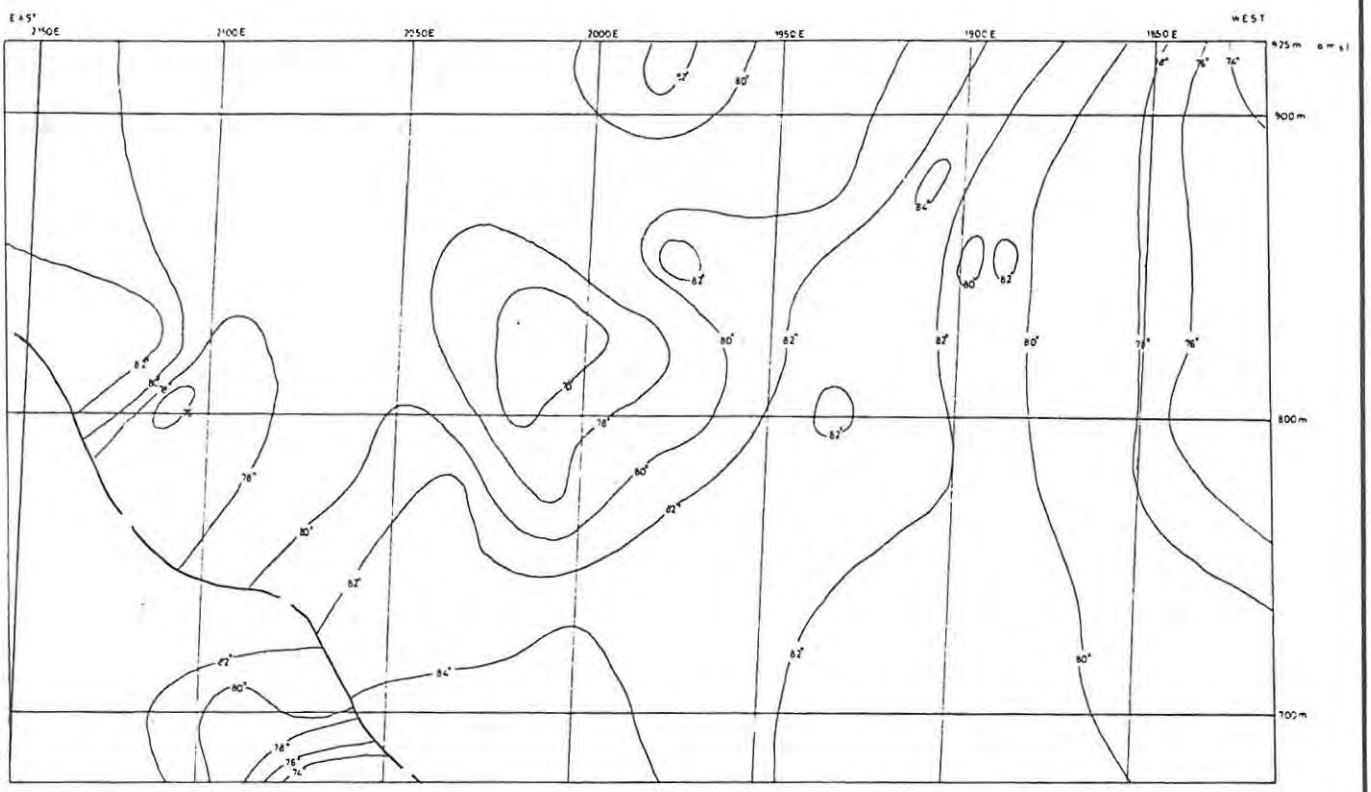

C. Change in dip.

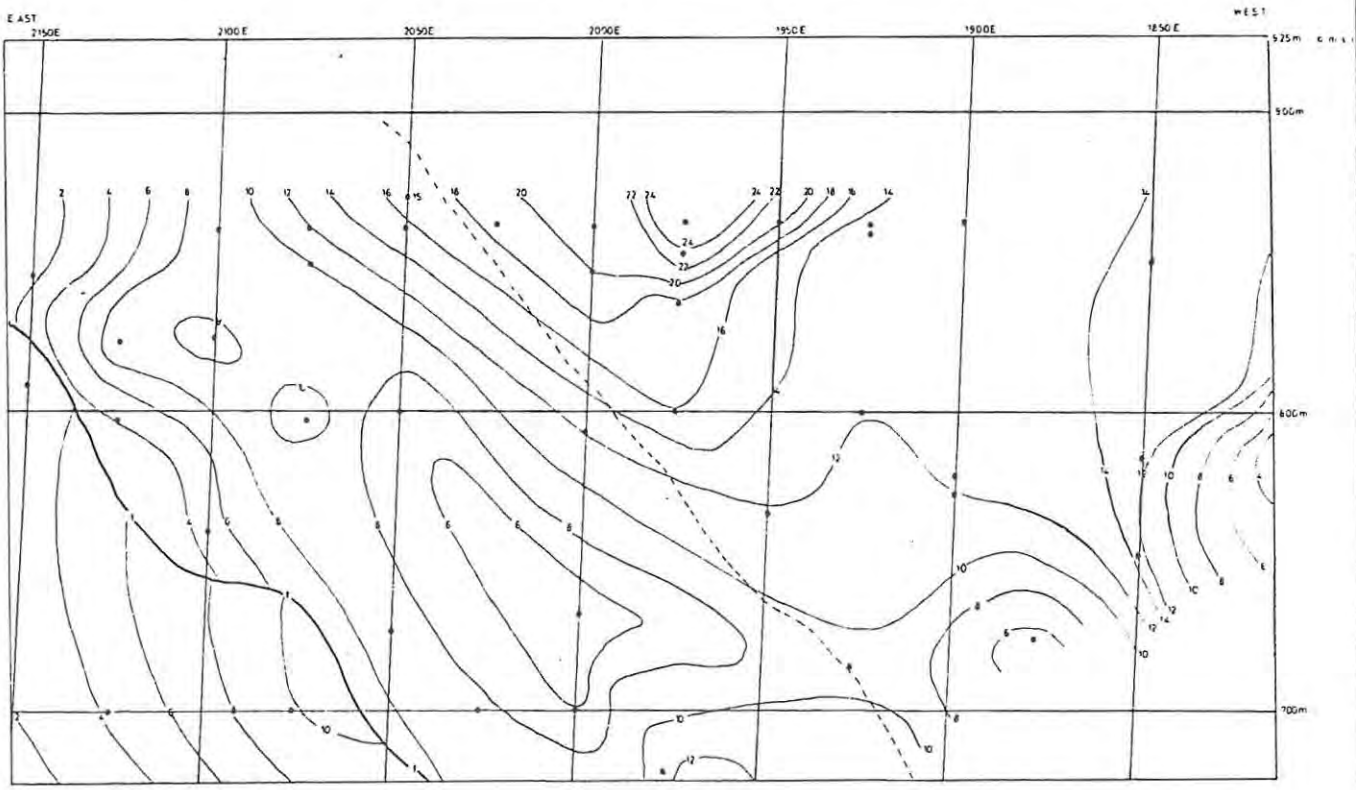

D. Zone thickness.

Trace of Pink Gneiss.

Although the accumulated thickness of vein material at any one point within Zone 4 does not vary greatly, the thickness of the zone itself varies widely, and is generally greater within the Dark Gneiss (Fig. 4.2.d). This behaviour is again due to the greater competency of the Pink Gneiss which, under stress, provided a small number of wide fractures, as opposed to the Dark Gneiss, which provided a large number of finer fractures and incorporated large amounts of country-rock.

Zone 5 has an average orientation of 78°/076°N and in contrast to the essentially vertical lineations seen in Zone 4 (Fig. 4.2.a), shows a pronounced horizontal lineation (Fig. 4.3.a).

The step-like features seen in figure 4.3.a are accentuated on figure 4.3.c, a longitudinal section contoured for dip, and relate to a series of E-W trending irregularities within the footwall surface.

In common with Zone 4, the thickest areas of Zone 5 are hosted by Dark Gneiss (Fig. 4.3.d), and again this feature relates to the larger amounts of Dark Gneiss country-rock included within the zone.

4.3 Determination of shear movement

A technique used to establish the relative direction and sense of fault movement is described by Schwartz (1986) and requires knowledge of the variation in the dip, strike and thickness of a vein.

The thickness of the vein is quoted as being either less than or greater than an arbitrary value, 'a', which is usually taken as the average thickness of that vein. The orientation of the vein at each selected intersection is plotted on a Wulff stereonet (Fig. 4.4 and 4.5) and given an appropriate symbol according to the vein thickness at that point (e.g. X for thickness >'a'). The great circle that best separates points representing thickness > 'a' from those representing thickness < 'a' is then constructed. The intersection ('b') of the pole of this great circle with the great circle that defines the average vein orientation, allows the measurement of the apparent slip of faulting.

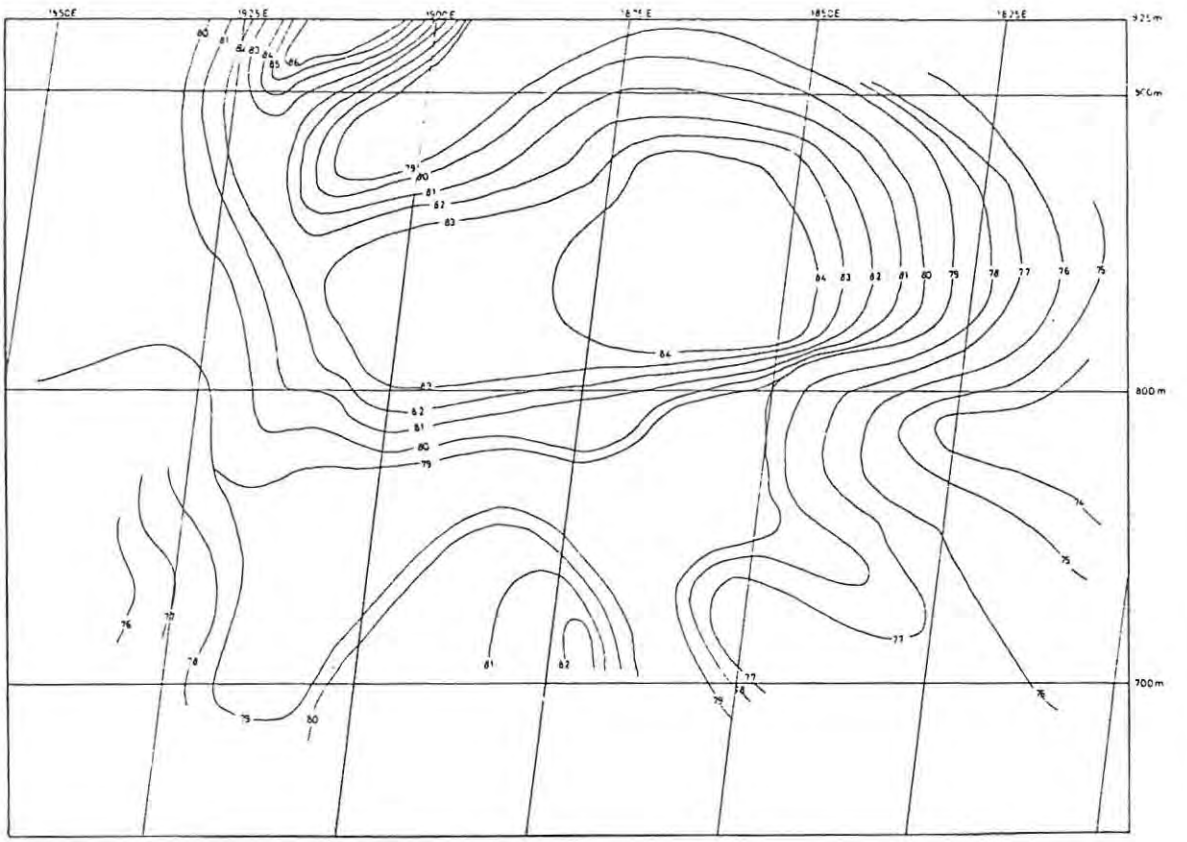

C. Change in dip.

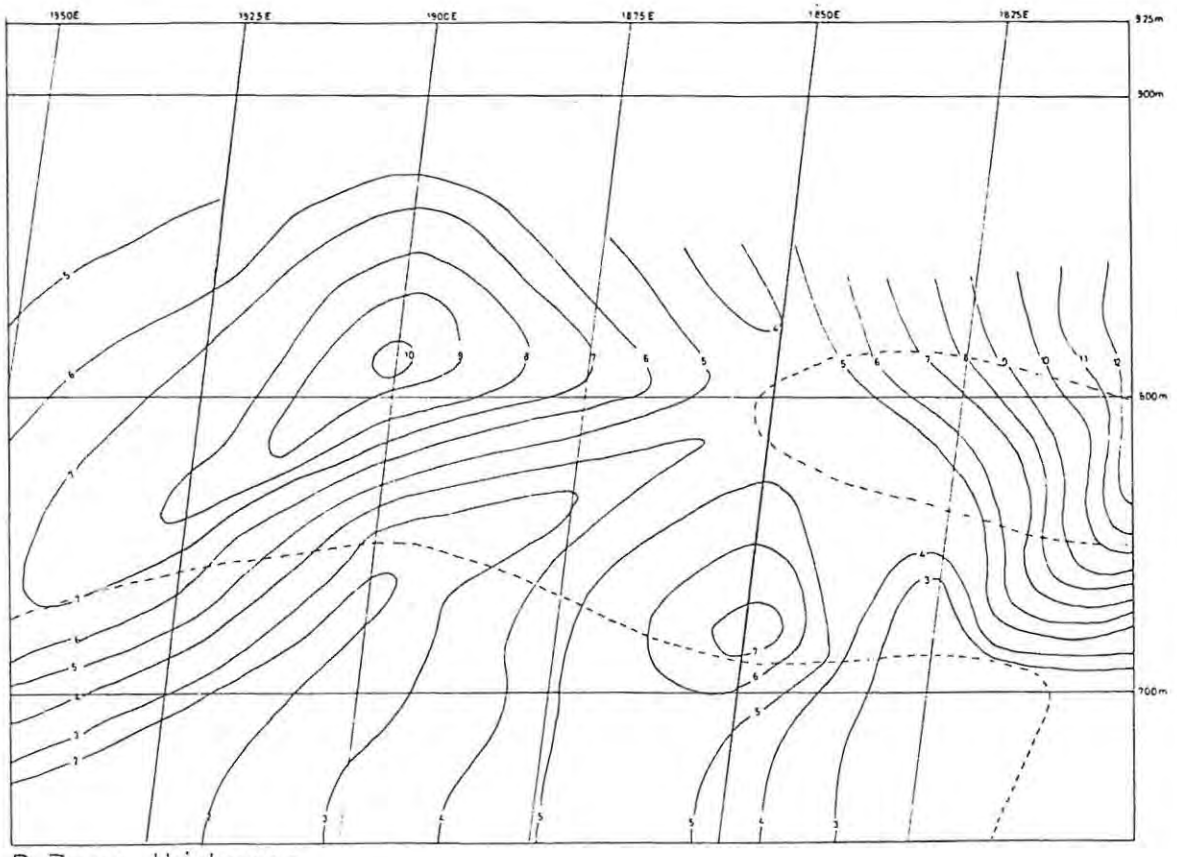

D. Zone thickness.

/ / Trace of Pink Gneiss.

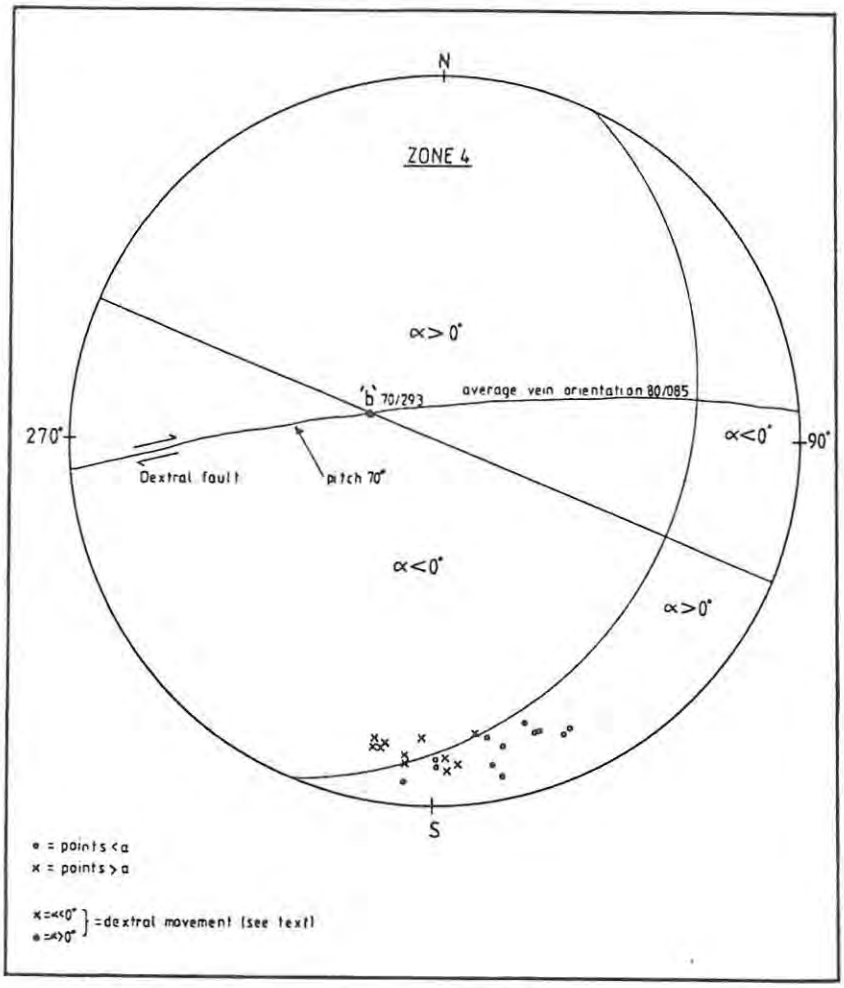

Figure 4.4. Stereogram showing attitude data for Zone 4 (see text). Wulff's stereographic projection, lower hemisphere. The intersection 'b' represents the apparent-slip direction along the vein (70/293) and 'a' is taken here to equal the average thickness of the vein. Movemenet along Zone 4 is dextral (see text), and, taking into account the westerly plunge of the zone, is also reverse.

A line drawn through the pole **'b'** and the centre of the stereonet divides the net into four sectors. Each pair of diagonally opposite sectors has an 'opening angle' ('α') of $> 0^{o}$ or $< 0^{o}$ respectively, where 'α' is the acute angle between the apparent slip (**'b'**) and the fault surface (see Fig.4.6). The sector which is clockwise adjacent to the pole **'b'**, has an

angle $\alpha > 0^\circ$ (Schwartz 1986) and if this sector, or its diagonally opposite sector, contains those points for vein intersections with thickness >a, then (as depicted on Fig. 4.6) the fault has a sinistral displacement. Conversely, if those points fall in a sector with $\alpha < 0^\circ$, the displacement is dextral.

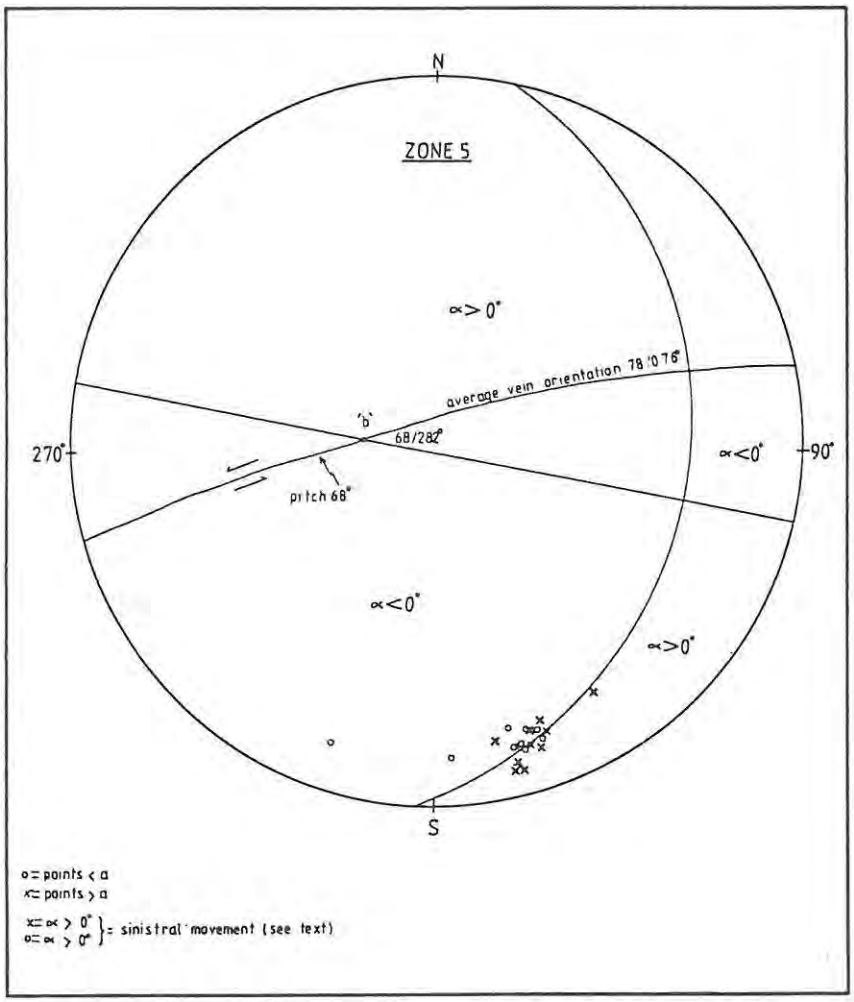

Figure 4.5. Stereogram showing attitude data for Zone 5. Symbols as for figure 4.4. Movement along Zone 5 is sinistral and normal.

The appropriate structural data pertinent to Zones 4 and 5 have been plotted on figures 4.4 and 4.5 respectively. From these constructions, and taking into account the westerly plunge of both Zones 4 and 5, it is apparent that movement along the two shear zones has been dextral-reverse and sinistral-normal respectively.

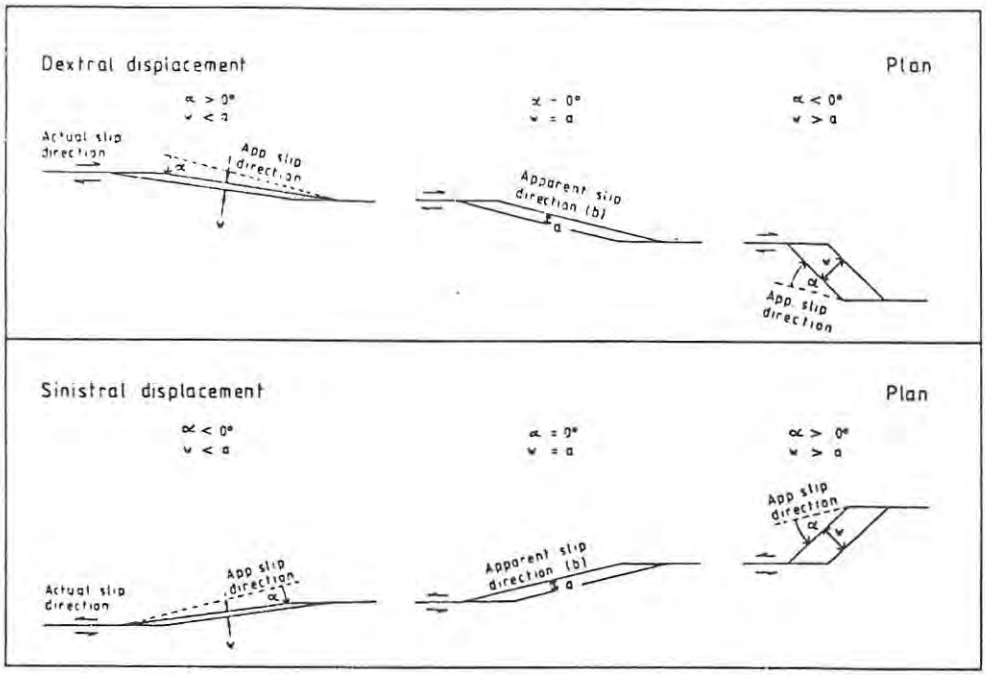

Figure 4.6. Diagram showing the mechanism of fissure opening along an irregular fault plane. See text for explanation. (after Schwartz 1986).

4.4 The formation of open-space, or low-pressure, zones

Because a decrease in pressure is a factor leading to the precipitation of most metals from solution, areas of **'open-space'**, or **'low-pressure zones'**, are favoured sites of ore deposition. In many cases the formation of low-pressure zones depends on the direction and sense of fault movement (Fig. 4.6), and on the attitude of the irregular fault surface (Schwartz 1986).

Taking the directions and sense of shearing, determined above for Zones 4 and 5, postulated irregularities in vein footwalls (indicated by changes in strike and dip - see Section 4.2.b) may be analysed in terms of their potential to form low-pressure zones. Commonly, proposed areas of low pressure do not coincide with areas of enhanced zone thickness, however, it must be remembered that zone thickness does not necessarily relate to the actual thickness of vein material.

Zone 4

-Because the rapid change in footwall strike (Fig. 4.2.b) between 2050^{O}E and 1950^{O}E (grid) forms an essentially vertical feature, only horizontal movement along the shear zone will cause this irregularity to produce low-pressure zones. In plan view, it can be seen that dextral movement along Zone 4 will lead to a low-pressure zone within, or immediately to the west of, the linear strike irregularity (Fig. 4.7). This open space is designated **4S.**

-A better idea of the nature of dip irregularities, at the time of shearing, can be gained by accounting for movement along East-Quarry-type faults, and reconstructing dip contours accordingly (Fig. 4.8). The dip irregularities thus seen are better defined and are orientated such that both vertical and horizontal movements along the shear will lead to the formation of low-pressure zones. Both the dextral and reverse components of shearing along Zone 4 cause the formation of low pressure zones within the same regions (Fig. 4.8), here designated **4Da, 4Db** and **4Dc.**

Zone 5

-Although strike contours for Zone 5 (Fig. 4.3.b) show no conclusive pattern, contours for dip show a series of E-W trending footwall irregularities and less distinct vertical irregularities. The irregularities are also orientated such that both vertical and horizontal shearing will lead to the formation of low pressure zones. The low pressure zones caused by sinistral and normal shear movement are shown in figure 4.9 and have been designated **5Da, and 5Db.**

The significance of areas of low pressure, within Zones 4 and 5, will become apparent in the next section (Section 5), when such areas are compared to areas of high Sn and/or W grades.

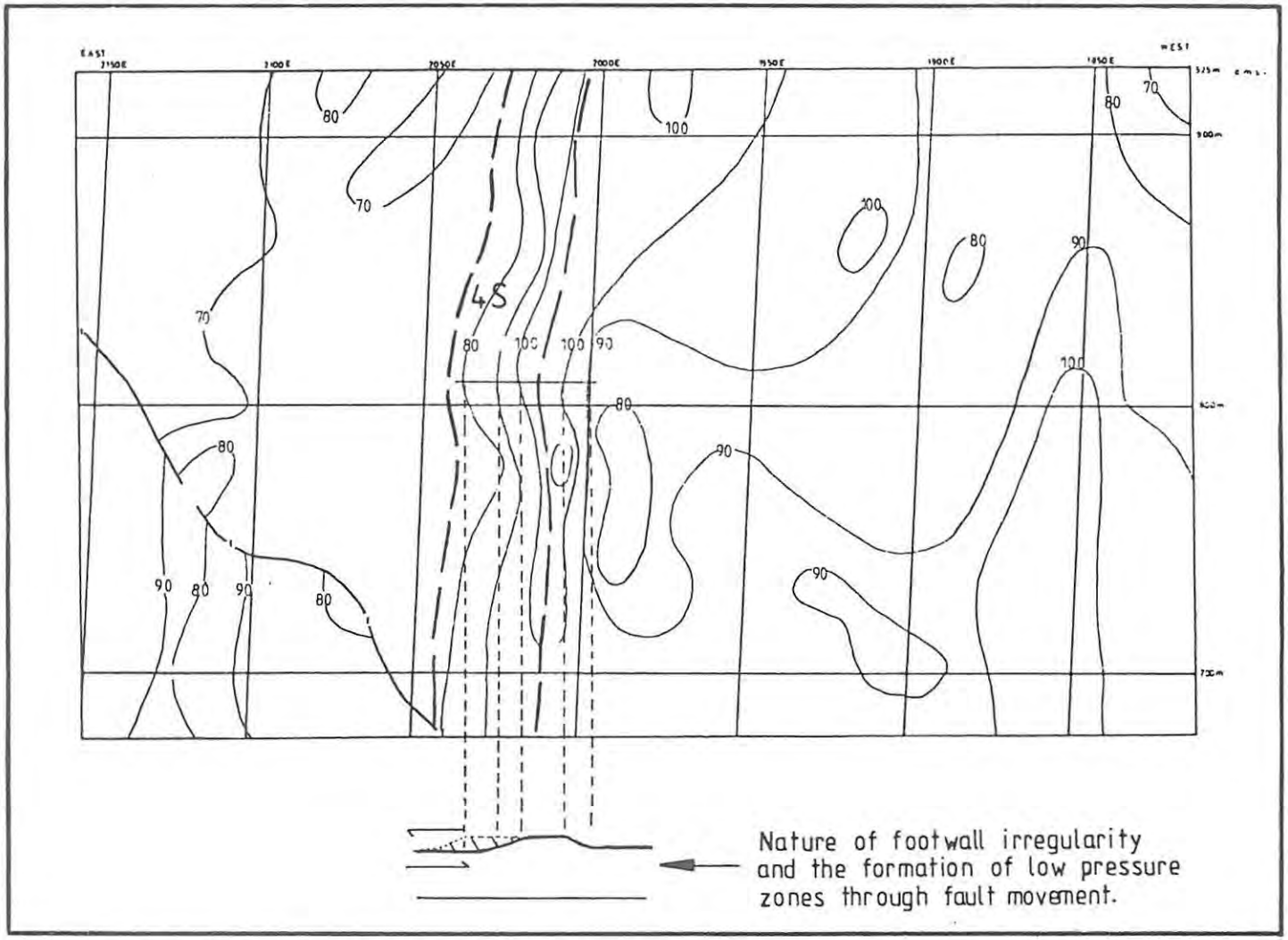

Figure 4.7. Longitudinal section of Zone 4 contoured for change in the strike of the footwall surface. Superimposed on these contours is the position of low-pressure zones (4S) caused by applying a dextral-reverse movement across the footwall surface.

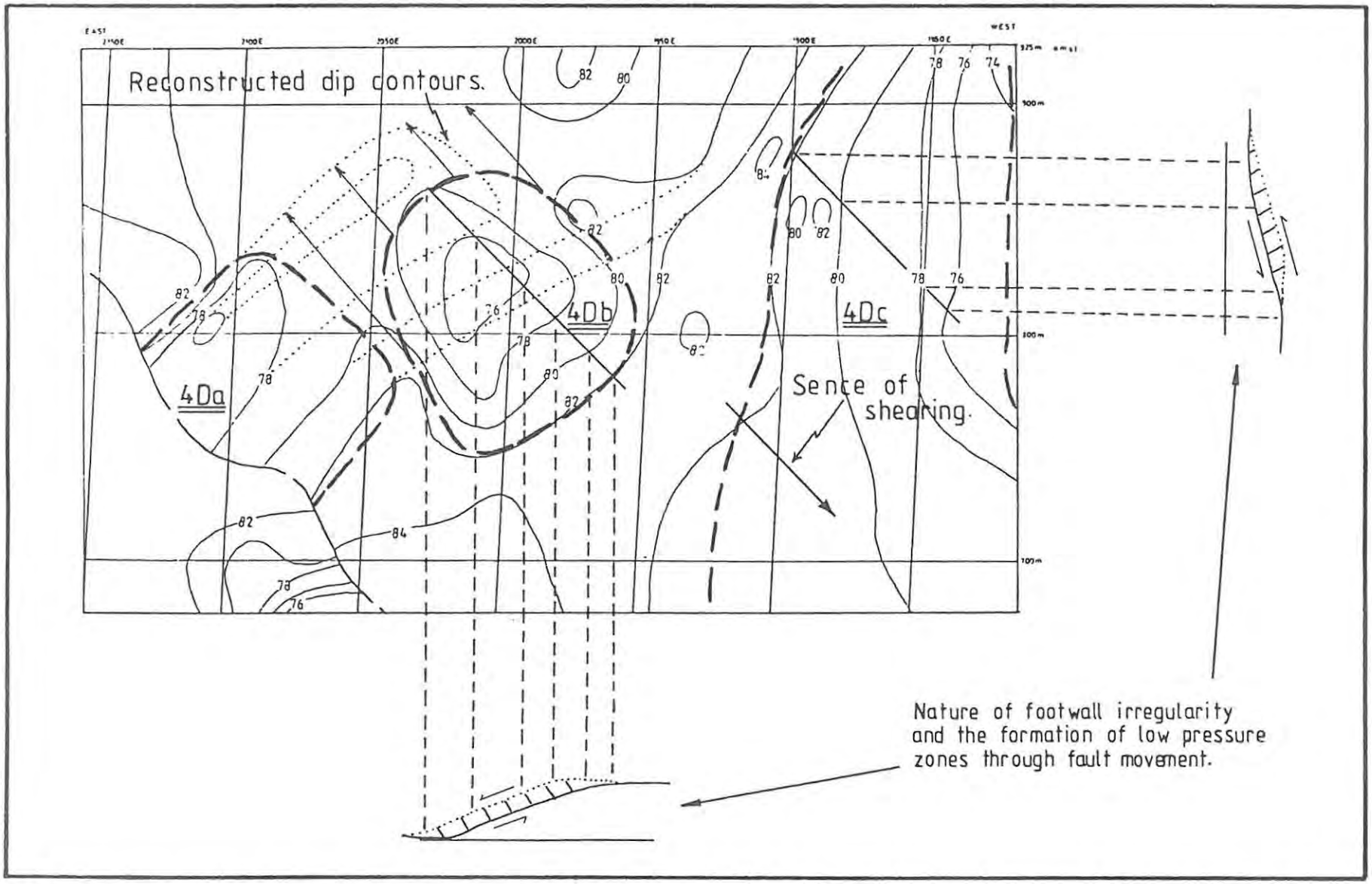

Figure 4.8. Longitudinal section of Zone 4 contoured for change in the dip of the footwall surface. Superimposed on these contours is the position of low-pressure zones (4Da, 4Db and 4Dc) caused by applying a dextral-reverse movement across the footwall surface.

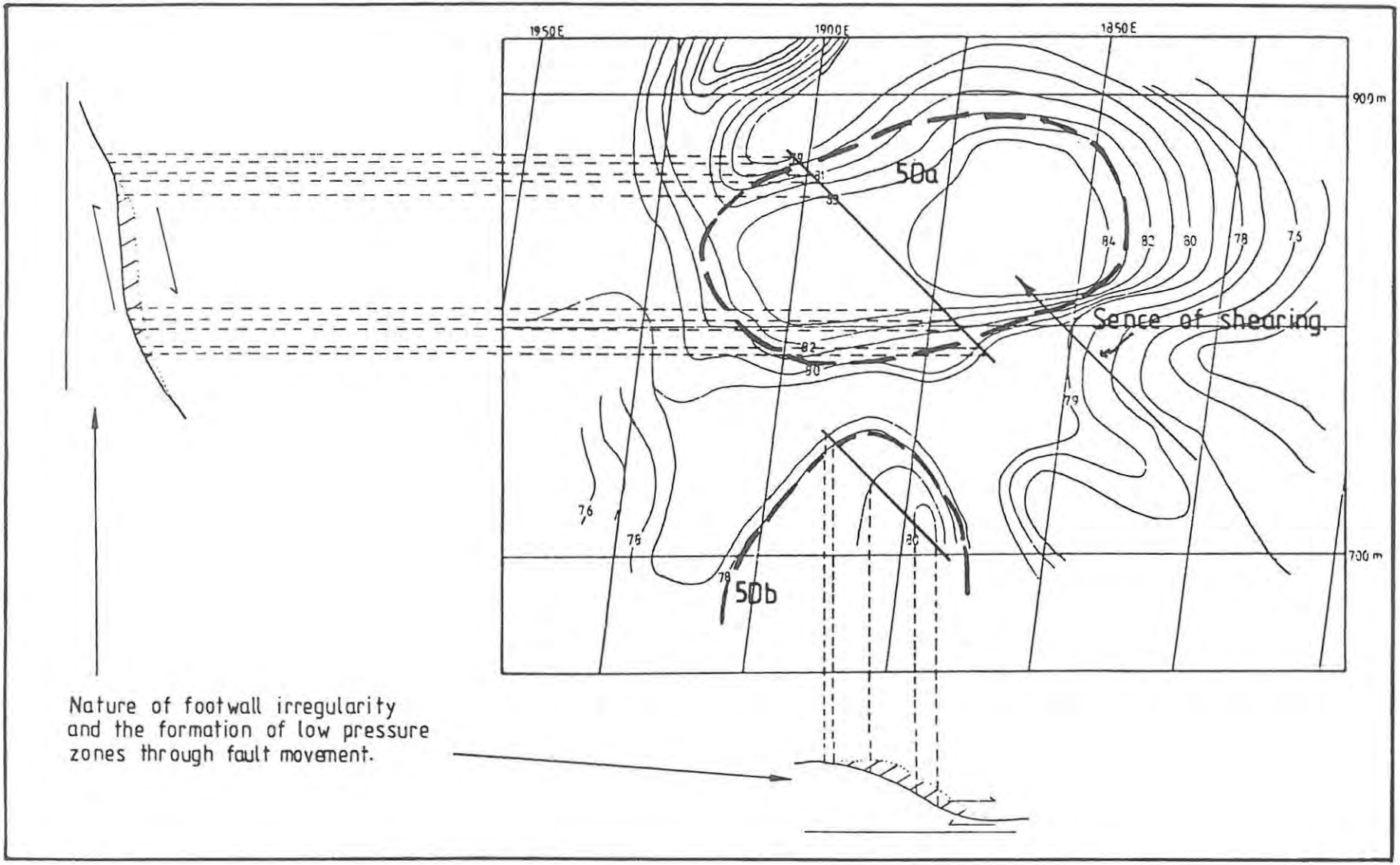

Figure 4.9. Longitudinal section of Zone 5 contoured for change in the dips of the footwall surface. Superimposed on these contours is the position of low-pressure zones (5Da and 5Db) caused by applying a sinistral-normal movement across the footwall surface.

5. STRUCTURAL CONTROLS ON THE DISTRIBUTION OF MINERALIZATION

5.1 Introduction

Longitudinal sections of Zones 4 and 5 were contoured for grades of Sn and W in order to investigate the distribution of mineralization. By comparing these distributions with longitudinal sections depicting host-lithology and structure of the veins, many important relationships become apparent.

5.2 Distribution of Sn

5.2.a Zone 4

The distribution of Sn within Zone 4 shows an excellent correlation with the position of low-pressure zones described in the previous section. Three major areas of high Sn concentrations are identified with Zone 4 and from east to west these correspond directly to low-pressure zones 4Da, 4Db and 4Dc (Fig. 5.1). Of these, 4Da hosts the largest and highest grade Sn concentration. Obviously, there is a strong structural control on the location of Sn-mineralization; the Sn-rich fluids preferentially permeated along zones of low-pressure that were created, upon shearing, by morphological irregularities within the vein. Within these zones of low-pressure, the initial deposition, and ultimate concentration, of Sn would depend mostly upon;

- the size of the low-pressure zone;
- the distance of the low-pressure zone from the feeder zone for the mineralizing fluids;
- the chemical environment within the low-pressure zone (ie. the host-lithology).

Low pressure zone 4Dc should contain the largest volume of low pressure space (Fig. 4.8), but corresponds to the smallest and lowest grade Sn anomaly. In the previous section it was suggested that the highly buckled and fractured contact area between the Pink Gneiss and Dark Gneiss probably offered the best pathway for the mineralizing fluids that entered Zone 4. It would then be expected that Sn-grades should decrease away from this

lithological contact area; 4Dc is the most distal anomaly and thus its low grades are not surprising.

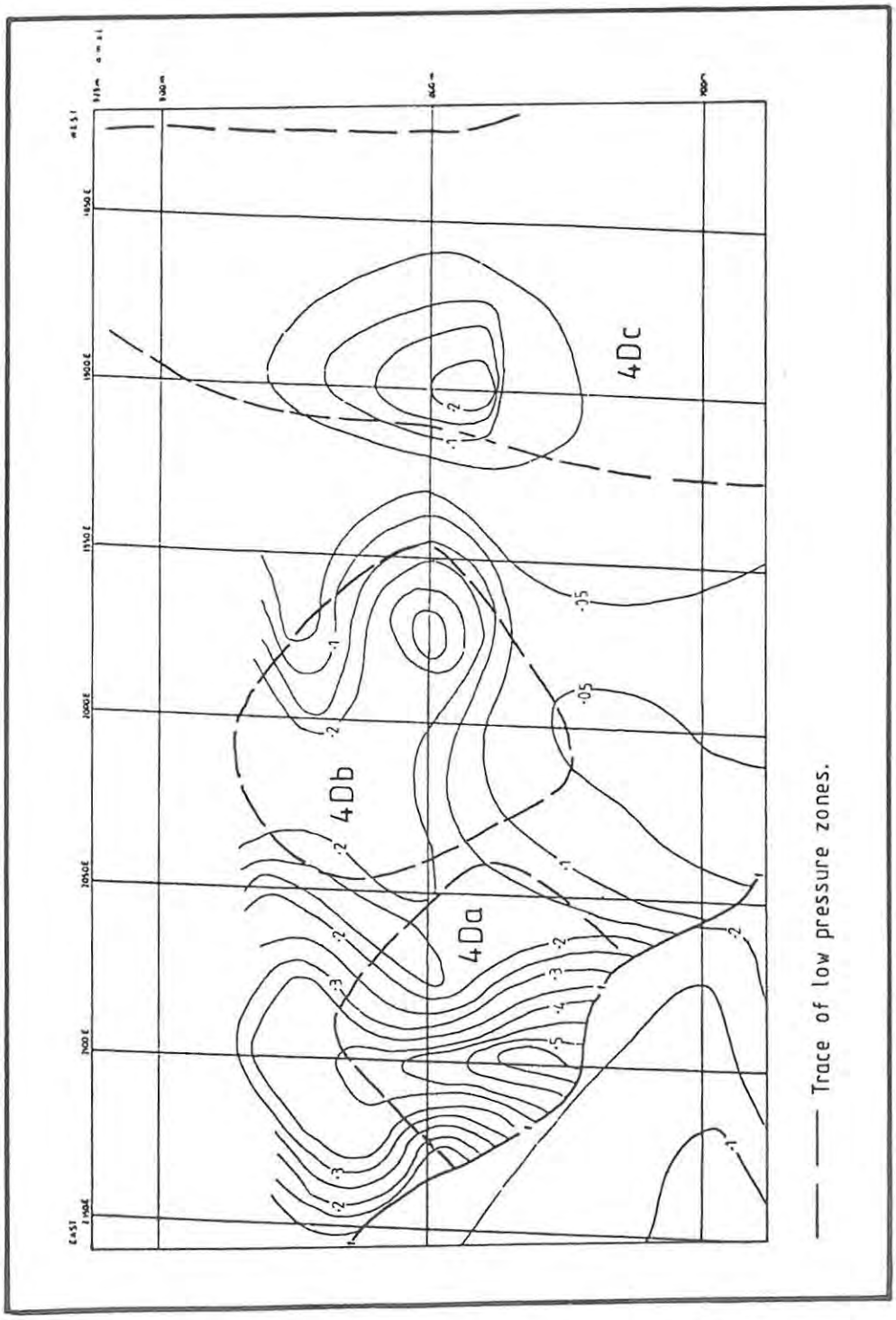

Figure 5.1. Longitudinal section of Zone 4 contoured for Sn-grade. Also shown are postulated zones of low-pressure.

An analysis of cassiterite grain sizes was carried out on numerous bore-hole intersections of Zone 4. Although results show a relatively simple distribution of cassiterite grains within Dark Gneiss-hosted regions, a distinct bimodal distribution is apparent for cassiterite grains within Pink Gneiss-hosted regions, (Fig. 5.2). These distributions suggest that whereas 4Db and 4Dc were subjected to only one phase of Sn-mineralization, 4Da was subjected to two such phases. The restriction of the second phase of Sn-mineralization to 4Da would explain why zone 4Da and 4Db can be situated at approximately equal distances from the inferred fluid feeder zone, and can have similar volumes of low-pressure space, yet differ so greatly in Sn-grade. The abovementioned restriction is probably a function of host-lithology; the chemistry of the Pink Gneiss (or its alteration product) being much more conducive to both phases of Sn-mineralization. Further evidence for a lighological control on the concentration of mineralization is presented in Sections 7 and 8.

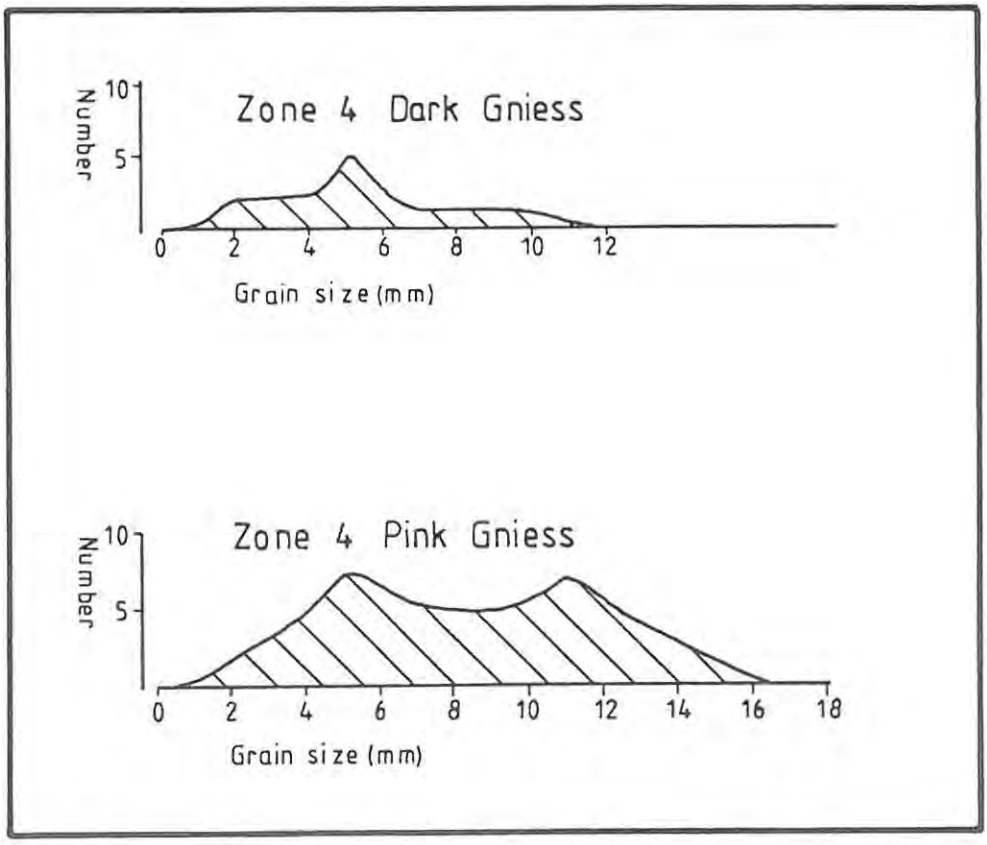

Figure 5.2. Frequency histograms of grain size measurements for cassiterite crystals within the Pink Gneiss and Dark Gneiss hosted areas of Zone 4. The histogram for grains within the Pink Gneiss hosted regions shows a second (and coarser) peak, implying that at least two phases of Sn-mineralization occurred within these regions.

Low pressure zone 4Da, and its corresponding Sn anomaly, are truncated by the East Quarry Fault. The continuation of 4Da cannot be located, however the sinistral reverse direction of displacement along the East Quarry Fault suggests that this continuation should occur beneath, and to the north of, 4Da.

5.2.b Zone 5

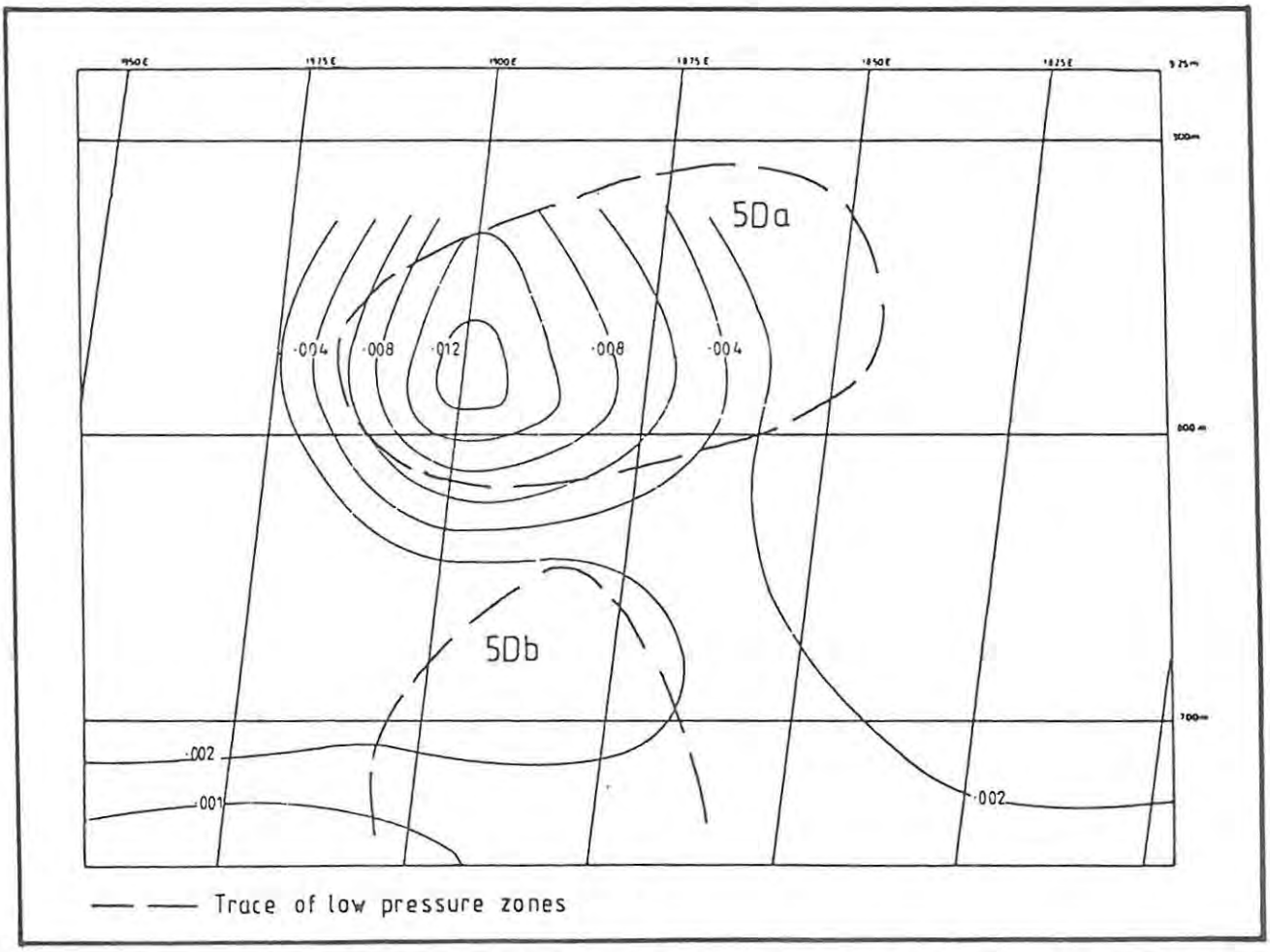

Figure 5.3. Longitudinal section of Zone 5, contoured for Sn-grade. Also shown are postulated zones of low-pressure.

Only one area of (albeit slight) Sn concentration is found within Zone 5 (Fig. 5.3) and is seen to correspond quite closely to the low pressure zone 5Da. This region also shows a good correlation with the area of greatest zone thickness (c.f. Figs. 5.3 and 4.3.d), and lies entirely within the Dark Gneiss. Unlike Sn-concentrations within Zone 4, no significant concentration of Sn occurs within the Pink Gneiss hosted areas of Zone 5. The Sn anomaly corresponding to 5Da is probably of the same origin as those corresponding to 4Db and 4Dc (low-grade anomalies also hosted within Dark Gneiss); the low grade of the Pink Gneiss hosted areas implies that only one Sn-mineralizing event affected Zone 5.

5.3 Distribution of W

5.3.a Zone 4

Two large areas of anomalous W values occur within Zone 4 (Fig. 5.4) and closely correspond to the Pink Gneiss-Dark Gneiss contact area; the inferred feeder zone for mineralizing fluids (c.f. Figs. 5.4 and 3.3). Away from this region, W concentrations decrease rapidly.

A relationship between Sn and W mineralization thus exists whereby mineralizing fluids permeated through the main fluid feeder zone, depositing W, before dispersing further into the country rocks and depositing Sn within (firstly) structurally and (later) chemically suitable sites. A similar phenomonon is common in many quartz vein - greisen deposits. For example, in describing the New Brunswick and Mount Pleasant deposits in Canada, Mulligan (1983) observed that W mineralization was confined to central quartz veins, surrounded by more disseminated, greisen bound, Sn and sulphide mineralization. Reasons for such element distribution are presented in Section 8.3.c.

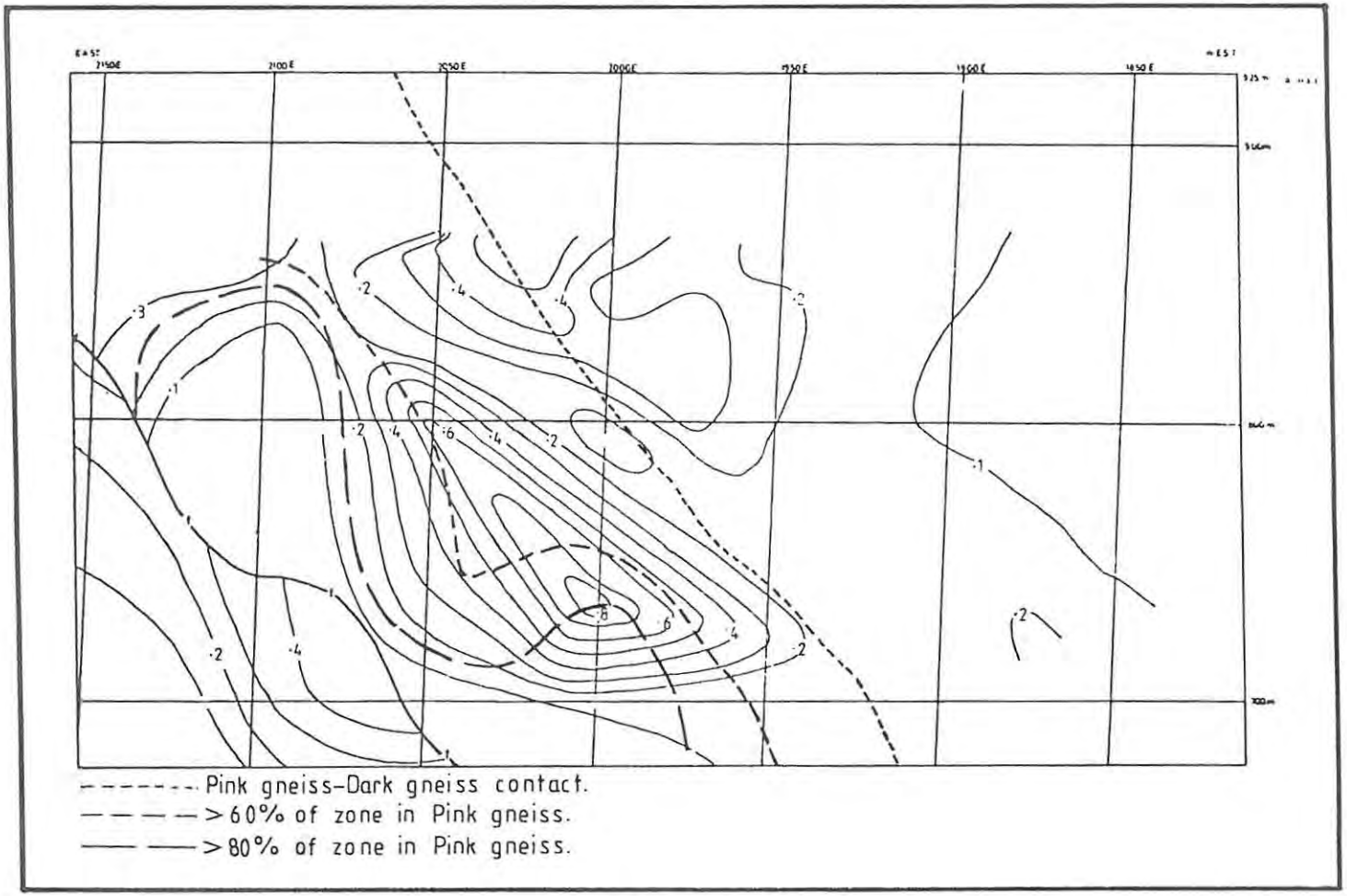

Figure 5.4. Longitudinal section of Zone 4, contoured for W-grade. Also shown is the intersection zone between the Pink Gneiss and the Dark Gneiss. The intersection zone was probably a major pathway for the mineralizing hydrothermal fluid.

5.3.d Zone 5

Although a close correspondence is seen between W concentrations and open space zones 5Da and 5Db, the highest W grades occur within the eastern portion of Zone 5, spatially associated with the area where Zone 4 and Zone 5 intersect (Fig. 5.5). Within Zone 4, high W grades are also associated with this intersection, which probably represents the point where mineralizing fluids entered Zone 5 (and possibly also Zone 4). Therefore, although 5Da and 5Db offered good structural traps for mineralization, W-mineralization was (again) mostly concentrated around the feeder zone, with W/Sn ratios generally decreasing outwards.

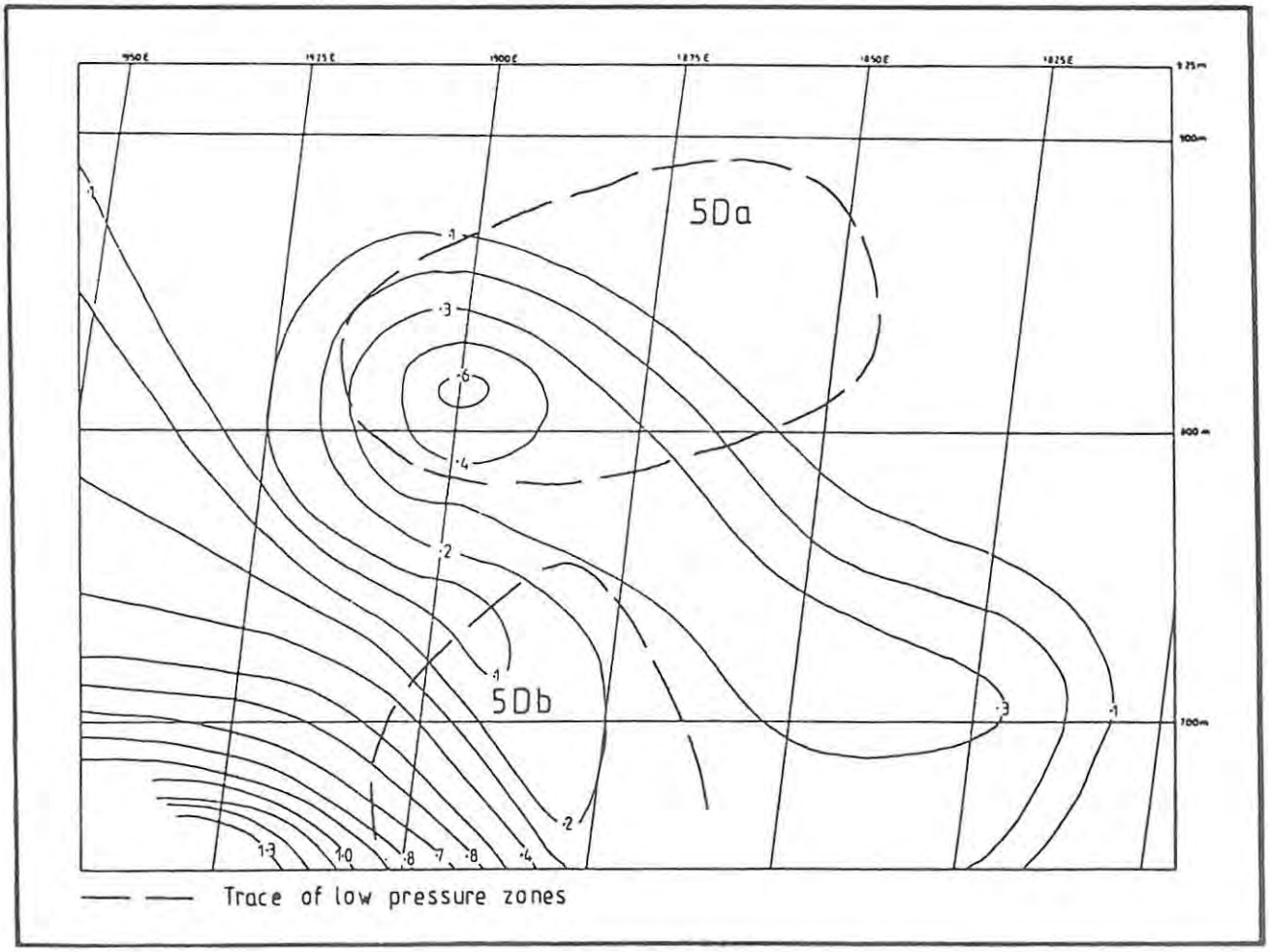

Figure 5.5. Longitudinal section of Zone 5, contoured for W-grade. Also shown are the postulated zones of low-pressure.

5.4 Distribution of other ore-elements

Longitudinal sections were not contoured for Cu or Mo, the only 'accessory' elements notably concentrated within Zones 4 and 5. Thus the relationship of these elements to structure and lithology cannot be assessed here. However, within both Zones 4 and 5 the concentrations of Cu and Mo never exceeds 0.16 wt% and 0.24 wt% respectively and averages around 0.01 wt % and 0.02 wt% respectively. The Van Rooi's Vley deposit does not show the high concentrations of elements such as As, Pb and Zn, which are associated with some Sn/W deposits.

The variation of Sn, W, Cu and Mo, across veins, was studied from numerous bore-hole intersections. Although many detailed variations exist, a general pattern (Fig. 5.6) is apparent and is independent of host lithology. High concentrations of Cu and Mo were commonly found to surround areas with high W/Sn ratios, and commonly coincide with areas of low W/Sn ratios. This relationship is to be expected, given that the areas with highest W/Sn ratios probably represent localized feeder zones. Tin and sulphides (chalcopyrite and molybdenite) would be enriched in the altered zones surrounding such feeders.

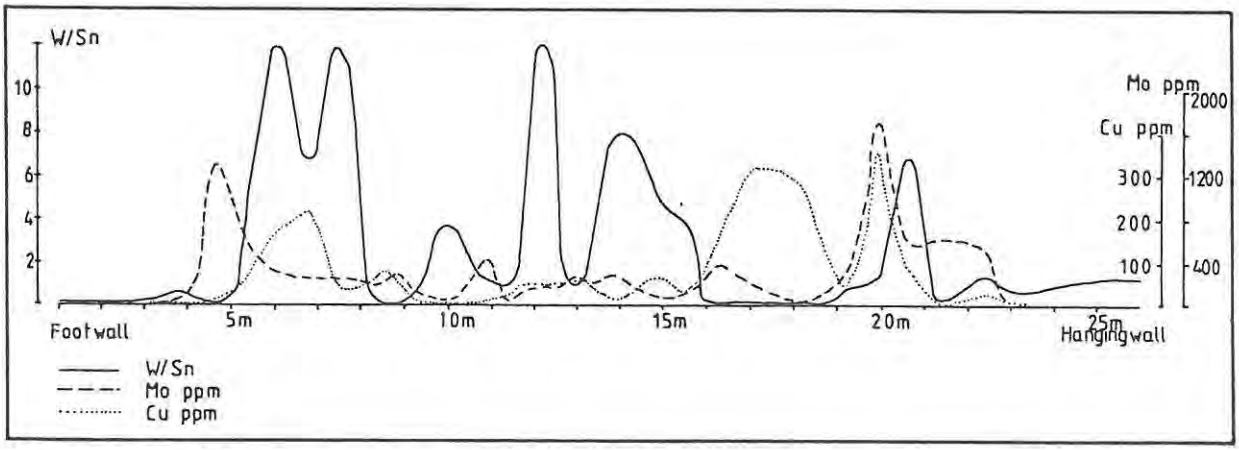

Figure 5.6. Hypothetical cross-section through a 'typical' vein zone, showing the distribution of the elements W, Sn, Mo and Cu. Areas of high Mo and Cu (both as sulphide minerals) are seen to envelope areas with high W/Sn ratios. This relationship is probably a result of changing temperatures of deposition (see text) and is apparently independant of host-lithology.

5.5 Conclusions

Structure has strongly controlled the location of mineralization at Van Rooi's Vley. However, the actual concentration of Sn and W, within structural sites, is a function of the prevaling phyicochemical environment, and is addressed in Section 8.

6. ORE MINERALOGY

6.1 Introduction

Scheelite, wolframite and cassiterite are the economically interesting ore minerals within the Van Rooi's Vley deposit. In addition, magnetite, pyrite and hematite are also common constituents of the ore assemblage, and molybdenite, sphalerite and chalcopyrite occur in minor to accessory amounts. The paragenesis of the ore minerals is outlined in table 6.1, and in table 7.1 it is directly compared to the paragenesis of alteration minerals. As can be seen from these tables, mineralization was prolonged and multi-staged, and consequently, many ore minerals are alterations of earlier ore phases.

TABLE 6.1
PARAGENESIS OF ORE MINERALS

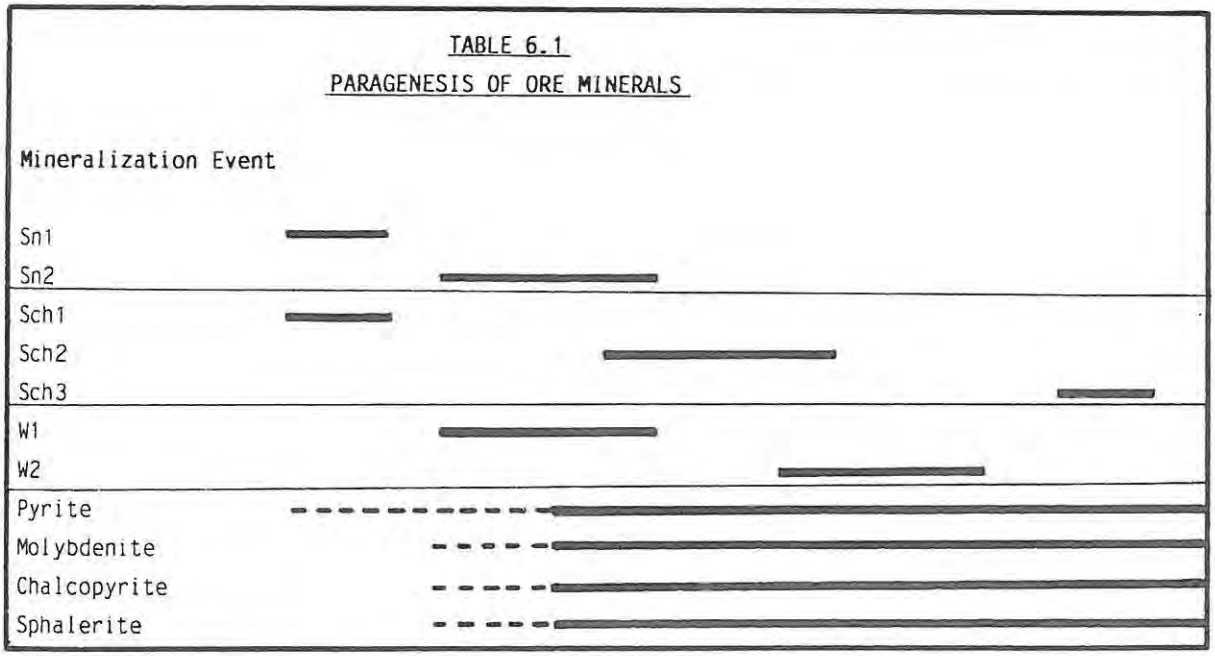

6.2. Cassiterite

As suggested in Section 5.2.a, at least two generations of Sn-mineralization occurred at Van Rooi's Vley. The early generation (Sn1) is the earliest mineralization event recognized and typically forms small anhedral to subhedral grains that average around 5mm in diameter (see Fig. 5.2). Sn1

is associated with an early phase of tourmalinization (Plate 6.1). The cassiterite crystals are most abundant within the tourmalinized selvage to the mineralized quartz-veins and are commonly brecciated by subsequent alteration events. Sn1 is the least important Sn-mineralizing event and its distribution is apparently independent of host lithology.

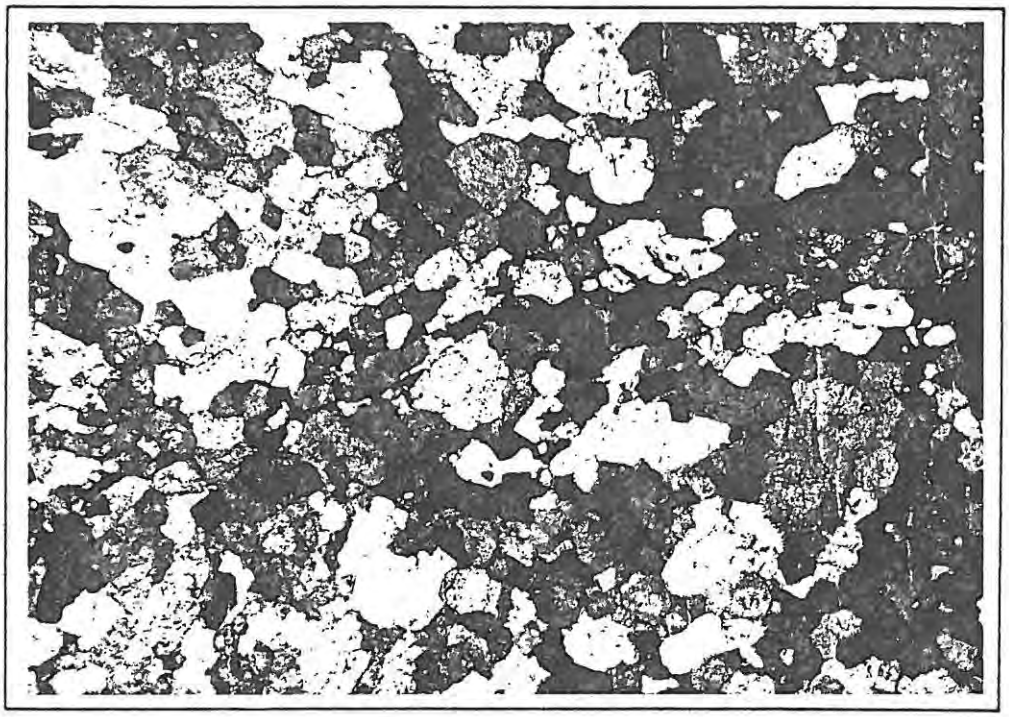

Plate 6.1. Cassiterite(ct) associated with an early stage of tourmalinization (T1-see Section 7). The Cassiterite is spatially associated with (but pre-dates) minor magnetite (black). (VR71, PPL, X20).

Cassiterite deposited during Sn2, the major Sn-mineralizing event, is subhedral to euhedral, with an average crystal size of around 11mm. Sn2 accompanied, or immediately post-dated, the deposition of tourmaline (green-brown and green-blue), magnetite, chlorite and (minor) pyrite (Table 7.1), all of which form inclusions within, or include, Sn2 cassiterite. Minor sericitic alteration of feldspars also occurs adjacent to cassiterite. Sn2 occurred within, or immediately adjacent to, Pink Gneiss hosted mineralized veins.

6.3 Scheelite

At least three generations of scheelite occur at Van Rooi's Vley. The first generation (Sch1) is the only wholly primary generation of scheelite, and forms either subhedral grains that average around 1.5cm in diameter, or clusters of smaller grains. These grains are predominantly found within the early tourmaline-rich selvages to the mineralized quartz-veins, sometimes in association with Sn1 cassiterite. The scheelite encloses the latter, and also "green-brown" tourmaline and pethite, and thus closely post-dates Sn1. Sch1 scheelite is always partially replaced by wolframite and fluorite (Plate 6.2), reflecting later Fe-rich and F-rich conditions.

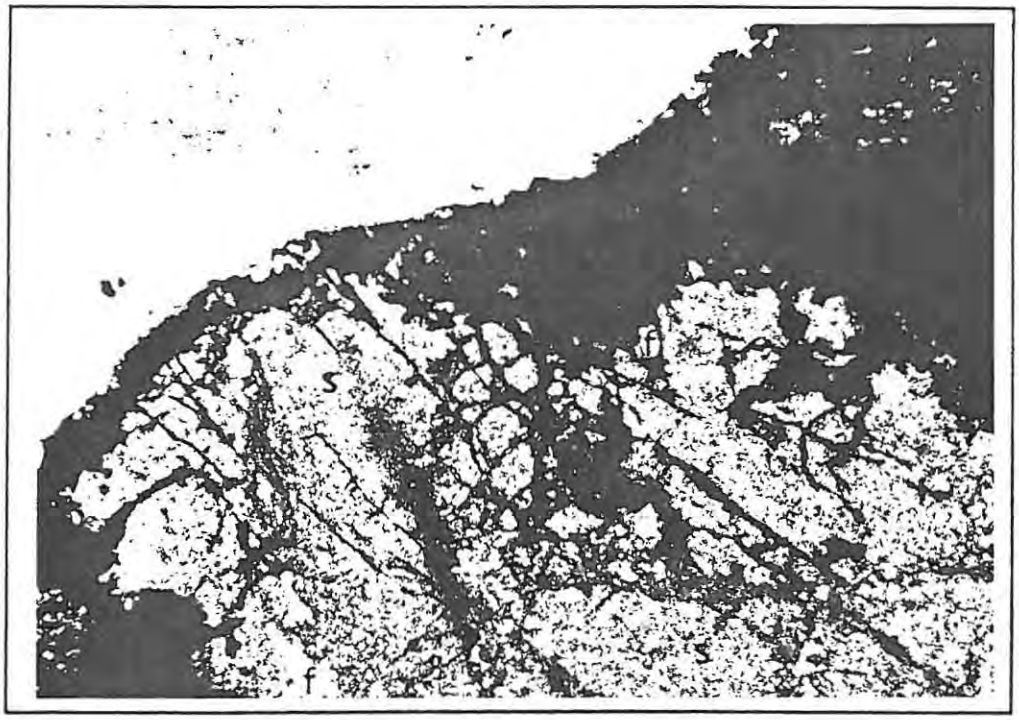

Plate 6.2. Photomicrograph showing wolframite (black) replacing scheelite(s). The wolframite (W2) forms rims around, and microfractures through, the scheelite (Sch1). This replacement reaction is always accompanied by the formation of fluorite(f) (VR55, PPL X20).

Second generation scheelite (Sch2) is dominantly primary and is probably the major generation of scheelite mineralization. Sch2 was deposited prior to a period of intense fluoritization (Table 7.1) and is enclosed by either fluorite or quartz. The scheelite grains never exceed 1.5mm in diameter but sometimes form into scheelite-fluorite clusters up to 1cm in diameter (Plate 6.3). All Sch2 grains are anhedral and have undergone extensive dissolution along their edges, presumably under conditions of high a_F (see Section 8.4.a). Where Fe-rich minerals (eg. magnetite) are also present, Sch2 scheelite undergoes extensive alteration to wolframite.

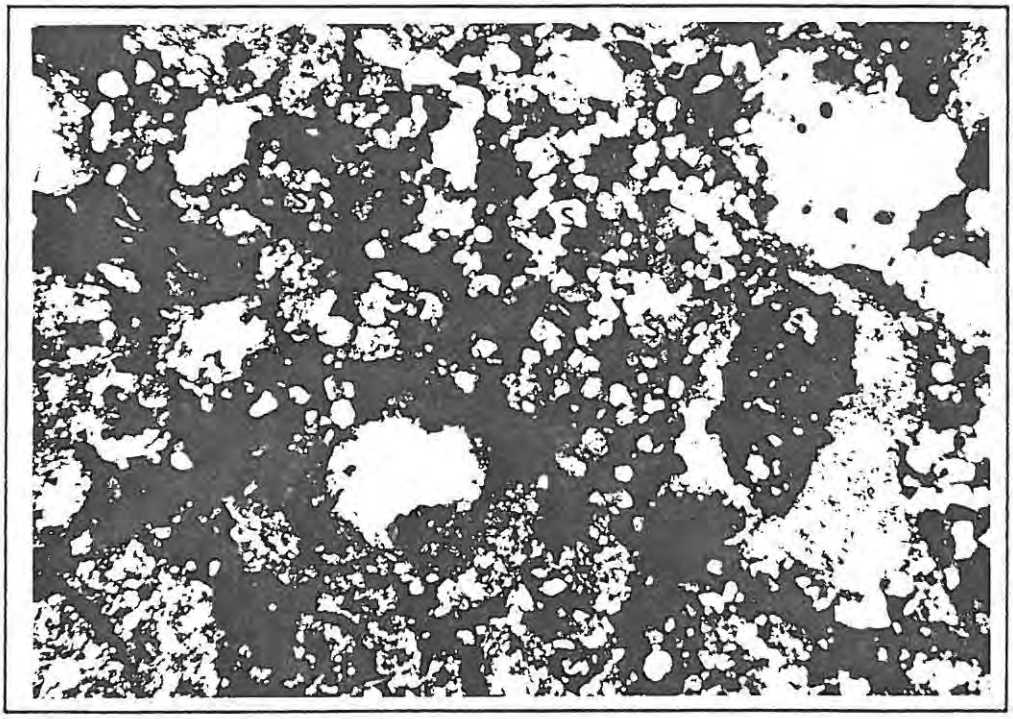

Plate 6.3. Photomicrograph showing scheelite(s)+ fluorite (black) clusters, formed by the alteration of scheelite (Sch2) during an intense period of fluoritization. Individual scheelite grains are highly rounded as a result of dissolution (VR20, XP, X20).

The last generation of scheelite (Sch3) occurs very late in the paragenetic sequence (Table 6.1) and is a quantitatively insignificant. Sch3 scheelite occurs in microfractures within, or (rarely) as veins around, wolframite and results entirely from the alteration of the latter.

6.4 Wolframite

Only two generations of wolframite are identified at Van Rooi's Vley. The first, and major, generation (**W1**) results in the primary deposition of subhedral to euhedral wolframite crystals, up to 3.5cm in size. These crystals may contain inclusions of tourmaline ("green-brown" and "green-blue") magnetite, pyrite and chlorite, indicating that W1 probably occurred during, and slightly outlived, Sn2 (Tables 6.1 and 7.1). However, no contact relationships between W1 wolframite and Sn2 cassiterite were seen, although this may simply reflect a slight spatial separation of the two minerals (noted in Section 5.3a), caused by slightly different requirements for deposition. Alteration of W1 wolframite to scheelite (Sch3) is never extensive, because Sch3 was only a minor mineralizing event.

The second generation of wolframite mineralization (**W2**) occurred after Sch2 (Table 6.1) and results from the alteration of both Sch1 and Sch2 scheelite grains. Fluorite always accompanies wolframite (Plate 6.2 - Table 7.1).

6.5 Fe-oxides

Concentrations of Fe-oxides occur in the form of magnetite and hematite. The latter mineral forms as a late stage replacement of magnetite and pyrite. Because of the abundance of these two oxides, they are considered within the following section, dealing with wall-rock alteration.

6.6 Sulphides

Pyrite greatly dominates the sulphide mineralogy and sometimes forms a major ore constituent. At least four generations can be identified although it is probable that pyrite was more or less continuously deposited throughout most stages of mineralization. Abundant pyrite is commonly associated with chloritic alteration events. Magnetite, deposited during the early mineralizing stages (Table 7.1) may be partially to completely altered to pyrite, which, in turn, may be partially to completely altered to hematite, during the final stages of mineralization.

Molybdenite is widespread, but only in minor amounts. It is sometimes accompanied by the rarer sulphides, **chalcopyrite** and **sphalerite**, and apparently was deposited throughout many stages of mineralization, and in numerous settings, eg;

1) as inclusions within quartz, fluorite, chlorite or pyrite ;
2) as partial rims to chlorite or pyrite ;
3) as late cross cutting micro veins.

7. WALL ROCK ALTERATION

7.1 Introduction

Pronounced wall rock alterations are associated with the mineralized veins at Van Rooi's Vley. Tourmalinization, silicification, potassic alteration and chloritization are the dominant alteration types although the nature and intensity of these alterations may differ slightly, depending on the nature of the host rock (ie. either Pink Gneiss or Dark Gneiss).

Table 7.1 outlines the paragenesis of alteration minerals found at Van Rooi's Vley whilst figure 7.1 presents an idealized section of the typically 'telescoped' veins. Silicification and the deposition of vein quartz has been omitted from table 7.1 because of the continuous nature of that alteration. The greatest amount of quartz deposition was, however, related to the main mineralizing stage (A2).

It should be noted that the actual sequence of alteration events is much more complex than is indicated in table 7.1. For example, not only does potassic alteration occur in three main events, readily apparent throughout the deposit, but it is also encountered as local potassic fronts, enveloping alteration types that result from the destruction of K-bearing minerals (eg. chloritization and tourmalinization). Furthermore, each potassic front is, in turn, enveloped by localized areas of sericitic alteration and chloritic alteration. This sequence (potassic-sericitic-chloritic) is commonly associated with Sn/W deposits (eg. see Taylor 1979 and Pollard et al., 1983) and in broad terms results from a progressive increase in the H^+/K^+ ratio of the altering fluids. Further complications to the alteration paragenesis arise from the fact that mineral deposition was prolonged and intense; as a result the preservation potential of early alteration types was low.

For the purpose of this study three alteration zones are recognized, viz;

- the **vein-zone**, including the mineralized veins (ie. gangue minerals)
- the **vein-margin zone**; a distinct selvage to the mineralized veins that results, at least in part, from the telescoping effect of successive alteration/mineralization events. Alteration within this zone, and

TABLE 7.1

PARAGENESIS OF ALTERATION MINERALS

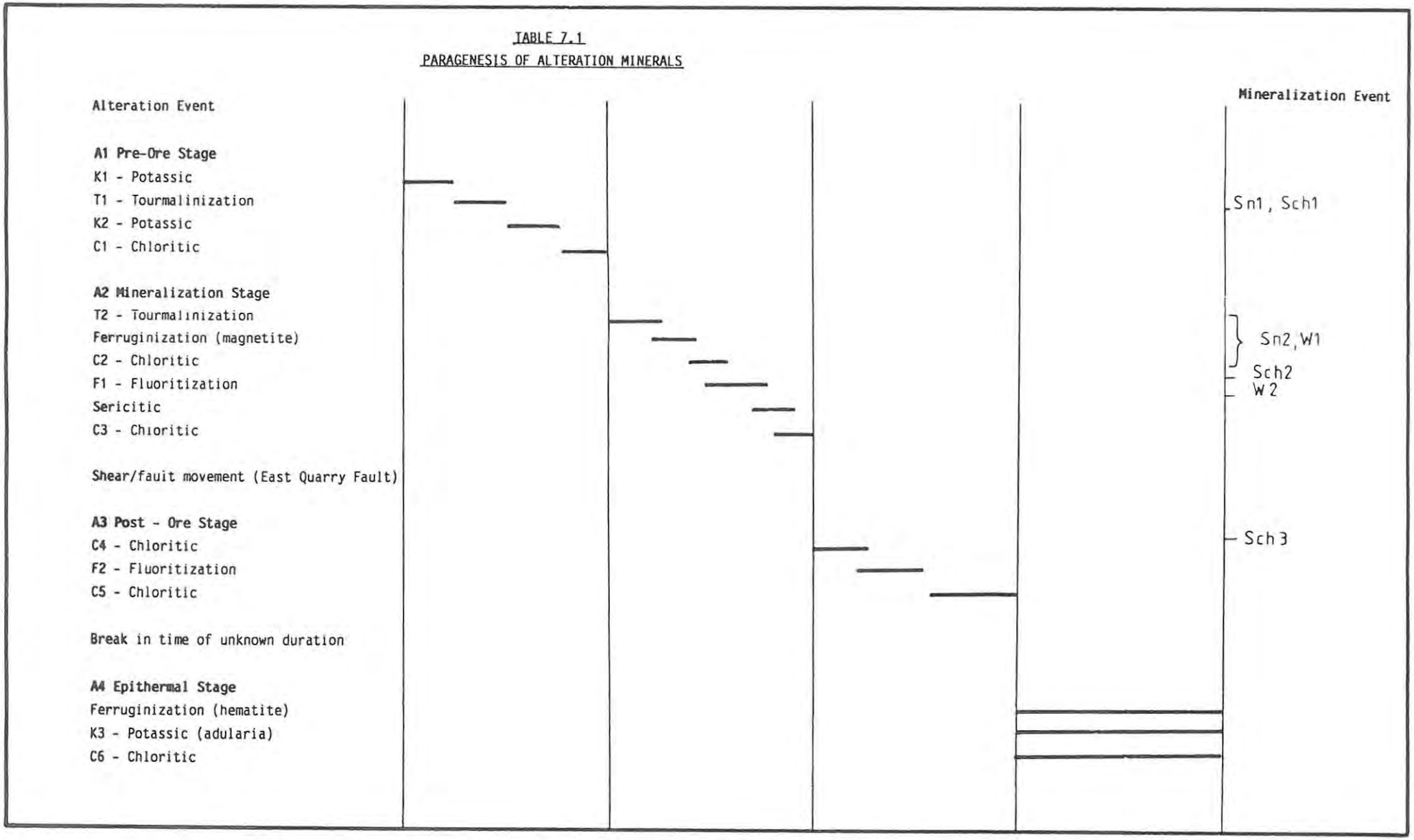

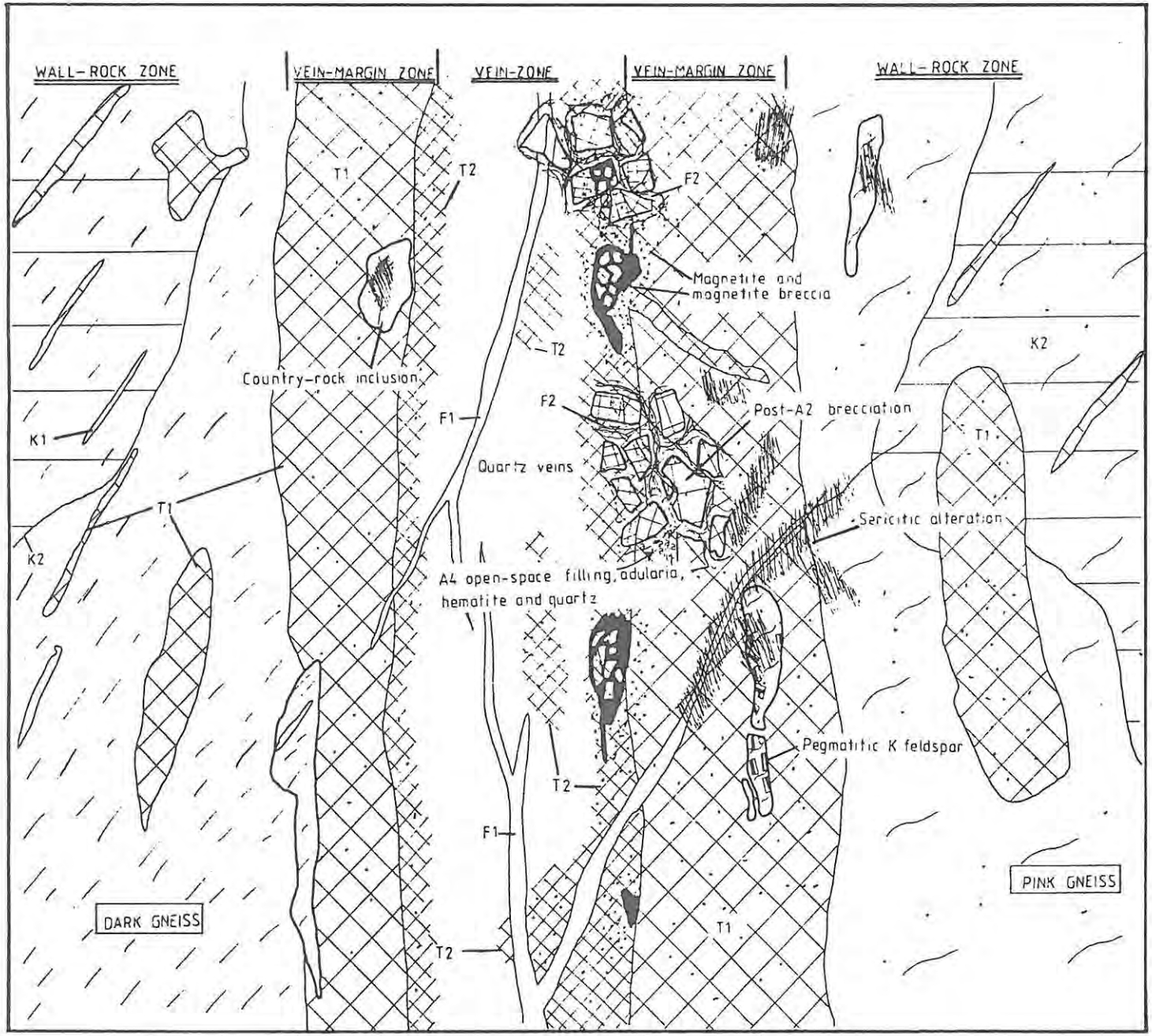

Figure 7.1. Schematic section through a 'typical' vein-zone and surrounding areas of extensive alteration. The diagram is drawn such that the right hand side represents events, and alterations, typical of Pink Gneiss hosted veins, whereas the left hand side of the diagram represents alterations typical of Dark Gneiss hosted veins. By necessity, this figure is highly simplistic (many alterations have been omitted) and must be considered in conjunction with the text.

within the vein zone, may commonly be complete.

- the **wall-rock zone**; an area of fracture-controlled to pervasive alteration of a still recognizable protolith. This zone surrounds the vein-margin zone and extends for up to 30m into the country rock.

Four main stages of alteration can be identified, vis; a **pre-ore stage (A1)**, a **mineralization stage (A2)**, a **post-ore stage (A3)** and an **epithermal stage (A4)**.

The original mineralogy of the high-grade gneissic country rocks, and the distribution of these rock types with respect to mineralized Zones 4 and 5 was discussed in Section 3.

7.2 Pre-Ore Stage (A1)

Potassic metasomatism (K1) is the earliest alteration event recognized within the deposit and is best identified within Dark Gneiss hosts. This alteration is distinguished from potassic-pegmatitic segregations of metamorphic origin (eg. see Plate 3.3) by both the cross-cutting relationships to the latter and by the more pervasive nature of K1.

Within the Dark Gneiss, K1 appears as a distinct pink colouration, paralleling foliation, with occasional K-feldspar veinlets cross-cutting this foliation. Perthitic feldspar $\pm$ biotite (brown-green) are the main alteration minerals and form at the expense of original feldspars (K-feldspar and plagioclase) and original biotite (brown).

The effects of K1 are not readily apparent within the Pink Gneiss, probably due to the alkaline nature of that rock type. The formation of low temperature alkali-feldspars (perthite and microcline) is possibly a result, in part, of K1, but more likely relates to a later period of potassic alteration (K2).

Primary tourmaline was only identified within the Dark Gneiss and never exceeded accessory proportions. It is a light green to brown Fe tourmaline (schorl) and is optically identical to tourmaline deposited during the first period of **tourmalinization (T1)**. As seen on figure 7.1, T1 is most intense

within the vein-margin zone, where a tourmaline-quartz ± feldspar assemblage forms a distinct selvage around the vein-zone. Where identified within the inner vein-margin zone or within the vein-zone, T1 tourmaline is commonly altered and brecciated by subsequent alteration events.

Magnetite is also associated with T1 assemblage, but rarely exceeds 5% of the mode, and minor Sn-mineralization may also occur (Sn1 - Plate 6.1). This magnetite was probably originally within, or remobilized from, the altered Pink Gneiss or Dark Gneiss host. In addition, T1 assemblages that developed within the Dark Gneiss may also contain accessory spinel (hercynite or gahnite) and garnet, both of which are original constituents of the host rock.

Within the wall-rock zone, T1 commonly produces discontinuous to continous tourmaline-rich layers that parallel the gneissic foliation of the host. Tourmaline-rich microfractures cross-cut this foliation. Tourmaline-quartz veins, up to 1m thick, also cross-cut the gneissic foliation of the wall-rock zone, carry minor mineralization (mostly Sn), and possibly reflect fluid permeation along small shears peripheral to the main shear zones.

Intense **potassic metasomatism (K2)** follows T1, often causing substantial alteration of the feldspar-rich Pink Gneiss and producing a medium-grained perthite - microcline - quartz - biotite assemblage. Turbid feldspars (ie. K-feldspar with submicroscopic hematite inclusions) are characteristic and cause a distinct reddening of the Pink Gneiss. Moderately fresh K2 feldspars are observed within the wall-rock zone, particularly within the Pink Gneiss, where cross-cutting relationships with the products of T1 are common (Plate 7.1).

Within the vein-zone and the vein-margin zone, biotite (original and K2) is chloritized and the feldspars (original, K1 and K2) have variously been chloritized and sericitized. This **chloritic alteration (C1)** may also alter tourmaline (T1) and ferromagnesian phases within the Dark Gneiss (ie. garnet, cordierite), and is the last recognizable event of the pre-ore stage.

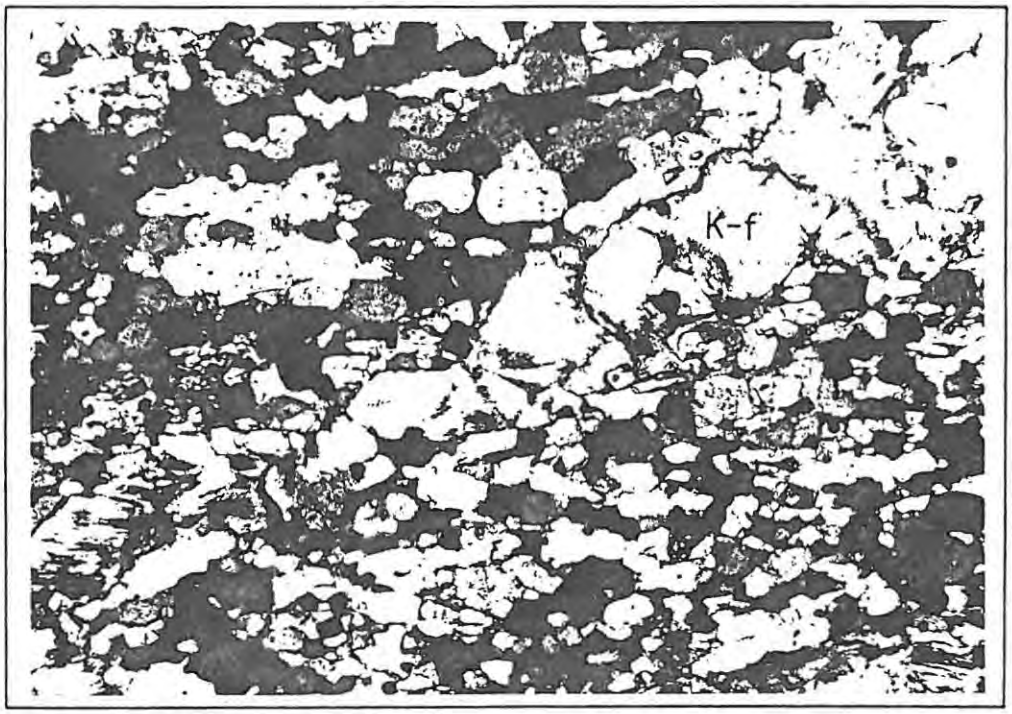

Plate 7.1. Photomicrograph showing a T1 tourmaline assembiage (light green-brown), cross cut by a K-feldspar vein (K-f), related to the K2 period of potassic metasomatism. The photomicrograph was taken of a sample (VRD11) collected from within the wall-rock zone of a Pink Gneiss hosted vein (Zone 4). (PPL ,X20).

7.3 Mineralization Stage (A2)

The mineralization stage (A2) was the most intense stage of alteration associated with the Van Rooi's Vley deposit and resulted in extensive mineralogical changes to both the original rock constituents and to assemblages produced during A1. The majority of the W/Sn mineralization was deposited in the early to middle periods of A2, during, or associated with, extensive tourmalinization (T2), ferruginization (magnetite), chloritization (C2) and fluoritization (F1). As noted in Section 3.1.c, many of these alterations are best developed within, or immediately adjacent to, the Pink Gneiss hosted regions of Zone 4 (in particular) and Zone 5. Fluid flow to, or effect upon, the Dark Gneiss hosted regions may therefore have decreased

during A2.

Intense **tourmalinization (T2)** is the first recognized event of A2. T2 tourmaline also has the composition of schorl (see Section 10) but is deep green to blue in colour, in contrast to the green to brown tourmalines of T1 (cf. Plates 7.1, 7.2 and 7.3). Where the two generations of tourmaline are seen together, T1 forms a finer grained selvage to veins comprised of coarse-grained (2-3mm), and commonly more euhedral, T2 (Plate 7.3). T2 is particularly well represented within the inner vein-margin zone and the vein-zone. Here, assemblages mineralogically similar to those formed during T1, are encountered, commonly forming a thick (up to 0.5m) selvage to well mineralized quartz, quartz-fluorite or quartz-fluorite-feldspar veins, and are often mineralized themselves.

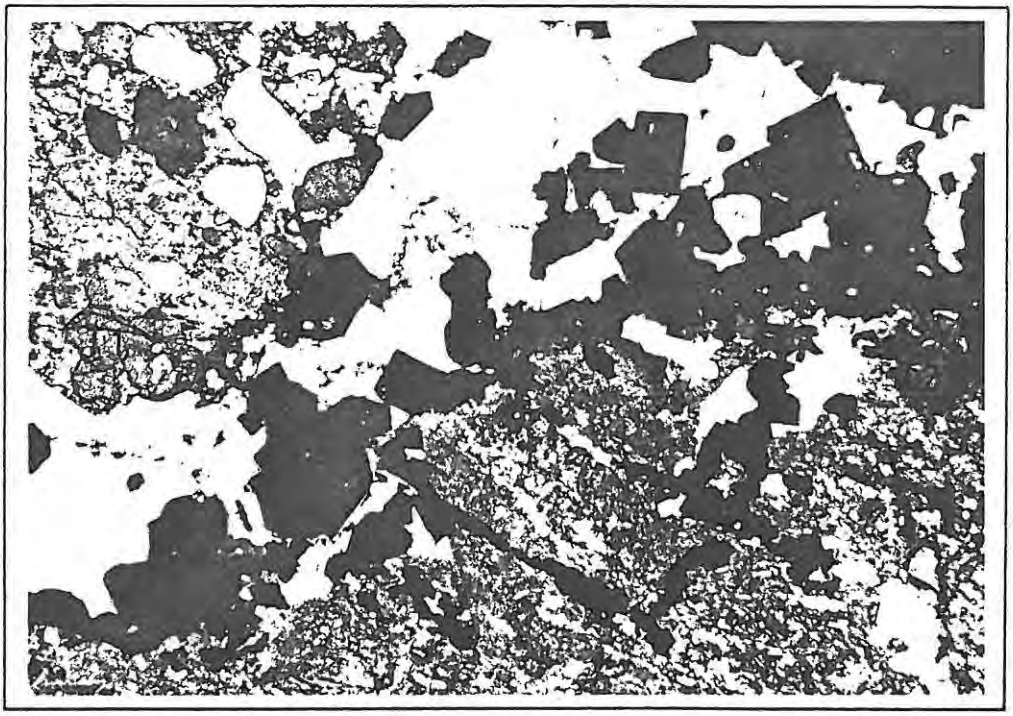

Plate 7.2. Photomicrograph taken to show the contrast in colour between tourmaline related to T1(T1) and tourmaline related to T2(T2) (VRD131, PPL, X20).

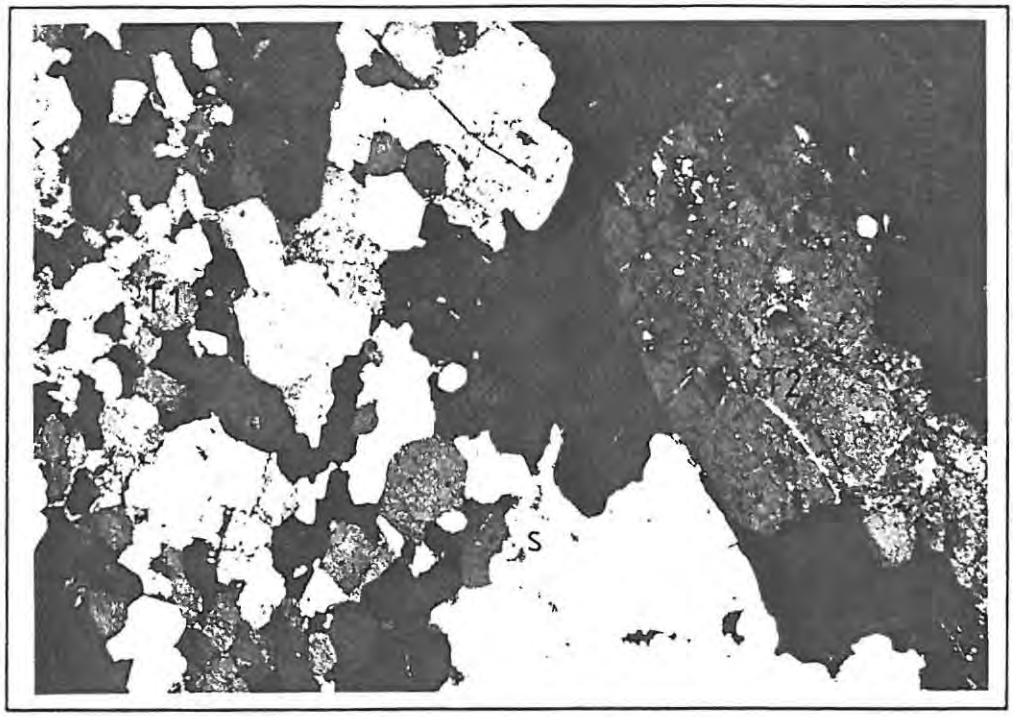

Plate 7.3. Photomicrograph taken to show the characteristically coarser-grained, and slightly more euhedral, nature of T2 tourmalines (T2), compared to T1 tourmalines (T1). This photomicrograph shows a fine-grained T1 selvage to a vein consisting of T2 tourmaline and fluorite (black). The sericitic alteration(s) follows the F2 period of fluoritization and is seen here to be altering T2 tourmalines (in particular). (VRD87, XP, X20).

Ferruginization (magnetite) follows T2. Magnetite veining within the Pink Gneiss (Plate 7.4) commonly increases in intensity from the inner wall-rock zone into the inner vein-margin zone and the vein-zone, where T2 assemblages locally become highly brecciated and replaced by magnetite (Plate 7.5). Within these inner alteration zones, the footwall is commonly richer in magnetite (up to 60% by mode) than the hanging wall, possibly as a result of minor density gradients within the altering fluids. Magnetite may directly form a selvage to the main quartz, and quartz-fluorite, veins of the inner vein-zone, although ferrugenized T2 tourmalinites more commonly form such selvages. As noted in Section 3.1.c (see Fig. 3.3), magnetite is not

abundant within the Dark Gneiss hosted areas of Zones 4 and 5; pyrite is the dominant Fe-phase and probably reflects the more reduced nature of this host-rock. The vein-margin zone and the vein zone within the Dark Gneiss are slightly enriched in magnetite with respect to the wall-rock zone, although it is presumed that much of this magnetite may be related to the T1 event. Ferruginization (magnetite) reflects conditions where Fe-rich fluids encountered a high fO_2 and/or low fS_2 environment. Given that such physico-chemical conditions would not be conducive to the local remobilization of original magnetite, and/or magnetite associated with T1, it seems likely that a large net input of Fe must have occurred. Indeed, the preceding event (T2) also required the involvement of Fe-rich fluids and it is possible that the change from tourmalinization to magnetite deposition simply reflects a reduction in the activity of B within the altering fluids. Notably, the period between the end of T2 and the beginning of F1

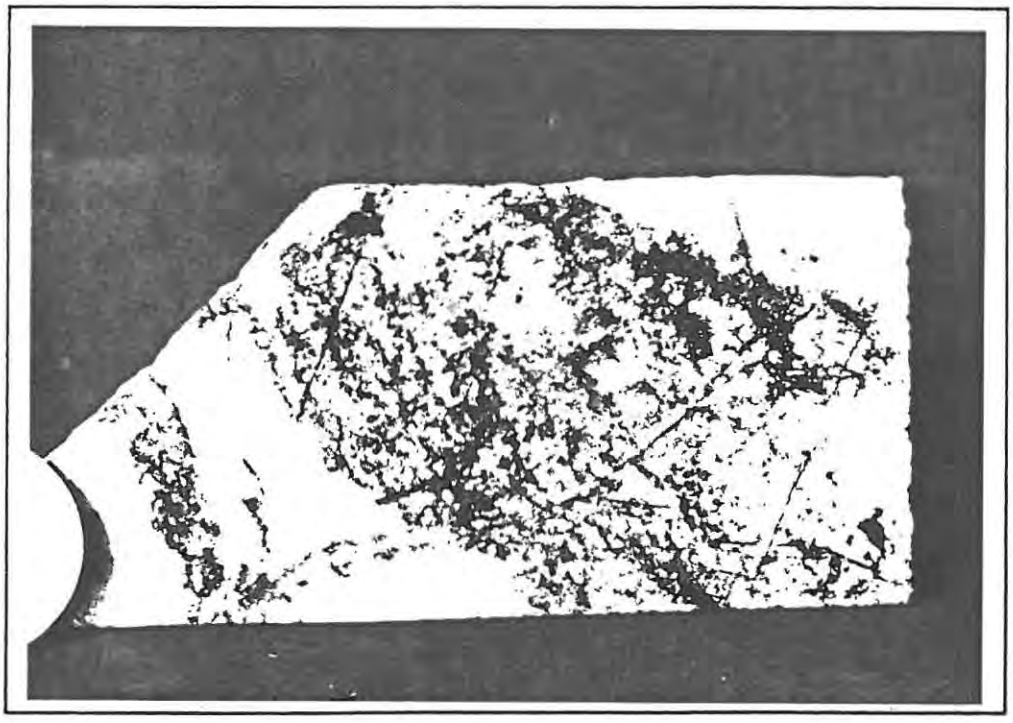

Plate 7.4. Magnetite veining within Pink Gneiss. The sample shown was collected from the outer vein-margin zone (VR74).

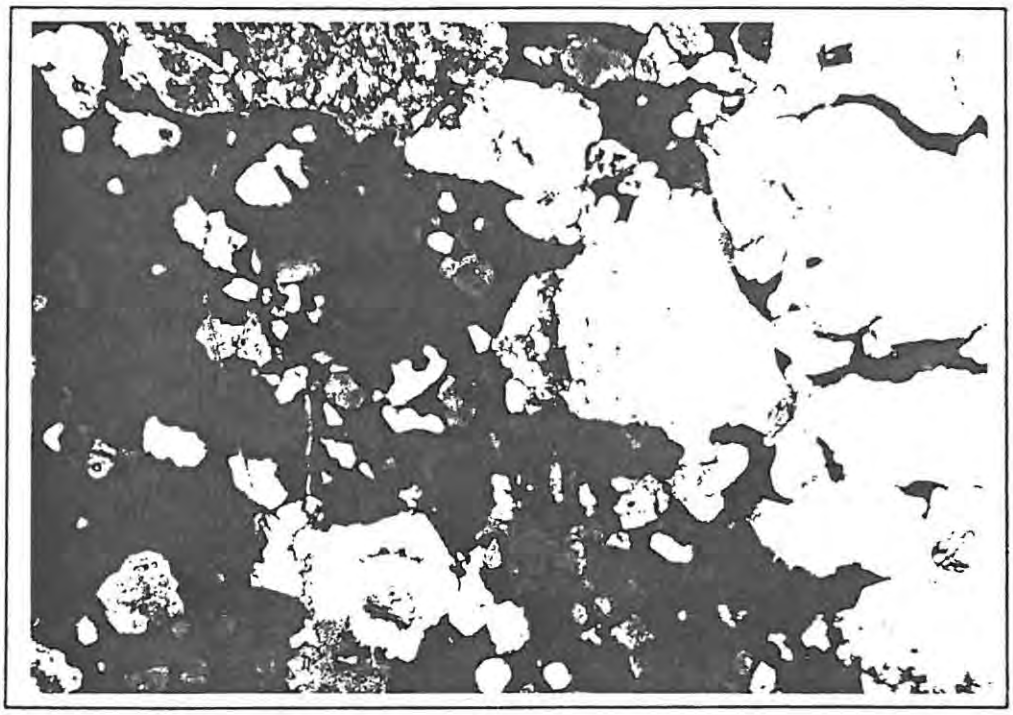

Plate 7.5. Photomicrograph showing a T2 tourmaline assemblage (dark green-blue) that has been brecciated and partially replaced by magnetite (black) within the vein-zone of Zone 4. (VRD 72, PPL, X20).

(fluoritization), marks a transition from a B-dominated system to a F-dominated system. The main phase of both Sn and wolframite deposition (see Section 6) seems to relate to the early stages of this transition period, whilst scheelite deposition relates more to the end of this transition, and is terminated by F1 (see Section 8.3.a).

Chloritization (C2) follows ferruginization (magnetite) and extensively alters tourmaline, magnetite, K-feldspar and biotite. The inner vein-margin zone and the vein-zone of the Pink Gneiss are particularly affected by C2. Intense quartz veining occurred during, and immediately after, C2 and caused the recrystallization of the Pink Gneiss into a coarse grained (up to 5cm) assemblage that is dominated by K-feldspar. Both the Pink Gneiss and the recrystallized Pink Gneiss were subsequently brecciated. In extreme cases of C2 the brecciated clasts are extensively chloritized (Plate 7.6); high Sn grades may also occur (see Section 8.4.c).

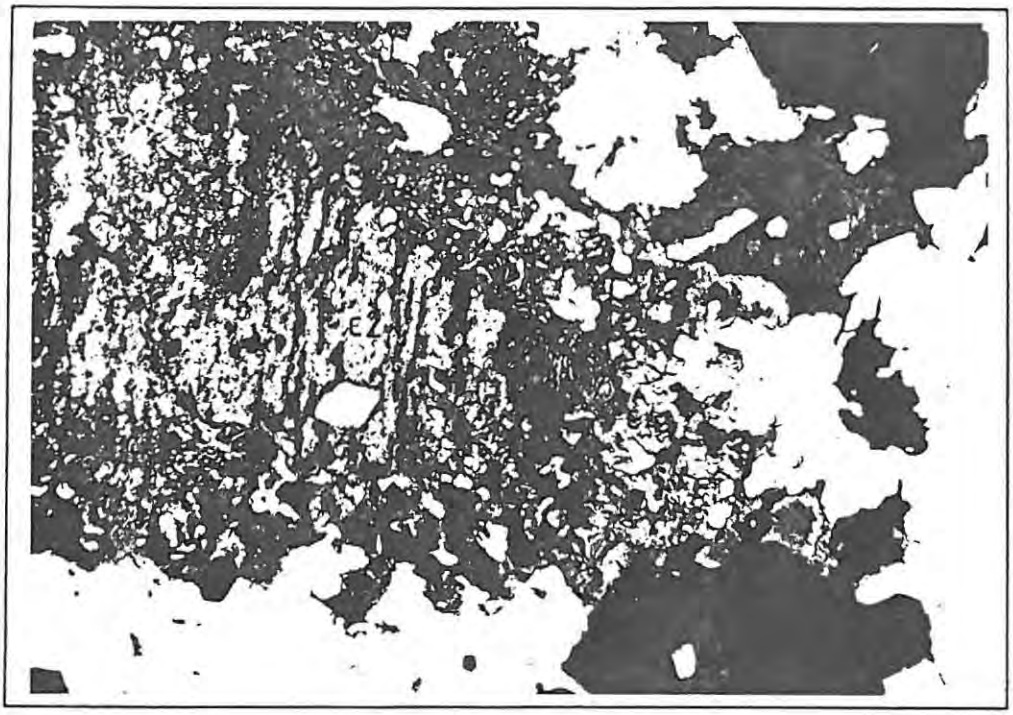

Plate 7.6. Photomicrograph showing what was once a piece of Pink Gneiss host-rock but has now been altered by the C2, C3, C4 and C5 periods of chloritization (VRD 91, PPL, X20).

During **fluoritization F1**, quartz veins within the middle of the vein-zone, and at the boundary between the vein-zone and the vein margin-zone, are brecciated and replaced by fluorite. Minor fluorite (± quartz) veins, up to 3mm in width, penetrate into the vein-margin zone and (rarely) into the wall-rock zone. Fluoritization of wall-rocks adjacent to fluorite veins is not intense and is confined to plagioclase-rich (ie. Ca-rich) areas, particularly within the Dark Gneiss. Clear, colourless fluorite is characteristic of F1 and commonly forms as fine (1mm) anhedral to subhedral crystals. Minor amounts of white mica (sericite) may occur along the grain boundaries of fluorite but probably relate to a period of sericitization that immediatly post-dates F1.

Only one significant event of **sericitization** has been identified. This event immediatly follows F1 and affects areas within, and peripheral to, the middle vein-margin zone. Such areas represent assemblages where chemically

suitable host minerals (ie. feldspar-tourmaline-biotite) still remain. Rare feldspar ± tourmaline rich areas, (particularly within the vein margin zone) are pervasively altered to sericite (or rarely muscovite) but greisen-type assemblages (eg. Plate 7.7) are rare. Assemblages, of both T1 and T2 origin, commonly show minor degrees of sericitization.

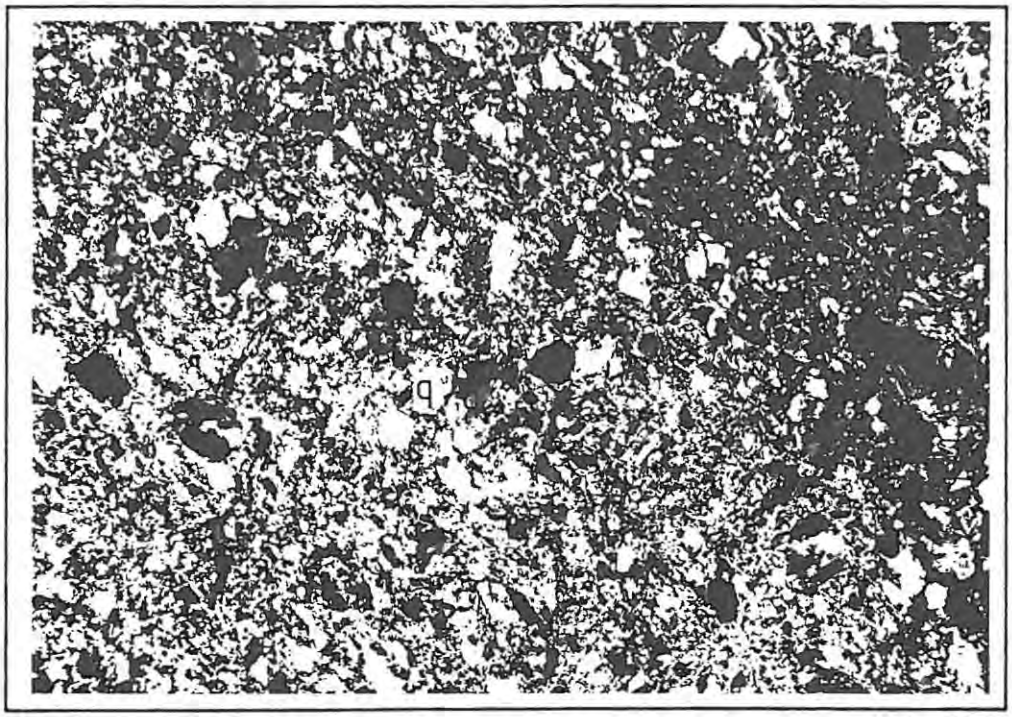

Plate 7.7. Photomicrograph of a (rare) greisen-like assemblage, found within the middle vein-margin zone. The original host, a Pink Gneiss, has be altered into the assemblage quartz (q), sericite (s) and minor tourmaline (t).(VR15, XP, X20).

No significant ore deposition was association with the abovementioned period of sericitization, however, minor sericitization is associated with all periods of Sn-mineralization (Table 7.1), altering feldspars adjacent to cassiterite crystals (Plate 3.7).

Pyrite commonly accompanies sericitization but is more abundantly associated with the **chloritization (C3)** that follows sericitization. Chlorite deposited during C3 is restricted to the vein-zone and inner vein-margin

zone, where extensive chloritization ± pyritization of tourmalinites, and of magnetite-rich tourmalinite, occurs. C3 is the last recognizable alteration event of the mineralization stage.

7.4 Post-Ore Stage (A3)

The **post-ore stage (A3)** of alteration is readily apparent within those Pink Gneiss hosted regions of Zone 4 that were fractured and brecciated by post A2 movement along the East Quarry Fault. The East Quarry Fault does not intersect Zone 5 which, like the remainder of Zone 4, shows very little evidence of A3 activity.

Alteration assemblages developed during the later part of A2 and during A3 are similar, indicating that the conditions of alteration had not changed significantly. It is likely that A3 closely follows A2 and does not simply represent a later, genetically unrelated, permeation of fluids along the East Quarry Fault. The East Quarry Fault was therefore active during the genesis of the deposit, although at a late and essentially barren stage. Alteration of scheelite to wolframite was the only feature of significance as regards mineralization.

Chloritic alteration (C4) closely follows brecciation of the Pink Gneiss and either forms a chloritic selvage to the brecciated vein walls, or rims brecciated clasts (Plate 7.6). Minor pyrite is associated with C4, as is minor alteration of wolframite to scheelite.

Fluoritization (F2), again associated with minor sericitization, immediately post-dates C4 and deposits pale green fluorite within the brecciated 'interclast' spaces. Like F1, F2 causes minor alteration, or removal, of scheelite.

Chloritic alteration (C5) occurred directly after F2, again associated with minor pyrite, and forms a second chlorite rim to brecciated clasts within the vein-zone. As shown in plate 7.6, silicification occurred between C4 and C5, possibly in association with F2. Abundant quartz is also associated with C5.

7.5 Epithermal Stage (A4)

Displacement along the East Quarry Fault included at least two major periods of movement, firstly immediately prior to A3 and secondly immediately prior to A4, the **epithermal stage** of alteration. The timing of A4, with respect to previous alteration events, cannot be established. However, by A4, the conditions under which alteration occurred had changed dramatically. This stage of alteration is only apparent where the East Quarry Fault intersects Zone 4.

The epithermal nature of A4 is characterized by an abundance of adularia and of large (up to 1.5 cm) euhedral quartz crystals (Plate 7.8). The latter contain up to three growth rings, defined by hematite inclusions, and probably crystallized during numerous rapidly consecutive fluid inpulses. Minor vugs are encountered (particularly within core from D.D.H. VRD 24/D_2) and indicate a very low pressure 'open-space filling' environment, as does the presence of adularia and large, euhedral, quartz crystals.

Extremely oxidized conditions prevailed during A4. Local areas of abundant hematite occur and can be traced into, or texturally matched with, sulphide- or magnetite-rich areas. The hematite is obviously an oxidation product of the latter two minerals.

No mineralization is known to be directly associated with A4, although alteration of a similar nature is characteristic of many high level Au deposits. The association of A4 with Sn/W mineralization at Van Rooi's Vley may simply be fortuitous, as no genetic relationship can be established.

7.6 Van Rooi's Vley - a greisen deposit?

A greisen can be defined as a peraluminous rock that has undergone H^+ metasomatism and consequently contains the assemblage quartz- muscovite (or lepidolite)-fluorite - topaz $\pm$ tourmaline $\pm$ cassiterite $\pm$ wolframite $\pm$ rutile $\pm$ apatite $\pm$ sulphides. This assemblage is characteristic of quartz vein-greisen Sn/W deposit, although such deposits invariably also show (often intense) alkali metasomatism, chloritization and sericitization.

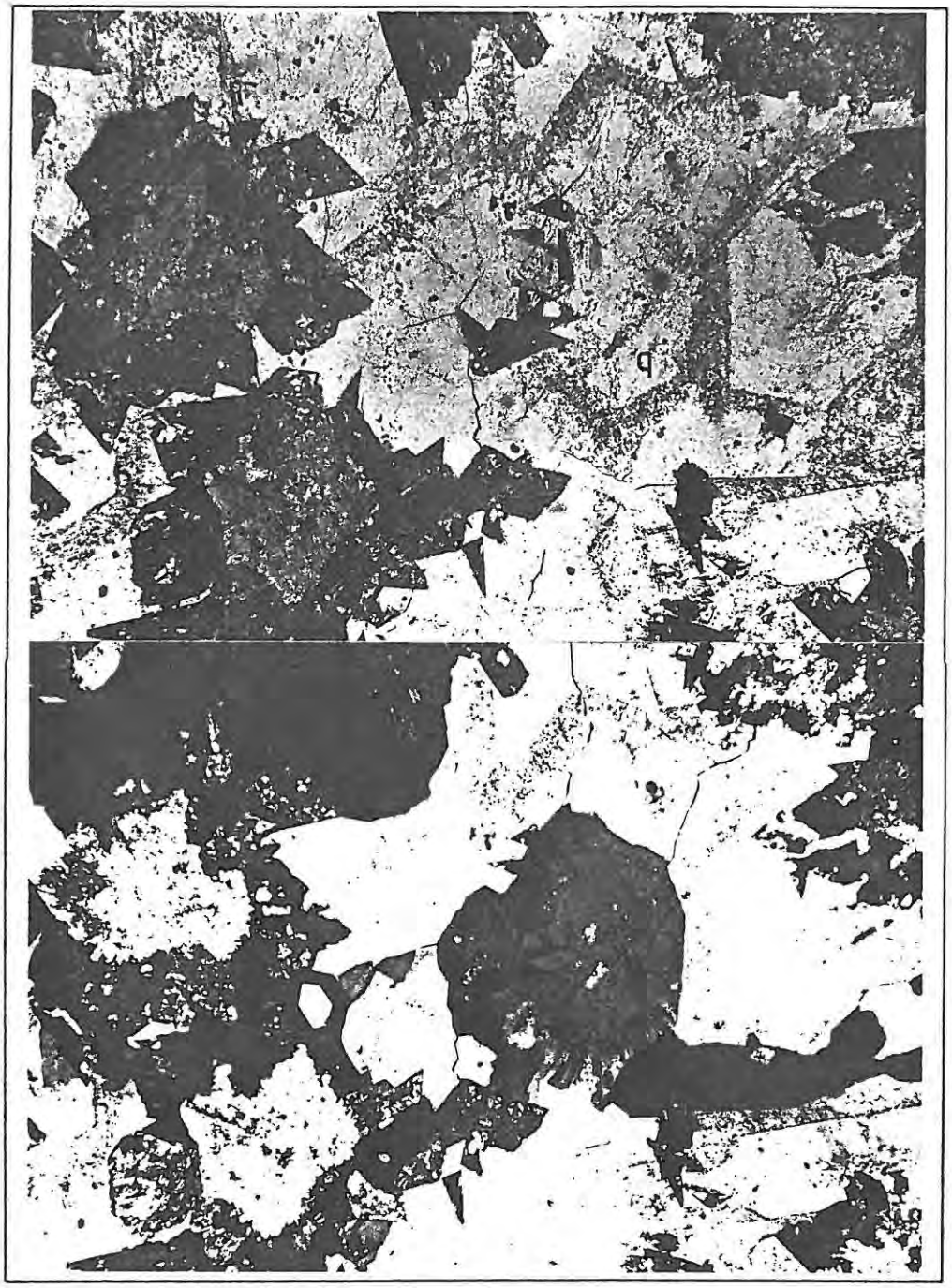

Plate 7.8. A4, the epithermal stage of alteration produces a distinctive assemblage that is confined to areas close to the intersection of the East Quarry Fault and Zone 4. The photomicrographs above show a typical epithermal assemblage, characterized by bladed and turbid K-feldspar (adularia - 'a') and multi-generation quartz (q). Each generation of quartz is defined by a series of fine-grained inclusions (i). (VRD 122, PPL and XP, X20).

Although no true greisen assemblage is found at Van Rooi's Vley, alkali metasomatism, chloritization and sericitization are common, and it is suggested here that, on the whole, the deposit is of a quartz vein - greisen affiliation. In this context, the lack of a typical greisen assemblage may relate to ;

(1) the lack of a suitable host assemblage. A wide vein selvage developed during T1 and T2 that contained a mineral assemblage which may have been stable under condition of low pH;

(2) low pressure during alteration. Given that the A4 Stage of alteration was epithermal in nature, the possibility exists that the entire mineralization/alteration event developed at low P, possibly below the muscovite stability field. At low P, K-feldspar is the stable potassic phase. The muscovite stability field has been determined at high P and T but, according to Miller et al., (1981), is not well defined under low P and T conditions;

(3) overprinting. A greisen assemblage may have developed, however, due to the very complex and prolonged alteration history of the deposit, this assemblage may not have been preserved;

(4) A lack of F within (or the loss of F from) the hydrothermal system. Because HF is an extremely powerful acid, an abundance of F may be essential in the development of a greisen. Compared to HF, boric acid is very weak, and it may then be expected that a system dominated by B would undergo less H^+ metasomatism than an otherwise similar F-dominated system. An overwhelming dominance of tourmaline, over fluorite, attests to the dominance of B within the Van Rooi's Vley system. Given that the solubility of fluorite is very low (Mulligan 1983), and that the stability field of tourmaline is extensive (Plimer 1983), decreasing F/B ratios within a fluid (and hence the tendency not to form greisenous alteration) may be a function of increasing distance from the fluid source. At Van Rooi's Vley, the source of mineralizing fluids is not seen and it can be assumed that it is distal; the tourmaline/fluorite ratio is correspondingly high and greisen assemblages are absent.

A similar situation is encountered within the Sn-fields associated with the acid phase of the Bushveld Igneous Complex. Here, 'endogranitic' mineralization (eg. Zaaiplaats - See Crocker 1986) is

often greisen-bound and associated with high F/B ratios, whereas distal, 'exogranitic', mineralization (eg. Rooiberg - See Rozendaal et al., 1986) shows minimal greisenization and is associated with low F/B ratios;

(5) the extent of country rock fracturing. In a tight (ie. almost closed) system, in which fluid movement is diffuse and slow, we would expect extensive greisens to form, whereas a well-fractured country rock is more likely to yield mineralized quartz veins (Eugster and Wilson 1986).

8. CONTROLS ON MINERALIZATION

8.1 Introduction

In Section 5 it was established that there was a strong structural control on the location of mineralization at Van Rooi's Vley, but that the concentration (i.e. grade) of mineralization was basically a function of physicochemical factors. Section 7 documents the progressive changes in host-rock mineralogy during mineralization. These mineralogical changes place some constraints on the physicochemical conditions under which accompanying mineralization occurred. Such conditions are further discussed below.

A brief study of fluid inclusions was also undertaken in order to constrain the temperature range, and fluid salinities, under which mineralization occurred. Unfortunately, only secondary fluid inclusions were identified and the measured temperatures of homogenization gave a rather obvious minimum temperature for mineralization of around 180° C. The failure to identify primary fluid inclusions is attributed here to poor sampling (particularly) and to the highly fractured nature of the mineral deposit.

8.2 Geochemistry of tungsten and tin

8.2.a Geochemistry of W and Sn

Tungsten and tin exhibit close geochemical similarities. Both elements are strongly incompatible and lithophile under most geological conditions and, as a result, they ;

- have an affinity for felsic (granitic), as opposed to mafic, igneous rock-types;
- do not enter into common, and early formed, felsic minerals (eg. quartz and feldspar), and are consequently concentrated within residual melts;
- form common stable compounds only in their highest valence state and

consequently exist as oxides;

- require similar physicochemical conditions (eg. an increase in fO_2, increase in pH, decrease in temperature) to destabilize their soluble complexes within hydrothermal fluids.

The valency of tungsten ranges from +1 to +6 although in nature it is almost exclusively hexavalent (+6), forming stable complexes mainly with oxygen (ie. as the wolframite and scheelite series of minerals), but also with halides and other elements.

Molybdenum and hexavalent W have the same valency. These two elements are separated by the Lanthanide group of elements and as such have greatly different atomic numbers (Mo = 42, W = 74), although, through the Lanthanide contraction phenomenon, their ionic radii are very similar ($\sim$0.062nm). As a result, W and Mo may substitute for each other within the scheelite ($CaWO_4$) - powellite ($CaMoO_4$) series of oxide minerals. However, covalent bonding of W to S is weak, partly because of the higher electronegativity of W (compared to that of Mo), and whereas Mo occurs predominantly as the sulphide molybdenite (MoS_2), the analogous W sulphide (tungstennite) is rare (Mulligan 1983).

Tin has only two valence states, +2 (stannous) and +4(stannic), and although most readily transported in the reduced state, stannic oxide (ie. cassiterite - SiO_2) is overwhelmingly the most abundant Sn-bearing mineral. Stannite (Cu_2FeSnS_4) may also be a significant concentrator of Sn^{4+}.

Bivalent Sn tends not to form natural stable compounds, except as rare sulfo-salts in combinations with Cu,As, Pb and Sn^{4+}. Native Sn is rare and possibly refelcts the later natural smelting of cassiterite, in the presence of both a reductant (e.g. oroganic matter) and a heat source (eg. a basalt flow).

8.2.b Concentration of W and Sn

A very close and almost universal relationship has been established between fractionated granitoids and deposits of W (eg. see Mulligan, 1983) and of Sn (eg. see Taylor, 1979). This relationship is discussed further in Sections

10 and 11 and is taken to be either ;

(a) genetic, the mineralization caused by classical magmatic-hydrothermal processes of incompatible element enrichment within, and subsequent fluid phase transport from, a highly fractionated granite;

or, in the case of many scheelite bearing veins,

(b) non-genetic, the W±Sn mobilized, through granitization and assimilation, from within bedded rocks surrounding granitic intrusions. Conceivably, high-grade regional metamorphism may also cause such remobilization, as has been suggested in connection with mineralization at Van Rooi's Vley (Wheatley and De Beer 1986).

At any rate, concentration of Sn and W within a fluid phase that coexisted with a highly felsic assemblage, is suggested in all cases.

8.2.c Transport and deposition of W

Although little work has been done concerning the transport of W within hydrothermal fluids, tungstic acids, halide complexes and polytungstates are the most commonly invoked agents for such transport.

According to Mulligan (1983), W is possibly transported as undissociated tungstic acid (eg. $H_2\ WO_4$), or as HWO_4, the former favouring temperatures above 350°C and the latter favoured by lower temperatures.

Various neutral, oxy-halogen complexes with W^{6+} have been proposed, in particular, WX_6, WOX_4 and WO_2X_2, (where X is Cl or F). These complexes may, however, be readily hydrolized and thus destabilized. According to Manning and Henderson (1984), protonated, anionic W-O-X species such as WOF_5, WO_3F^{3-} and $(WO_3)_2\ Cl^-$, are more likely to be present in aqueous solutions at high temperatures and pressures.

Manning and Henderson (1984) consider isopolytungstates (eg. $H_6[H_2W_{12}O_{40}]$) and heteropolytungstates, where elements such as P, As, Si and B substitute for H within the isopolytungstate structure (eg. $H_3[PW_{12}O_{40}]$), as possibly

significant transporters of W.

Deposition of W from a hydrothermal fluid will occur through changes in the physicochemical environment. In particular, decreasing temperature, decreasing pressure, increasing fO_2 and increasing pH will effectively destablize all of the abovementioned W complexes.

The P/T conditions at the site of W (and Sn) deposition are obviously dependant upon such parameters as the prevailing regional and/or contact metamorphic grade, distance to the hydrothermal source and the initial temperature at that source, and on the structure of the fluid pathway (ie. open or closed). The latter parameter is of particular importance. Within an open system only minimal wall rock reaction will occur and W-deposition will largely be a function of 'physical' (eg. P/T) variables, whereas, within a more closed system, more extensive wall rock alterations (eg. greisenization) will occur, and chemical means of ore deposition may be important.

It was suggested in Sections 4 and 5 that, at Van Rooi's Vley, W mineralization is closely associated with the pathways of the mineralizing fluids, whilst Sn may be dispersed away from such zones. Therefore physical variables (particularly temperature) possibly played a greater role in the deposition of W than in the deposition of Sn.

8.2.d Transport and deposition of Sn

Tin is transported within hydrothermal fluids as Sn^{2+} and, according to Patterson et al. (1981) and Eugster (1984), is only significantly soluble as the chloride complexes $SnCl^+$, $SnCl_2$ and $SnCl^-_3$. Patterson et al. (1981), also suggest that under a very low pH and/or a high a_F, SnF^+, and higher fluoride complexes, may readily form. However, the low solubility of fluorite within hydrothermal fluids would control the concentration of F, and such complexes may not be important.

Deposition of Sn, as cassiterite, requires the same physicochemical changes as described for W deposition. However, deposition of Sn requires both the destabilization of a chloride complex and a valence change in Sn (ie.

$Sn^{2+} \rightarrow Sn^{4+}$), and consequently, a change in pH and (particularly) oxidation must be involved.

8.3 Ore mineral relationships at Van Rooi's Vley - Chemical controls on mineralization

8.3.a Scheelite - Wolframite

It is apparent from Section 6, that the W-mineralogy at Van Rooi's Vley is complex. Although the major developments of both scheelite and ferberite are primary features, later generations of these minerals show a replacement nature. Ferberite commonly replaces scheelite, although the opposite reaction also occurs. Variations in the activity of Fe, Ca, F and CO_2, within the mineralizing system, can explain the relationships between these W-phases and also the high scheelite/wolframite ratio of this essentially greisen-affiliated deposit.

Because of the very low solubility of wolframite (Eugster 1984), it is unlikely that W could be transported within the same fluids as Fe and Mn. Eugster (1984) suggests that W derives from the hydrothermal fluids while $FeCl_2$ and $MnCl_2$ are provided by acid alteration of the country rocks, through reactions such as,

$$3\ Fe_3O_4\ (\text{mt. or biot. etc.}) + 18\ HCl + 3H_2 \rightleftharpoons 9\ FeCl_2 + 12\ H_2O$$

In this respect it is significant that the main phase of primary ferberite deposition (W1) at Van Rooi's Vley occurred immediately following the ferruginization (magnetite) stage of alteration. Minor alteration of this Fe-rich assemblage, during the C2 period of chloritization to which the ferberite relates, may have increased the a_{Fe} within the W-rich hydrothermal fluids enough to cause primary ferberite precipitation. Because no scheelite accompanies ferberite, the relatively lower activities of Ca, F and CO_2 must have been unimportant under these Fe-rich conditions. Furthermore, given the large amount of magnetite, the fO_2 of the system would have been buffered, at a high value, further aiding the formation of ferberite.

Scheelite is the normal W mineral in association with carbonate rocks and is accounted for either through direct precipitation, eg.

$$H_2WO_4 + CaCO_3\ (CC) \rightleftharpoons Ca\ WO_4\ (sch) + H_2\ CO_3$$

or through exchange reactions, eg.

$$Fe\ WO_4\ (wolf) + CaCl_2 \rightleftharpoons CaWO_4\ (sch) + FeCl_2$$

It may be argued that the abundance of scheelite at Van Rooi's Vley, and the high scheelite/wolframite ratio, reflects skarn-style mineralization. Indeed, the same may be said of fluorite which, although quite a common phase, is not as abundant as within most greisen-style deposits, where large fluorite-rich sheets occur. However, the fact that normal greisen deposits are greatly enriched in fluorite indicates that even a pelitic (peraluminous) rock-type (eg. the gneissic rock at Van Rooi's Vley) can supply a moderate amount of Ca to a mineralizing system. Therefore, it is probable that the lack of extensive fluorite at Van Rooi's Vley indicates that the system was deficient in F, not Ca. Such a situation would lead to the formation of scheelite (even though it is more soluble than fluorite - Mulligan 1983), because more Ca would be present than is required to fix all F as fluorite. In support of the above hypothesis, it has already been noted that, unlike other Sn/W deposits, Van Rooi's Vley is a B-dominated system. In fact, the B/F ratio probably only approached unity immediatly prior to F1, after the main stage of mineralization.

The main stage of primary scheelite deposition (Sch2) occurred after primary wolframite deposition (W1) and immediatly prior to F1. During Sch2 the a_{Fe} of the system must have been low, requiring a marked change in conditions from those under which W1 occurred. Such a change may have been brought about by the abundant deposition of vein-quartz. Consequently, the old Fe-rich inner selvage to the vein system was inhibited from reacting with incoming fluids, by the new quartz selvage. Such a mechanism explains why much of the primary scheelite lies within the inner vein-zone, whilst primary ferberite is more confined to the outer vein-zone.

Like the magnetite rich assemblage, primary ferberite would, to some extent,

have been isolated from the scheelite depositing fluids. As a result, only minimal scheelite replacement of ferberite occurs at this stage.

The influence of F upon scheelite-wolframite stabilities is demonstrated on figure 8.1. As predicted by figure 8.1, the deposition of primary scheelite ended during F1 (Table 7.1), when the a_F became too great and ferberite (W2) replaced scheelite as the stable W mineral. High concentrations of F during F1 led to a partial destruction of the preceding scheelite assemblages. Isolated scheelite grains, or partially dissolved scheelite masses (Sch2 - Plate 6.3), remain within the quartz-fluorite dominated inner vein-zone, whereas partial replacement of scheelite (Sch1 and Sch2), by ferberite (W2), occurs within the Fe-rich (ie. magnetite-tourmaline) outer vein-zone and vein-margin zone (Plate 6.2). Here, ferberite probably forms according to the reaction,

$$CaWO_4 + FeO \text{ (any mineral)} + F_2O \rightleftharpoons FeWO_4 + CaF_2 \text{ (see plate 6.2)}$$

A net input of W need not have occurred. The small amount of Fe required during W2 was not as great as during W1, and was probably met through (the albeit inhibited) reaction with the Fe-rich outer-vein zone. Possibly, brecciation of the vein zones, during F1, increased fluid flow to the Fe-rich and scheelite-rich regions.

After F1 the a_F again decreased. Scheelite (Sch3) once more became the stable W-phase (Fig. 8.1) and formed minor replacements of ferberite (W1 and W2) during later alteration events.

8.3.b Cassiterite

The concentrations and distribution of cassiterite ,the only Sn-rich phase identified at Van Rooi's Vley, was discussed in Section 5. The first concentration of cassiterite (Sn1) occurred near the end of T1 (Table 7.1). The second, and major, generation of cassiterite (Sn2) occurred near the end of T2 (Table 7.1) , continued throughout ferrugenization (magnetite), and into C2. Cassiterite deposition during Sn2 is basically restricted to areas of Zones 4 and 5 that are hosted by Pink Gneiss.

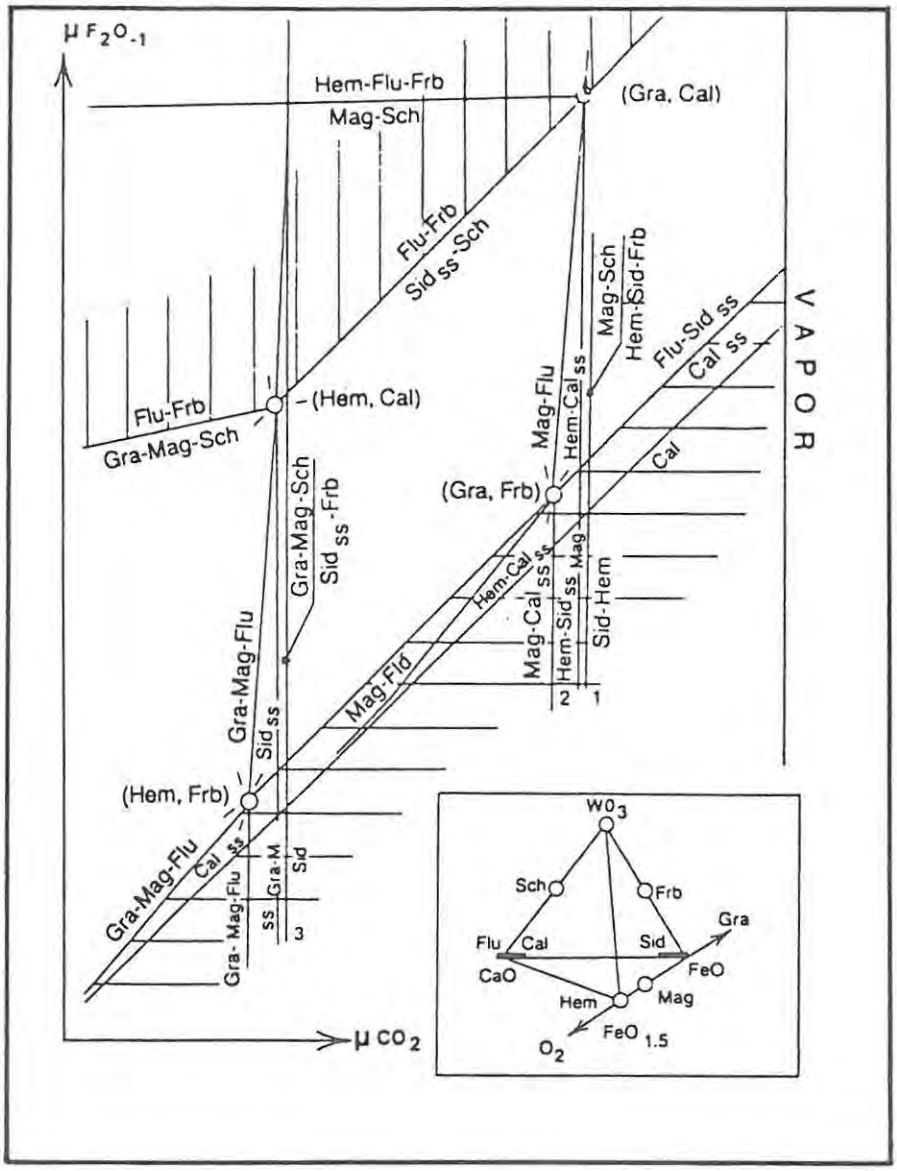

Figure 8.1. Schematic μF_2O_{-1} - μCO_2 projection of the system Ca-Fe-W-C-O-F in skarns, veins and greisens. The assemblage fluorite-ferberite, characteristic of greisens and veins, is stable in the area with vertical hachures. The assemblage calcite-scheelite, characteristic of skarns, is stable in the area with horizontal hachures (after Burt, 1972).

The precipitation of cassiterite involves changes in both the pH and the oxidation state of a mineralizing system, and may be represented by the reaction :

$$SnCl^{+} + 2H_2O \rightleftharpoons SnO_2 + 2H^{+} + Cl^{-} + H_2$$

Because the solubility of cassiterite increases with increasing pH and decreasing fO_2, additional reactions must occur to counter-act the effect of the above reaction. If substantial amounts of cassiterite are deposited, the effects of such counter-reactions, or buffers, should be detected within the wall rocks. Such reactions include K-feldspar→muscovite, biotite→muscovite and biotite→chlorite, and, combined with the reaction for cassiterite deposition may be writen as (for example),

$$SnCl_2 + 3(Na,K)\ Al\ Si_3O_8\ (K\text{-feld}) + 2H_2O \rightleftharpoons SnO_2 + KAl_3\ Si_3O_{10}(OH)_2\ (mus) + 6\ SiO_2 + 2\ NaCl + H_2$$

At Van Rooi's Vley, conditions were apparently more conducive to Sn deposition during Sn2 than during Sn1. In Section 5.5, it was stated that although structure controlled the location of mineralization, physico-chemical variables (eg. T, pH, fO_2) controlled the concentration. Following Section 7, we can now assess the nature of the host rock, and alterations, prior to Sn1 and Sn2, and thus the nature of the physicochemical controls on these mineralizing events.

Prior to Sn1 an almost monomineralic assemblage of tourmaline (T1) formed as a wide selvage to fractures and inclusions of potassically (K1) altered country rock that remained within the vein zones.

For the reasons discussed above, such an assemblage has no long-term potential to maintain the conditions required for Sn deposition; sericitic alteration of the volumetrically insignificant K-feldspar has occurred and completion of this reaction would have been a factor limiting mineralization. However, it is probable that during this early stage in the development of the deposit, high temperatures, high pressures and low Sn concentrations may have been equally, if not more, important than host-rock controls in limiting the amount of Sn-mineralization.

In contrast to Sn1, the wall-rock assemblage prior to Sn2 was both alkali-rich and greatly oxidized, and as such could maintain conditions of Sn-deposition.

Mineralization during Sn2 is again associated with minor sericitic alteration, particularly of partially altered inclusions of Pink Gneiss within the vein-zone, and of the leucogranite sheet (Plate 3.7 - Section 3.4.c) that intrudes the vein-zone. Chloritization (C2) of these wall rocks is also prominent, affecting biotite and tourmaline- K-feldspar-magnetite assemblages. Such reactions may possibly have maintained the pH at high enough levels for the continuation of Sn deposition.

Minor pyrite is also associated with Sn2, particularly during C2, and forms mainly as a replacement of magnetite. This reaction is probably a response both to an increasing fS_2 within the system, and, more importantly, a decreasing fO_2 due to cassiterite deposition. The magnetite rich wall-rocks thus effectively buffered the mineralizing environment against a decrease (or increase) in the fO_2, again maintaining conditions conducive to Sn deposition. As noted in Section 3.1.c, the Dark Gneiss hosted region of Zones 4 and 5 are pyrite-rich and magnetite-poor (Fig. 3.3) and would thus not be chemically conducive to Sn deposition.

8.3.c. The zonation and separation of Sn and W mineralization

The location of structural sites (eg. low pressure zones) is the principal control on the location of Sn mineralization, which typically occurs in structurally prepared pockets, at various distances from the pathway of the mineralizing fluid. For Zone 4, the pathway was along the Pink Gneiss - Dark Gneiss contact, whilst for Zone 5, it was the intersection between Zone 4 and Zone 5. Tungsten is more-or-less confined to areas within, or immediately adjacent to, these pathways, and is thus also structurally located.

Obviously, temperature (and a_F, a_{Ca}, a_{Fe}, fO_2, fS_2, Ph etc) also had a control on the location of Sn and W mineralization, and in the spatial

separation of these elements. Wolframite and (under conditions of high a_{Ca} and low a_F) scheelite will become insoluable within an aqueous solution at a higher temperature than will cassiterite, and would thus tend to be located more proximally to a fluid pathway than would cassiterite (e.g. Fig. 3.3).

9. THE WITKOP W/Sn DEPOSIT - A COMPARISON WITH VAN ROOI'S VLEY

9.1. Introduction

The Witkop deposit lies approximately 1km NW of Van Rooi's Vley and displays many features that are of critical importance in the understanding of W and Sn metallogenesis within the Van Rooi's Vley - McTaggarts Camp district. Given the time available for this study, the Witkop deposit could not be investigated in the same detail as was Van Rooi's Vley. Therefore, only salient features of the deposit will be discussed below, particularly those that draw contrasts with the Van Rooi's Vley deposit.

9.2 Local Geology

Mineralization at Witkop dominantly occurs within a series of quartz (± tourmaline ± fluorite) veins, hosted within a 'quarter-moon' shaped sliver of micaceous gneiss, tectonically isolated within rocks of the Riemvasmaak Formation (Fig. 9.1) micaceous gneiss. The micaceous gneiss strikes approximately E-W and dips almost vertically, at surface, but rapidly flattens out at depth, to an average dip of 53°N (Fig. 9.1). The origin of the micaceous gneiss is unclear, however, a strongly pelitic mineralogy (biotite - sillimanite - cordierite - Plate 9.1) suggests that the gneiss belongs to either the Toeslaan Formation, or more likely, to the Biesjepoort Formation. The micaceous gneiss differs from the Dark Gneiss at Van Rooi's Vley, in that primary biotite is much more abundant within the former, and in places may constitute up to 85% (by mode) of the rocks.

9.3 Ore Mineralogy

The ore assemblage at Witkop is dominated by scheelite, with lesser amounts of wolframite and only minor cassiterite. Scheelite occurs in at least two generations, the original generation being primary and volumetrically the most significant. The second generation of scheelite is probably also primary, but is only minor and occurs very late in the ore paragenesis. Much of the wolframite occurs as an alteration of early scheelite, although

the dominant deposition of wolframite is also primary, post-dates the early generation of scheelite and is accompanied by abundant deposition of fluorite (Plate 9.2).

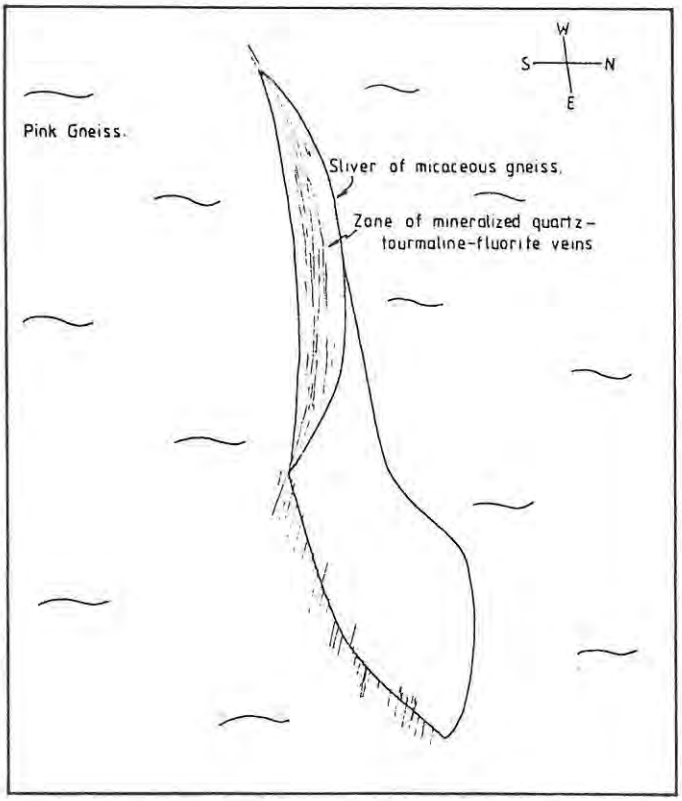

Figure 9.1. Schematic representation of the geology of the Witkop W/Sn deposit.

Magnetite is common, both within the altered wall-rocks and within the ore assemblage, however, it is present in much lesser amounts than within the Van Rooi's Vley deposit. No hematite is seen within the Witkop ore assemblage.

Pyrite is usually the dominant sulphide although pyrrhotite is common and in some cases may constitute up to 70% (by mode) of the ore assemblage. Pyrrhotite and pyrite often occur together and grain boundary relationships indicate a stable co-existence (Plate 9.3). Magnetite is not stable within the sulphide assemblage, and where present, is seen to be altering to

pyrrhotite (Plate 9.3). The deposition of pyrrhotite post-dates the main deposition of scheelite, wolframite and of cassiterite, and is apparently only associated with quartz, pyrite, chlorite ± fluorite. Minor chalcopyrite and molybdenite also occur within the Witkop ore assemblage, commonly associated with the other sulphides.

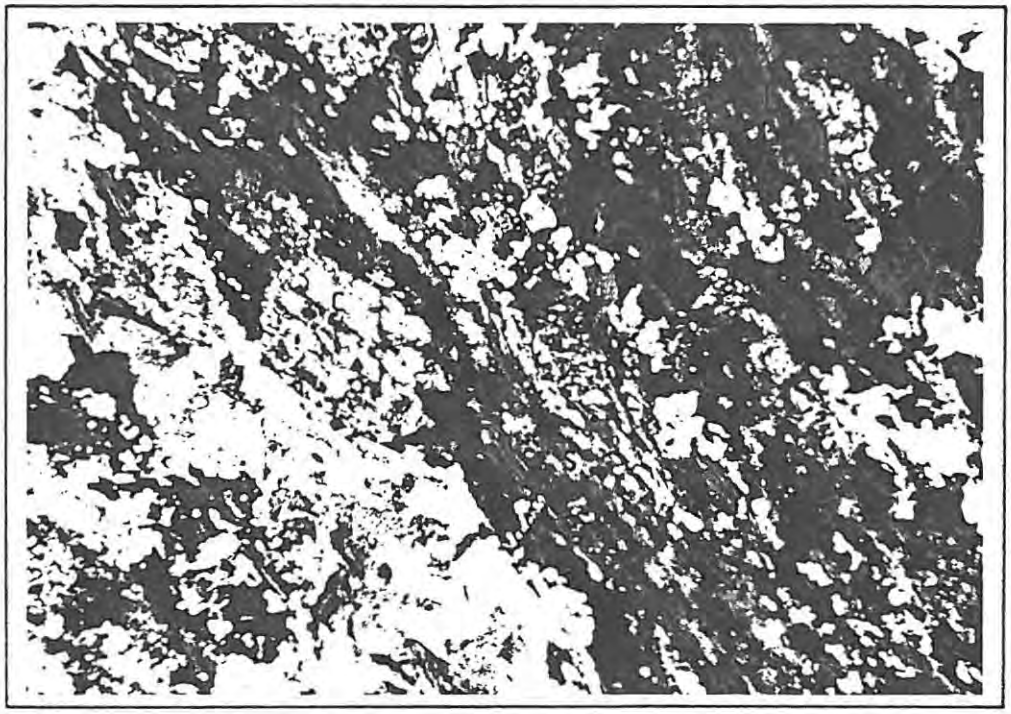

Plate 9.1. Photomicrograph of the pelitic micaceous gneiss found at the Witkop deposit. Important mineralogical features include the presence of biotite (b), sillimanite (s) and cordierite(c). (WK51, PPL, X20).

9.4 Wall-rock Alteration

Wall-rock alterations developed at Witkop differ only in relative intensity, from those developed at Van Rooi's Vley. The same alteration types (e.g. tourmalinization, potassic alteration, fluoritization etc.) are developed in both deposits.

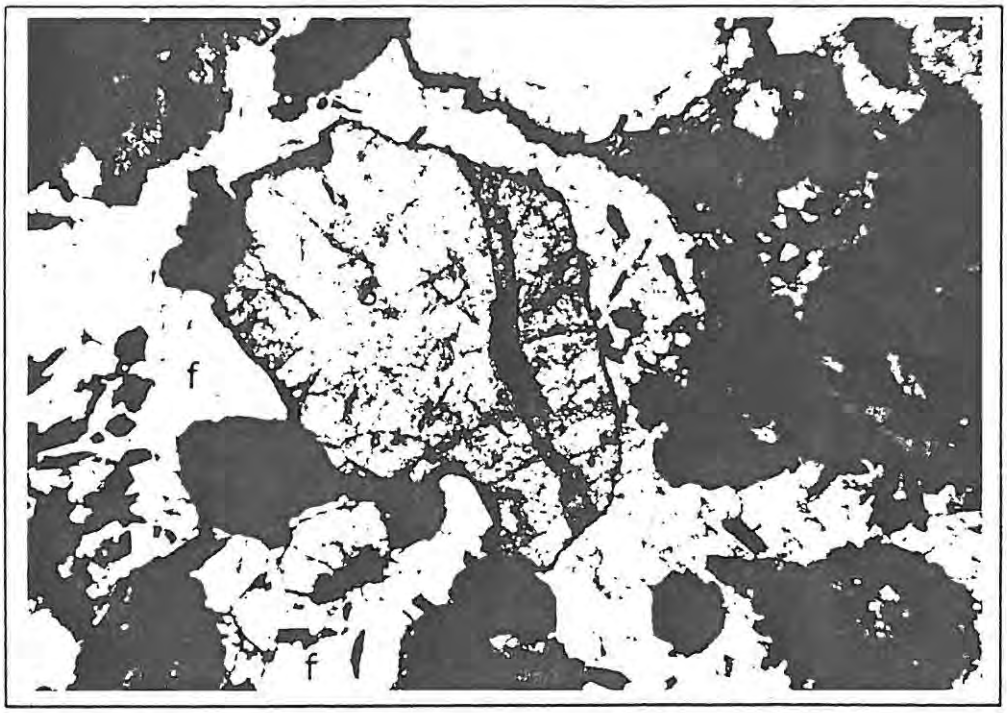

Plate 9.2. Photomicrograph showing primary wolframite (black) and scheelite (s). Deposition of wolframite was accompanied by deposition of fluorite (f), reflecting conditions of high a_F, under which scheelite is not stable. At least some of the wolframite may represent an alteration product of scheelite. (WK 65, PPL, X20).

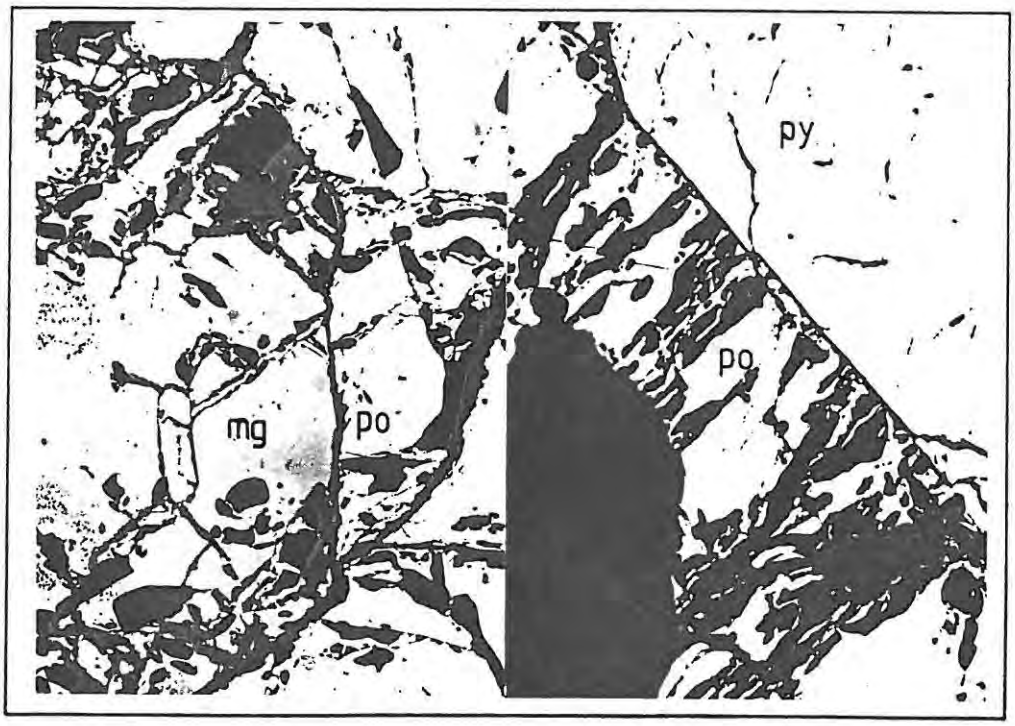

Plate 9.3. Photomicrograph showing the pyrrhotite-rich sulphide assemblage developed at the Witkop deposit. No reaction relationship is seen between pyrrhotite (po) and pyrite (py), indicating that these two minerals stably co-exist. Magnetite (mg) is, however, not stable within this assemblage, as evidenced by reaction rims around all magnetite grains (WK66, Reflected lenght, X20).

In particular, the ratio of fluorite to tourmaline, within the alteration paragenesis as a whole, seems slightly lower at Witkop than at Van Rooi's Vley. The same two phases of tourmaline that were identified within the latter also affect the former, however later fluoritization is more intense at Witkop. Abundant deposition of wolframite relates to an early phase of fluoritization (Plate 9.2), which immediately post-dates the deposition of the first generation of scheelite.

Muscovite locally forms an extensive alteration of original feldspars and biotite (Plate 9.4), indicating that H^+ metasomatism (greisenization) may have been a significant alteration process within the Witkop deposit. This alteration immediately post-dates the second phase of tourmalinization (as evidenced by inclusions of euhedral tourmaline crystals within muscovite), and possibly relates closely to cassiterite and wolframite mineralization.

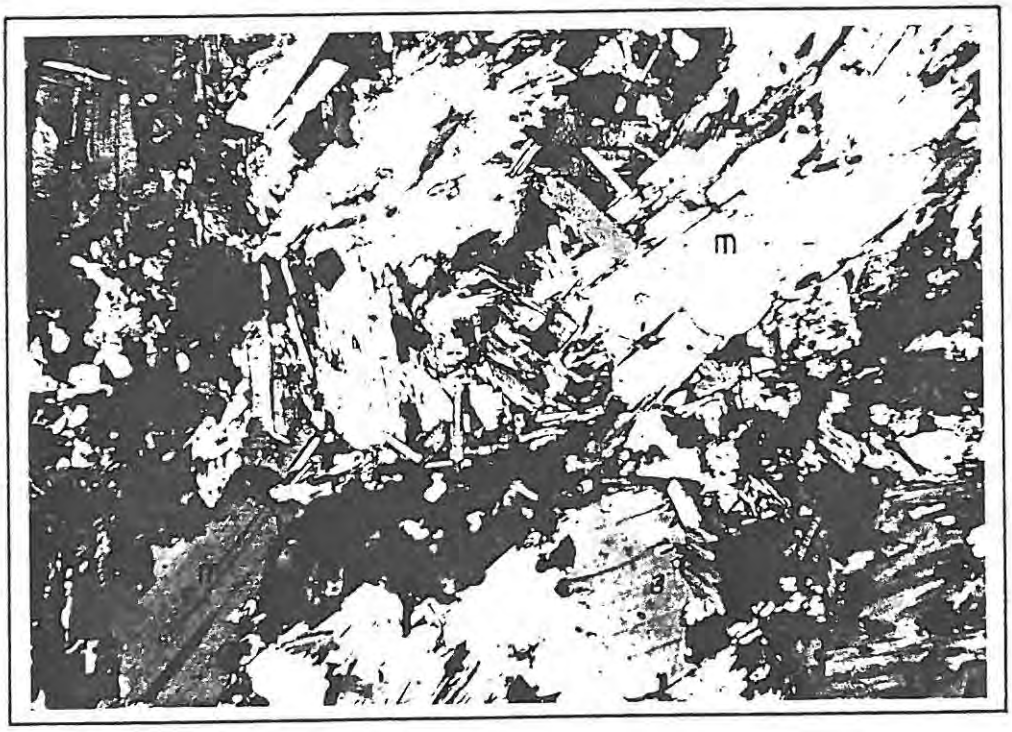

Plate 9.4. Photomicrograph showing a greisenous assemblage rich in coarse grain muscovite (m) with lesser amounts of fluorite (f) and tourmaline. (WK45, XP, X20).

9.5 Comparison with Van Rooi's Vley

The Witkop and Van Rooi's Vley deposits share many close similarities apart from an obvious spatial relationship. Most importantly, both of these deposits have ;

- the same geological setting and associations;
- the same alteration types and paragenesis;
- similar ore mineralogy.

Although not proven, it is likely that the two deposits are of a similar age, the above similarities impose similar constraints on the genesis of these deposits. It is also probable that both deposits are the result of the same hydrothermal event and as such, the following differences must be explained ;

- the higher W/Sn ratios at Witkop;
- the slightly higher F/B ratios at Witkop;
- the presences of greisenous alteration only at Witkop;
- the presences of pyrrhotite only at Witkop.

Interestingly, the Witkop deposit and the McTaggarts Camp deposits are also quite similar, although the latter has even higher W/Sn and F/B ratios, and greisenous alteration is more abundant, but has no pyrrhotite. It was suggested in Section 3.5 that the McTaggarts Camp deposits probably also relate to the same hydrothermal event that produced mineralization at Van Rooi's Vley.

In Section 7.6 it was suggested that the F/B ratio within a mineralizing system may decrease with increasing distance from the mineralizing source. The change in the F/B ratio would be reflected by a decrease in the ratio of fluorite (or topaz) to tourmaline. If such a relationship holds true, it would imply that the Witkop deposit formed closer to a mineralizing source that did mineralization at Van Rooi's Vley. The McTaggarts Camp deposit would have formed still closer to such a source.

The presence of a greisenous assemblage at Witkop supports the

abovementioned spatial relationships. Greisenization is probably best affected by dissociation of the powerful acid, HF. This would be a rapid reaction in the presence of a plagioclase-rich assemblage, and would cause H^+ metasomatism (of that assemblage) and the deposition of fluorite and/or topaz. Greisenous assemblages are therefore characteristically F-rich and occur proximal to the source of volatile-rich hydrothermal fluids.

From the discussions above, it would follow that the Witkop deposit formed at higher temperatures than the Van Rooi's Vley deposit. This may explain not only the higher W/Sn ratios at Witkop (see discussions in Section 8.3.c) but, as figure 9.2 indicates, it may also explain the differing Fe-sulphide mineralogy between the two deposits; pyrrhotite only forming at Witkop, within the slightly higher temperature ore assemblage.

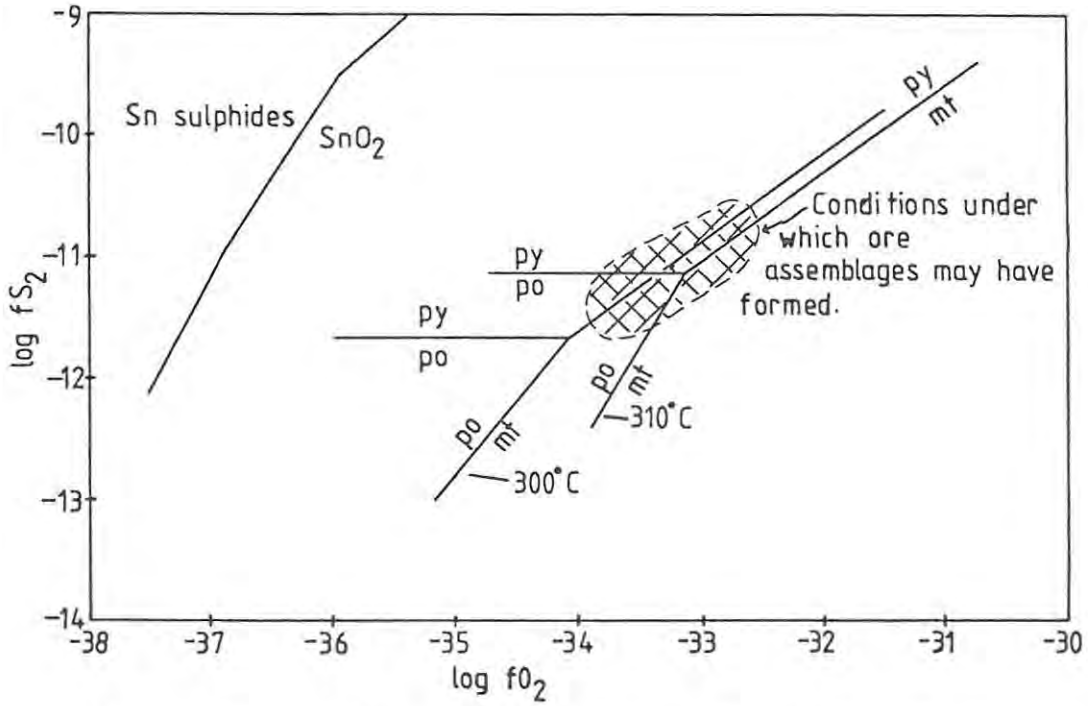

Figure 9.2. Log fS_2 - Log fO_2 diagram showing how a small decrease in temperature ($\sim$ 10°C) can cause a change in a sulphide mineral assemblage. The assemblage pyrite - pyrrhotite - magnetite occurs at Witkop, whereas the assemblage pyrite-magnetite is typical of the Van Rooi's Vley deposit.

10. PREVIOUS GENETIC MODELS FOR MINERALIZATION AT VAN ROOI'S VLEY

10.1 Introduction

To explain the formation of the Van Rooi's Vley Sn/W deposit, a genetic model must also be able to account for W/Sn mineralization at Witkop and at McTaggarts Camp. Mineralization at both Van Rooi's Vley and McTaggarts Camp is synchronous with, or slightly post-dates, the intrusion of leucogranites that are late-to-post-tectonic (i.e. unfoliated) with respect to the Namaqua event. The distinct similarities between the Witkop and Van Rooi's Vley deposits further suggest a similar age of mineralization. It is therefore likely that a late-to-post-tectonic age can be placed on all of the hydrothermal mineralization within the Van Rooi's Vley-McTaggarts Camp district in general.

The genesis of the Van Rooi's Vley deposit has, however, been a matter for conjecture mainly because nowhere within the Van Rooi's Vley - McTaggarts Camp district can a strikingly obvious source for mineralization be identified. Similar problems are encountered in deciphering the metallogenesis of many high-grade metamorphic terranes and, unfortunately, necessitate the more extensive use of circumstantial data than would otherwise be desirable.

10.2 Two contrasting models for the genesis of the Van Rooi's Vley deposit

Wheatley and De Beer (1980) outline two principle alternative models for the genesis of mineralization at Van Rooi's Vley, vis ;

1. the **metamorphic remobilization** of a sedimentary/exhalative proto-ore during the waning stages of the Namaqua event (see Section 3.4) ;

2. the degassing of a **'specialized' granitoid.**

The remobilization model envokes a close genetic relationship between the

Van Rooi's Vley deposit and tourmalinites, that are located near the top of both the Riemvasmaak and Biesjepoort Formations. Metamorphic remobilization of these tourmalinites is envisaged to have provided B for the deposit (as tourmaline selvages), and also to have provided a ligand for the transport of Sn and W. Both Sn and W are thought to have been leached from the Biesjepoort Formation. Tourmalinites within the Riemvasmaak Formation crop-out near Kakamas, some 40km west of Van Rooi's Vley, and are well bedded (Plate 3.1). They are not found at Van Rooi's Vley. Tourmalinites are, however, also found within the Biesjepoort Formation, just to the south of Van Rooi's Vley, (Fig. 3.1) and crop-out mostly as scattered rubble. It is unlikely that these tourmalinites are as well bedded as the Kakamas tourmalinite, and it is possibly that they are not of a sedimentary origin.

However, it is perhaps significant that, in view of the absence of the Goede Hoop Formation (correlated with the Pella Quartzite of the Bushmanland Sequence?) from the stratigraphy at Van Rooi's Vley, tourmalinites at the top of the Biesjepoort Formation may lie stratigraphically close to the Aggeneys-Gamsberg-Fe formation (see discussion Section 3.4 and c.f. Tables 3.1 and 3.2). The latter formation hosts the Aggeneys-Gamsberg series of sedimentary exhalative Cu-Pb-Zn deposits, and correlation with the Biesjepoort tourmalinites (exhalatives?) may indicate a regional stratigraphic interval, rich in exhalative products. Such products may include a proto-ore for the Van Rooi's Vley deposit.

The following points do, nevertheless, argue against the remobilized exhalative model.

- No Sn and/or W deposit has satisfactorily been shown to be of exhalative origin.

- Mineralization apparently post-dates intrusion of late- to post tectonic leucogranites and is thus not synchronous with the thermal peak of the Namaqua event.

- No local unmineralized supracrustal unit is known to be anomalous in Sn or W (P. Friggens pers. comm), i.e. no sedimentary source (proto-ore) of Sn or W is known.

- The sedimentary (exhalative) nature of the 'tourmalinites' in question is far from established.

- Late to post-tectonic granitoids intrude the region and are anomalous in W and Sn.

It is hard to attempt to model the genesis of any Sn/W deposit without showing a bias for processes genetically related to granitic magmatism. Such are the relationships established between Sn/W deposits and highly fractionated 'specialized' granites, that even when these granitic bodies are not seen, their presence is always inferred. Evidence for a granitic influence on the Van Rooi's Vley deposit is not quite so circumstantial. Although no granitoids crop-out at Van Rooi's Vley, they are encountered in drill core, and do crop-out at McTaggarts Camp. The former granitoids consist of at least three generations (Section 3.4), the latest being leucocratic and late to post-tectonic in age (but pre-mineralization). The granitoids at McTaggarts Camp are tourmaline-rich leucogranites that are late to post-tectonic in age and closely relate to mineralization (Section 3.5). In view of these leucogranitic occurrences, one cannot help but consider the tourmaline-rich leucogranitic phases of the Cnydas granite complex as a possible source of mineralization within the Van Rooi's Vley - McTaggarts Camp district. These phases are late-to-post-tectonic in age, anomalous in Sn and W and may be linked to the abovementioned district by the Cnydas shear zone (Section 3.4c). Granitoids of a similar nature may very well occur beneath the Van Rooi's Vley-McTaggarts Camp district.

An abundance of tourmaline is a feature common to both the sites of mineralization and, therefore, probably also to the source of mineralization. Possibly, tourmaline from the former may adopt some compositional features of the tourmaline from the latter. Because the composition of granitic tourmaline and sedimentary/exhalative tourmaline contrast so greatly (Plimer, 1986; Henry and Guidoffi, 1985) an attempt was made to characterize the tourmaline associated with the Van Rooi's Vley - McTaggarts Camp deposits.

10.3 The geochemistry of tourmaline - a clue to the origin of mineralization

10.3.a. The tourmaline system

Tourmaline is a complex borosilicate with a general formula of

$$XY_3Z_6(BO_3)_3SiO_{18}(OH,F,Cl)_4$$

where

X = Na, Ca, K,
Y = Al, Fe, Fe, Li, Mg, Mn
Z = Al, Fe, Cr, V.

The principal end-members are :

elbaite, $Na(Li, Al)_3Al_6(BO_3)Si_6O_{18}(OH)_4$
schorl $NaFe^{2+}{}_3Al_6(BO_3)_3Si_6O_{18}(OH)_4$,
dravite $NaMgAl_6(BO_3)_3Si_6O_{18}(OH)_4$,
and uvite $CaMg_3(MgAl_5)(BO_3)_3Si_6O_{18}(OH)_4$.

According to Henry and Guidotti (1985), most natural tourmalines belong to two completely miscible solid solutions ; schorl-dravite and schorl-elbaite. An apparent miscibility gap exists between dravrite and elbaite.

The very large stability field (Plimer 1986) and complex chemical variability of tourmaline make this mineral a potential indicator of the environment in which it formed. In fact, certain compositions of tourmaline are specific to certain hydrothermal ore-deposits. In particular, dravite is commonly associated with sedimentary/exhalative deposits (massive sulphide deposits) whilst granitic related deposits commonly contain schorl. The potential of tourmaline as an exploration guide for such mineralization, is obvious.

10.3.b The nature of tourmaline of Van Rooi's Vley and McTaggarts Camp

The composition of tourmaline from Van Rooi's Vley, Witkop, McTaggarts Camp,

the Kakamas tourmalinite, the Biesjepoort tourmalinite and the Cnydas leucogranite, were analysed by electron microprobe. Tourmaline analyses are given in table 10.1 and are plotted on figure 10.1.

Tourmaline from all populations analysed, fall within the schorl-dravrite solid solution series with only limited substitutions with the uvite (CaMg) component (Table 10.1). The best discrimination between populations was obtained by comparing MgO vs. FeO/(FeO + MgO) (Fig. 10.1).

Tourmaline from the Kakamas tourmalinite has a composition close to that of pure dravrite, and lies within the field of sedimentary/exhalative tourmaline (Fig. 10.1), whilst tourmaline from tourmaline pods within the Cnydas leucogranites has a composition close to that of pure schorl, and lies within the field of granitic tourmaline. Tourmaline from the Biesjepoort tourmalinite also lies within the compositional field for granitic tourmalines indicating a non-sedimentary origin for this tourmalinite.

Tourmaline associated with mineralization contains more of the schorl component than of the dravite component, and lies within, or near, the compositional field for granitic tourmaline. Tourmaline from tourmalinized selvages at McTaggarts Camp is closer to pure schorl in composition than is tourmaline from the Cnydas leucogranites, whilst tourmaline from the leucogranite bands at McTaggarts Camp is almost pure schorl (Fig. 10.1). First generation tourmaline (T1) from tourmalinized selvages at Van Rooi's Vley, and at Witkop, is slightly more Mg (dravite)-rich than tourmaline from the Cnydas leucogranites. Second generation tourmaline (T2), from both deposits, may contain up to 40% of the dravite component and falls just outside the compositional field for granitic tourmaline, but is distinctly separate from the compositional field for sedimentary/exhalative tourmaline (Fig. 10.1). Both the T1 and T2 tourmalines from Witkop are slightly more Fe (Schorl)-rich than the corresponding tourmalines from Van Rooi's Vley.

TABLE 10.1

PARTIAL CHEMICAL ANALYSES OF TOURMALINES

T1-TOURMALINES

	VRV87/1	VRV87/2	VRV87/3	VRV87/4	VRV87/5	VR71/1	VR71/2	VR71/3	WK25/1	WK25/2	WK25/3	WK25/4
SIO2	34.73	33.55	33.56	33.37	32.27	34.46	32.36	33.94	35.33	33.14	34.77	33.13
TIO2	0.78	0.82	0.84	0.86	0.86	1.07	0.81	0.95	0.73	1.16	0.98	1.35
AL2O3	28.20	28.81	28.27	27.91	27.81	28.42	28.56	29.61	30.35	30.51	30.06	30.87
FEO	14.21	14.36	14.09	14.13	15.54	13.93	15.52	13.35	12.70	13.19	12.58	13.41
MNO	0.04	ND	0.01	0.01	0.02	0.03	0.08	0.03	0.05	ND	0.01	0.02
MGO	4.41	4.29	4.57	4.48	4.64	4.58	4.42	4.51	3.64	3.48	3.93	3.50
CAO	1.20	2.23	2.72	3.09	3.07	1.28	1.72	1.84	0.19	1.69	0.81	1.43
NA2O	2.20	1.59	1.36	1.14	0.99	1.99	1.59	1.77	2.30	1.59	2.02	1.56
TOTAL	85.77	85.66	85.42	84.97	85.19	85.76	85.06	86.00	85.30	84.77	85.16	85.27
FEO#	0.76	0.77	0.76	0.76	0.77	0.75	0.78	0.75	0.78	0.79	0.76	0.79

T2-TOURMALINES

	VRV141/1	VRV141/2	VRV141/3	VRV141/4	VR73/1	VR73/2	VR73/3	VR73/4	WK21/1	WK21/2	WK21/3
SIO2	35.30	33.65	35.32	34.92	34.35	35.26	35.19	35.17	32.95	34.95	33.55
TIO2	0.67	0.70	0.53	0.58	0.48	0.60	0.59	0.46	1.38	0.36	1.03
AL2O3	30.47	31.16	30.62	30.68	31.24	29.99	30.28	30.17	28.46	30.57	29.60
FEO	11.64	12.00	11.64	11.92	9.46	9.58	9.82	8.96	12.53	11.74	11.89
MNO	0.01	ND	0.04	0.01	0.03	0.02	0.03	0.02	0.07	0.08	0.11
MGO	5.34	5.07	5.32	5.21	5.93	6.10	5.92	6.06	5.38	4.85	5.22
CAO	1.51	2.28	1.10	1.45	1.47	0.78	0.78	0.93	3.69	1.12	2.81
NA2O	1.92	1.48	2.20	1.90	1.95	2.30	2.32	2.04	0.75	2.03	1.23
TOTAL	86.86	86.33	86.77	86.67	84.90	84.63	84.92	83.82	85.19	85.69	85.44
FEO#	0.69	0.70	0.69	0.70	0.61	0.61	0.62	0.60	0.70	0.71	0.69

CNYDAS GRANITE TOURMALINES

	CGT/1	CGT/2	CGT/3	CGT/4	CGT/5	CGT/6	CGT/7	CGT/8
SIO2	34.55	35.04	34.32	34.89	35.81	34.96	35.08	34.50
TIO2	0.82	0.73	0.83	0.42	0.29	0.77	0.54	0.84
AL2O3	32.15	32.12	32.15	32.22	32.24	31.56	33.32	31.53
FEO	12.64	12.36	12.88	12.70	12.47	12.55	11.33	13.01
MNO	0.09	0.11	0.08	0.07	0.12	0.09	0.08	0.11
MGO	2.64	2.91	2.59	2.67	2.60	3.16	2.78	2.67
CAO	0.55	0.48	0.63	0.39	0.26	0.53	0.45	0.46
NA2O	2.11	2.00	2.02	2.02	1.97	2.06	1.96	2.05
TOTAL	85.55	85.75	85.50	85.38	85.76	85.68	85.54	85.17
FEO#	0.83	0.81	0.83	0.83	0.83	0.80	0.80	0.83

TABLE 10.1

PARTIAL CHEMICAL ANALYSES OF TOURMALINES

	GRANITE(McT)		TOURMALINES-McTAGGARTS CAMP					
	MT/1	MT/2	MT/3	MT/4	MT/5	MT/6	MT/7	MT/8
SIO2	34.83	33.86	35.63	35.34	34.99	33.46	35.00	34.62
TIO2	0.10	0.15	0.34	0.21	0.39	0.90	0.66	0.89
AL2O3	32.14	32.95	32.57	33.17	32.43	33.73	32.68	32.27
FEO	14.71	14.84	12.60	13.75	13.56	12.04	12.81	12.47
MNO	0.07	0.10	0.02	0.03	0.01	ND	ND	ND
MGO	0.87	0.60	2.42	1.57	1.77	2.33	2.57	2.48
CAO	0.13	0.44	0.20	0.20	0.38	0.65	0.51	0.66
NA2O	1.53	1.76	1.94	1.81	1.79	1.79	1.81	1.75
TOTAL	84.38	84.70	85.72	86.08	85.32	84.90	86.04	85.14
FEO#	0.94	0.96	0.84	0.90	0.88	0.84	0.83	0.83

	TOURMALINES-ZAAIPLATS				TOURMALINES-ROOIBERG				
	Z/1	Z/2	Z/3	Z/4	R/1	R/2	R/3	R/4	R/5
SIO2	34.87	35.58	34.83	34.68	36.12	35.83	36.04	36.07	35.72
TIO2	0.04	0.00	0.04	0.04	0.41	0.68	0.97	0.37	0.26
AL2O3	28.39	31.70	28.32	28.81	27.69	28.04	29.42	28.80	27.35
FEO	20.48	17.26	21.05	21.14	10.99	10.43	9.71	11.08	12.82
MNO	ND	0.01	0.01	0.01	ND	ND	ND	ND	ND
MGO	0.13	0.09	0.16	0.13	7.03	7.53	7.15	6.65	6.49
CAO	ND	ND	ND	ND	0.35	1.03	0.81	0.33	0.10
NA2O	2.39	1.50	2.52	2.27	2.58	2.20	2.48	2.88	2.96
TOTAL	86.30	86.14	86.93	87.08	85.17	85.74	86.58	86.18	85.70
FEO#	0.99	0.99	0.99	0.99	0.61	0.58	0.58	0.62	0.66

	SEDIMENTARY TOURMALINES (*1)								
	VT 105	EZ 272	AM 2	CP 16	JS 79	BH-D-2	BH-D-4	BH-D-9	BH-D-15
SIO2	38.36	38.84	39.72	38.05	38.88	37.24	36.44	37.17	38.20
TIO2	0.45	0.45	0.08	1.54	0.33	0.21	0.19	0.23	0.26
AL2O3	33.29	34.48	36.14	32.22	36.64	32.73	33.92	32.68	35.90
FEO	2.78	2.78	1.47	3.02	3.55	1.07	3.15	0.90	2.33
MNO	ND	ND	ND	ND	ND	ND	ND	ND	ND
MGO	11.77	11.36	11.43	11.92	9.67	12.18	8.62	12.38	9.21
CAO	0.43	0.80	0.28	1.54	0.88	2.68	0.71	2.67	0.47
NA2O	2.81	2.35	2.95	2.33	3.03	1.21	2.49	1.21	2.08
TOTAL	89.89	91.06	92.07	90.62	92.98	87.32	85.52	87.24	88.45
FEO#	0.19	0.20	0.11	0.20	0.27	0.08	0.27	0.07	0.20

(*1) Analyses from Taylor and Slack (1984)

TABLE 10.1

PARTIAL CHEMICAL ANALYSES OF TOURMALINES

	KAKAMAS TOURMALINITE			BIESJEPOORT TOURMALINITE		
	K/1	K/2	K/3	BP1	BP2	BP3
SIO2	35.76	35.91	35.78	32.94	34.94	33.52
TIO2	0.40	0.43	0.38	1.38	0.36	0.85
AL2O3	32.13	32.59	32.57	27.95	29.61	29.04
FEO	3.68	3.50	3.23	12.65	12.14	12.16
MNO	0.03	0.05	0.05	0.07	0.08	0.08
MGO	8.75	9.01	8.84	5.38	4.75	5.12
CAO	1.35	1.43	1.15	2.95	1.02	1.50
NA2O	1.91	1.90	2.09	0.73	1.91	1.85
TOTAL	84.01	84.82	84.09	84.05	84.81	84.12
FEO#	0.30	0.28	0.27	0.70	0.72	0.70

TOURMALINES FROM GRANITES, APLITES & PEGMATITES. (*2)

	T1	T2	T3	T6	T7	T8	T9	T10	T11
SIO2	35.61	36.00	34.90	35.00	35.07	35.17	35.10	35.10	35.92
TIO2	0.68	0.77	0.73	0.31	0.58	0.13	0.48	0.66	0.41
AL2O3	33.16	31.65	36.04	33.67	33.30	34.47	33.91	33.00	33.67
FEO	11.66	14.54	10.47	13.22	12.90	14.73	11.90	13.10	13.29
MNO	0.13	0.12	0.08	0.21	0.21	0.40	0.15	0.13	0.25
MGO	3.26	2.64	4.39	2.67	2.07	0.21	3.04	2.94	2.15
CAO	0.12	ND	0.24	0.04	0.23	0.04	ND	0.03	0.19
NA2O	1.88	1.95	2.11	1.96	1.93	1.92	1.90	1.43	1.97
TOTAL	86.50	87.67	88.96	87.08	86.29	87.07	86.48	86.39	87.85
FEO#	0.78	0.85	0.70	0.83	0.86	0.99	0.80	0.82	0.86

	T15	T16	T17	T18	T19	T20	T23	T24	T25
SIO2	34.40	35.13	34.55	34.15	35.22	35.22	34.95	34.41	34.83
TIO2	0.29	0.47	0.46	0.58	0.25	0.40	0.53	0.18	0.54
AL2O3	32.62	33.45	33.08	32.09	33.11	33.08	32.93	32.24	33.26
FEO	16.52	13.12	14.24	15.00	14.32	13.12	14.59	15.93	15.19
MNO	0.28	0.15	0.20	0.19	0.28	0.20	0.26	0.23	0.23
MGO	1.05	3.12	2.72	1.51	2.02	2.75	1.80	1.10	1.63
CAO	ND	0.03	0.05	ND	0.09	0.04	0.10	ND	ND
NA2O	2.30	1.98	1.76	2.54	1.75	1.97	2.15	1.97	1.93
TOTAL	87.46	87.45	87.06	86.06	87.04	86.78	87.31	86.06	87.61
FEO#	0.94	0.81	0.84	0.91	0.88	0.83	0.89	0.94	0.90

(*2) Analyses from Neiva (1974)

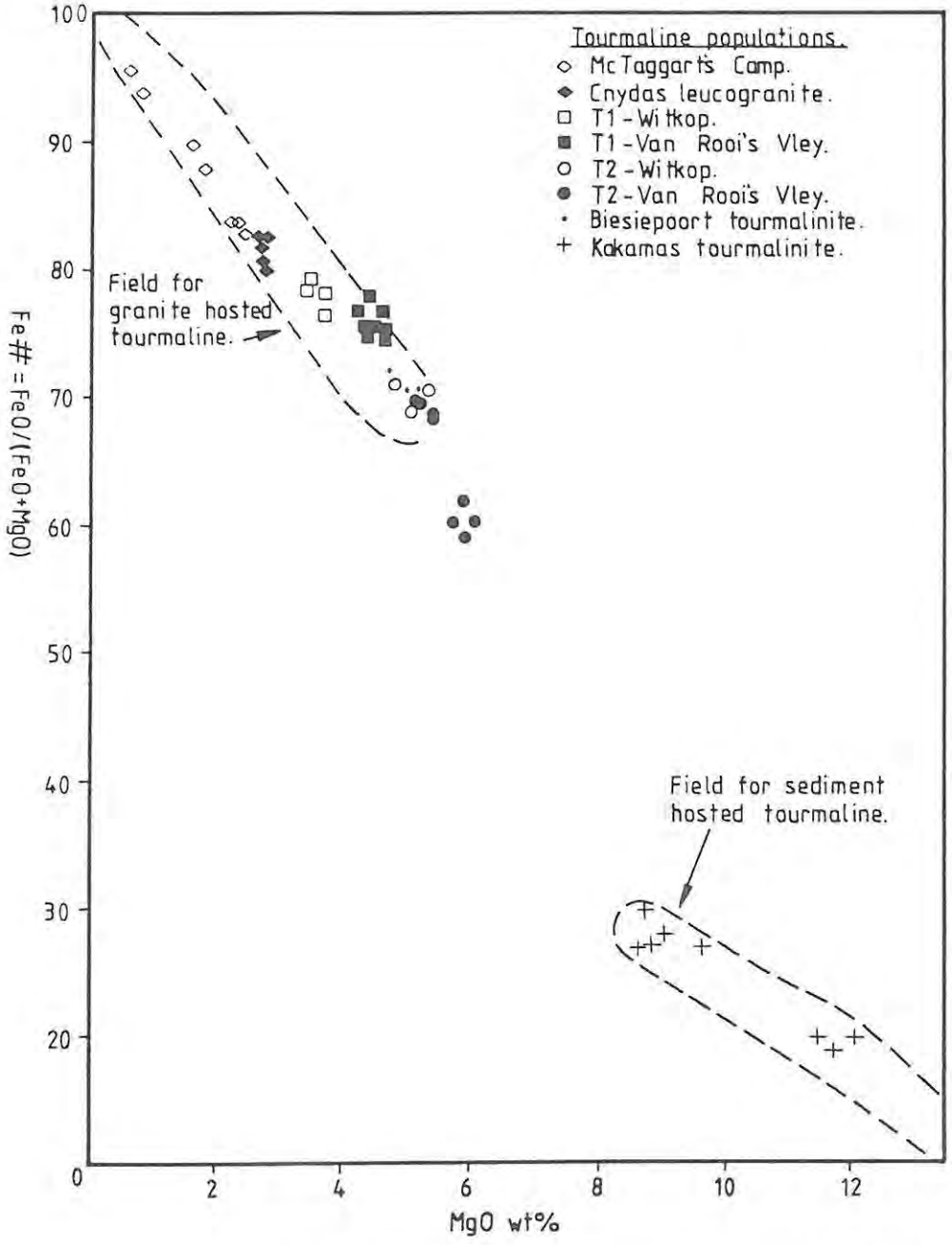

Figure 10.1. Fe#vs. MgO diagram showing the compositional variation of tourmaline from various locations within, and around, Van Rooi's Vley. Also shown are the compositional fields for tourmaline from granites and from sedimentary/exhalative tourmaline beds.

10.3.c Discussion

On the basis of information presented in figure 10.1, it seems unlikely that the tourmaline selvages within the Van Rooi's Vley-McTaggarts Camp series of deposits are related to sedimentary/exhalative tourmalinites. Tourmaline from the Kakamas tourmalinite is characteristic of sedimentary/exhalative tourmaline and is very different in composition from all other tourmaline populations studied here. Tourmaline from the Biesjepoort tourmalinite is, however, not of a sedimentary/exhalative origin, but is granitic in composition. The Biesjepoort tourmalinite is therefore more likely to be a replacement feature, related to the same event that caused tourmalinization at Van Rooi's Vley.

The remaining tourmaline populations clearly show compositional similarities to granitic tourmaline and strongly favour a granitic-related mode of genesis for the abovementioned mineralization.

The Fe#(ie. FeO/(FeO+MgO)) of T1 and T2 tourmalines is higher at Witkop than at Van Rooi's Vley, but is lower than the Fe#of tourmalines from the Cnydas leucogranite (an inferred source of mineralization). A similar change in the Fe#of tourmaline is also displayed by analyses from the Zaaiplaats and Rooiberg Sn-deposits (Fig. 10.2) , in central Transvaal, which are considered here to represent a classic exogranitic-endogranitic Sn-mineralized system. It therefore seems that, in a relative sense, the Fe# of tourmaiine may be inversely proportional to the distance from a source of Sn/W mineralization. This relationship is, however, probably a combined result of fluid/wall-rock conditions. For example, the progressive leaching of Mg (in preference to Fe) from wall rocks or the progressive precipitation of Fe (sulphides) from a sulphidic fluid.

Tourmaline at McTaggarts Camp has a higher Fe#than tourmaline from the Cnydas leucogranite, and thus, seem inconsistent with the abovementioned relationship. However, the latter are from tourmaline pods (see Section 3.4.c) that clearly formed as a replacement of the host leucogranite. As such, this tourmaline would also be enriched in Mg with respect to tourmaline at the (unseen) source of the B-rich fluids, deeper within the leucogranite body. Tourmaline from the leucogranite bands at McTaggarts

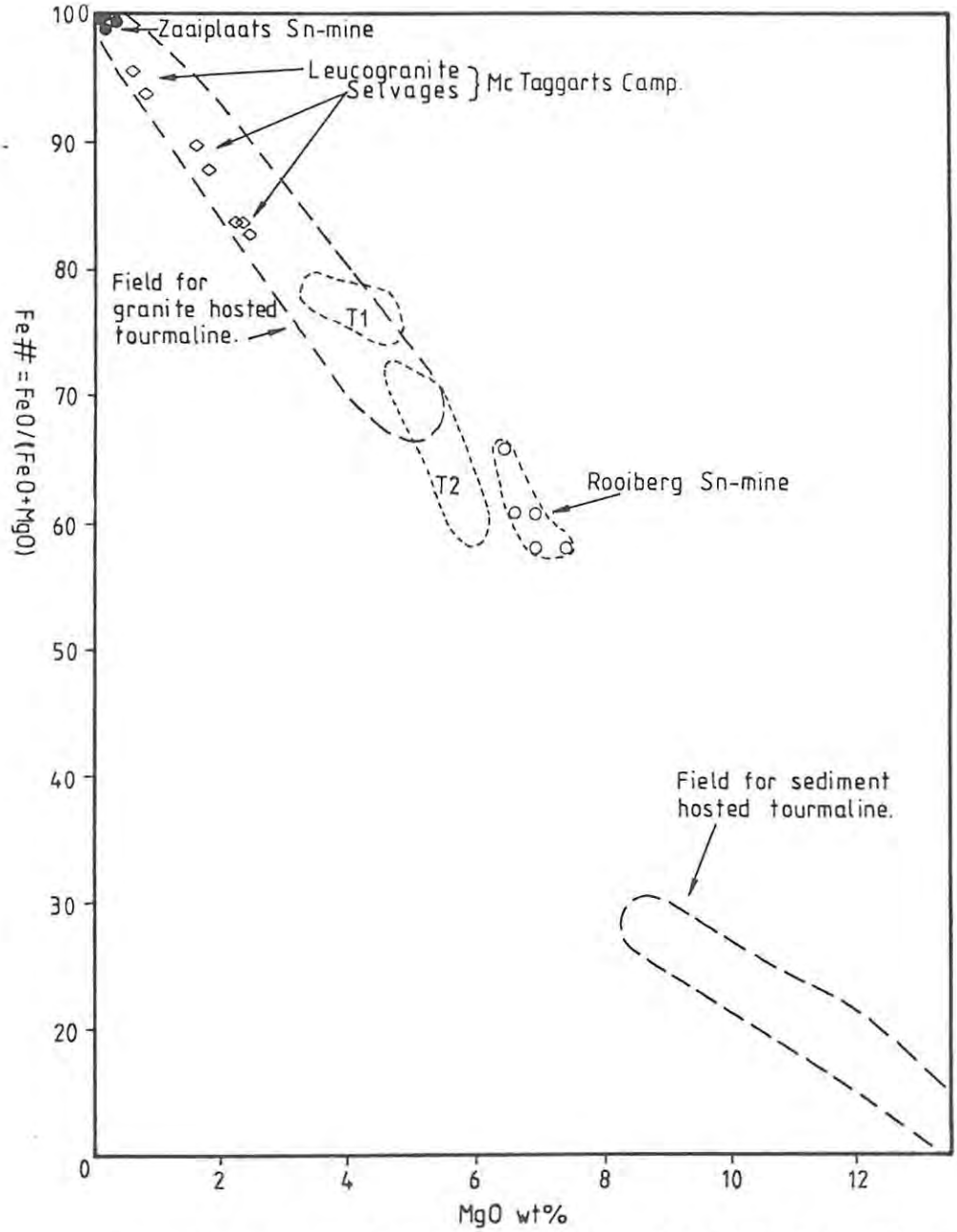

Figure 10.2. As for figure 10.1, but including (for comparative purposes) analyses of tourmaline from the Zaaiplaats and Rooiberg Sn-mines, central Transvaal.

Camp (Fig. 10.2) is euhedral in shape and probably represent a primary phase of that rock. Therefore, the composition of tourmaline from McTaggarts Camp is probably more representative of the composition of tourmaline at the source of mineralization. The tourmaline-rich leucogranite bands either belong to the Cnydas complex itself, or to a granitic body very similar to the Cnydas complex.

Taking the tourmaline within the leucogranite bands at McTaggarts Camp as source tourmaline, the Fe# of tourmaline is seen to progressively decrease in the order ; McTaggarts Camp selvages (adjacent to the leucogranite bands), Witkop, Van Rooi's Vley. This spatial relationship repeats relationships already established based on changing F/B ratio, alteration (greisenization) and ore-mineralogy (Section 9.5), and substantiates not only an affiliation of the mineralization to a granitic source, but also the hypothesis that mineralization at McTaggarts Camp, Witkop and Van Rooi's Vley formed (in that order) at successively greater distance from that mineralizing source.

10.4 Conclusions

The genesis of mineralization within the Van Rooi's Vley - McTaggarts Camp district seems best related to the degassing of a specialized granite. Leucogranitic dykes occur within the area and resemble leucocratic phases of the Cnydas granite complex, which are known to be anomalous in Sn and W. The geochemistry of tourmaline, associated with mineralization, also indicates a granitic origin for mineralization rather than an origin through the remobilization of a sedimentary/exhalative proto-ore. The remobilization model is inadequate in explaining mineralization at Van Rooi's Vley, for numerous reasons, as outlined in Section 10.2.

11. CONCLUSIONS:- THE GENESIS OF THE VAN ROOI'S VLEY DEPOSIT, AND RELATED MINERAL OCCURRENCES

At approximately 1.0 to 1.1 Ga, granitoids that were late-to-post-tectonic, with respect to the Namaqua event, were generated, and intruded the Gordonia Subprovince along numerous NE trending shears. This magmatism was probably the result of a continent-continent collision, between the Namaqua Province and a 'southern continent' (Stage 6 - Section 2.6). Apparently, both I- and S-type granitoids were generated, reflecting a complex source region which probably included sediments that were rich in refractory minerals (e.g. zircon, cassiterite) and that were derived from basement granites of the Kaapvaal Province.

Through processes of magmatic fractionation, each successive phase of the intruding granitoid bodies became more extreme in composition. The Cnydas granite complex intruded along the Cnydas shear zone (a major crustal suture) and evolved leucocratic phases that were highly B(+F?)-rich and that concentrated large amounts of incompatible elements (including W and Sn). According to Jankowitz (1986), the Cnydas granite complex is I-type in composition, despite its anomalous Sn and W contents ; a feature more commonly associated with S-type granitoids.

The surface of the Cnydas granite complex, as a whole, is thought to be inclined towards the south (P.Friggens pers. comm), in the direction of the Van Rooi's Vley - McTaggarts Camp district. The Complex may very well underly that district, as suggested by the presence of unfoliated leucogranitic dykes as far south as McTaggarts Camp.

Tourmaline is very abundant within the Cnydas leucogranites and is commonly concentrated into distinct pods (Plate 3.5). These pods could represent the frozen early stages in the development of a magmatic/hydrothermal system (F. Pirajno pers. comm). Evidence that these tourmaline pods acted in a similar way to bubble within a liquid, is seen in plate 11.1, which shows comet-like tails on the ends of individual tourmaline pods. These pods would stream upwards, through the dense, and largely consolidated magma, to concentrate in the apical regions of the leucogranite body. Extreme oversaturation,

with respect to volatiles such as B, Cl ± F and Li, would occur within these apical regions and a separate fluid phase would exist. Furthermore, according to London (1986), the crystallization of tourmaline, from a silicic melt, is a reaction that leads to the exsolution of large amounts of H_2O (approximately 8 mol of H_2O per mol of tourmaline). Therefore, any fluid phase present within the apical regions of the Cnydas leucogranite would also be aqueous.

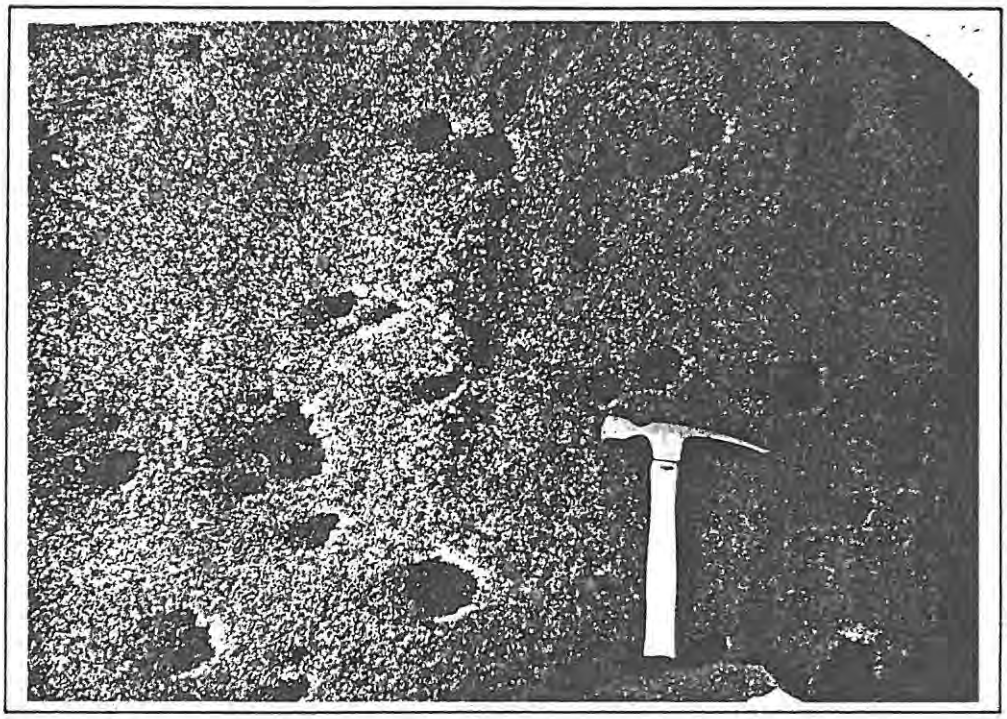

Plate 11.1. Comet-like tails on the ends of tourmaline pods form within the Cnydas Leucogranites. These pods seem to have 'streamed' up through the leucogranite, like gas bubbles through water.

Rare-elements, such as Sn, Mo, W, Nb,Ta etc would partition strongly towards a volatile rich aqueous phase (London 1987). The release of the aqueous phase (and associated rare-element complexes) from the leucogranites could have initiated a large-scale hydrothermal system, with the potential to form rale-element deposits. A viable release mechanism could have been hydrostatic overpressuring, simply due to crystallization and the consequent evolution of the magmatic aqueous phase. Alternatively, movement along

the Cnydas shear zone may have caused fluid release.

Hydrothermal fluids emanating from the Cnydas leucogranites would follow paths of least resistance through the high-grade gneisses that characterize the region. The Cnydas shear zone, and related shears such as the Van Rooi's Vley and Witkop shears, would offer excellent fluid pathways. Mineralization would occur along the fluid pathways, in structural sites where local physicochemical conditions drastically decrease the solubility of W and Sn within the fluid.

In the simplest terms, individual deposits within the Van Rooi's Vley - McTaggarts Camp district may be modelled as representing specific levels within one hydrothermal system that derived from the Cnydas (or similar) leucogranites. These deposits may be classified on a 'proximal' to 'distal' facies basis according to the systematic changes in five variables, vis ;

- the F/B ratio of the deposit as a whole;
- the W/Sn ratio of the ore assemblage ;
- the presence or absence of greisenous alteration ;
- the nature of the Fe-sulphide assemblage ;
- the Fe# of tourmaline.

Apparently, the F/B ratio of the mineralizing fluids changed, not only with distance from the source, but also with time. Changes in the F/B (or more correctly, the a_F of the fluid) caused changes in the W mineralogy of the ore assemblage at Withkop and (particularly) at Van Rooi's Vley. Initially B-rich fluid conditions were favourable to both wolframite and scheelite deposition, depending on local activities of Fe and Ca. However, later fluctuations in the F/B ratio meant that, under periodic conditions of high a_F, Ca complexed with F in preference to W, increasing the solubility of scheelite within the hydrothermal fluids. Periodic dissolution of scheelite, and formation of wolframite rims around scheelite, occurred.

A general increase in the F/B ratio, with time, can be explained in terms of the contrasting behaviour of F and B, in the presence of a silica melt and a co-existing fluid phase. Under such conditions, F partitions towards the melt phase (Manning 1981), whilst B partitions in favour of the fluid phase

(Burnham and Nekvasil 1986). Fluorite would thus concentrate in late-magmatic minerals (eg. fluorite, muscovite, topaz), but may, however, be readily released from the minerals during subsolidus (hydrothermal/ autometasomatic) alteration. Consequently, the first fluids to leave the oversaturated apical regions of a leucogranite would be aqueous B-rich magmatic fluids. However, as these fluids progressively alter the late magmatic (F-rich) assemblage, through which they pass, they become enriched in F.

The McTaggarts Camp deposit represents the highest temperature phase of mineralization, forming adjacent to leucogranite dykes that originate from an underlying magma chamber (Fig. 11.1). Greisenization, high F/B ratios, high W/Sn ratios and tourmalines with a high Fe#(~90) characterize this **'proximal facies'** of mineralization (Table 11.1). Further greisen-sheet style mineralization may occur at deeper levels, within (and adjacent to) a **'cupola facies'** of the hydrothermal system (Fig. 11.1).

TABLE 11.1
COMPARISON OF LOCAL W/Sn DEPOSITS

Deposit	F/B ratio	W/Sn ratio	greisenization, present/absent	Fe-sulphide assemblage	Fe# of tourmaline
Mclaggarts Camp	high	high	common	?	90
Witkop	medium-low	high-medium	noticable	+ pyrrhotite	70
Van Rooi's Vley	low	medium	absent	no pyrrhotite	65

The Witkop deposit would represent an **'intermediate facies'** of mineralization, characterized by lower F/B and W/Sn ratios, tourmalines with Fe# s around 70, minor greisenization and a moderate temperature sulphide assemblage.

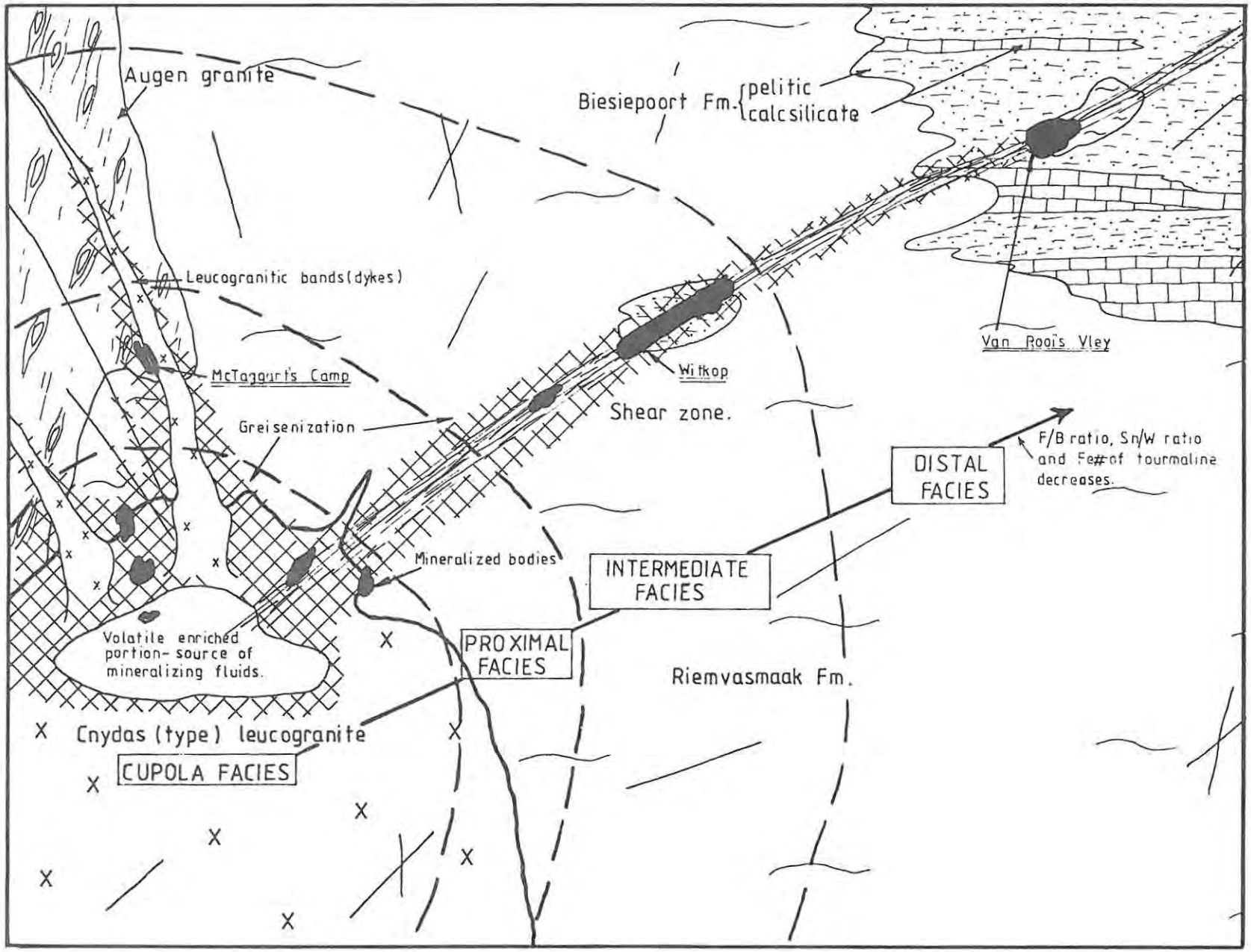

Figure 11.1. Schematic model showing the relationship between mineralization at Van Rooi's Vley, Witkop and McTaggarts Camp. These deposits have been classified on a 'proximal' to 'distal' basis according to numerous criterion (see text).

Mineralization at Van Rooi's Vley would represent the most 'distal facies' of hydrothermal mineralization seen within the district (Fig. 11.1) and is characterized by still lower F/B and W/Sn ratios, tourmalines with Fe# around 65 and a lower temperature sulphide assemblage than at Witkop (assuming similar values for fO_2 and fS_2). No greisenous alteration occurs at Van Rooi's Vley, although the deposit is definetely affiliated to greisen-style deposits. The Van Rooi's Vley deposit would be more correctly classified as a granite-related quartz - lode deposit.

12. ACKNOWLEDGEMENTS

I would first of all like to thank Professor F. Pirajno for his supervision, endless enthusiasm and expert guidance throughout the duration of this study.

Many thanks are also due to, Professor R. Jacob, Dr. R. Scoon and Messers C. Mallinson, J. Potgieter, N. Franey, G. Rankine, T. Tregoning, F. Walraven, B. Teigler and J. Misiewicz, for their help, discussions and friendship throughout the period of my study.

I would like to gratefully acknowledge Shell South Africa, Metals Division, for financial assistance, and for providing such an interesting area for study. P. Friggens and F. Dooge, (from the Upington Office) are particularly thanked for their advise and hospitality.

The C.S.I.R. (FRD) is also thanked for finantial assistance during 1986 and 1987.

Instructions and assistance in the study of fluid inclusions was given by Dr. A. Harwood (University of Natal - Durban), whilst Mr. R. Skae and B. de Klerk assisted with probe and X.R.F. determinations respectively. The text of this thesis was typed by Mrs. G. Bezuidenhout and Mrs. C. Mentoor, and was proof-read by Ms. C. Schulte. To all of the above I am very grateful.

Finally, I would like to thank my father, and family in Australia, for their encouragement and assistance throughout all of my years spent studying.

13. REFERENCES

Albat, A.H. (1984). The Proterozoic granulite facies terrane around Kliprand, Namaqualand Metamorphic Complex. Bull. Precambrian Res. Unit. Univ. Cape Town, 33, 382pp.

Barton, E.S. and Burger, A.J. (1983). Reconnaissance isotopic investigations in the Namaqua Mobile Belt and implications for Proterozoic crustal evolution - Upington Geotraverse. Special Publ. Geol. Soc. S.Afr., 10, p173-191.

Blignault, H.J., van Aswegen, G., van der Merwe, S.W. and Colliston, W.P., (1983). The Namaqualand geotraverse and environs : Part of the Proterozoic Namaqua Mobile Belt. Special Publ. Geol. Soc. S. Afr., 10, 1-29.

Botha, B.J.V., Grobler, N.J. Linstrom, W., Smit, C.A. (1976). Stratigraphic correlation between the Kheis and Matsap formations and their relation to the Namaqualand Metamorphic Complex. Geol. Soc. S. Afr. Trans. 79 p304-311.

Burnham, C.W., and Nekvasil, H. (1986). Equilibrium properties of granite pegmatite magmas. American Min. 71 : p239-263.

Burt D.M. (1972). The influence of fluorine in the facies of Ca-Fe-Si skarns; Carnegie Institute Yearbook 71, p 443-450.

Chappell, B.W., and White A.J.R., (1974). Two contrasting granite types Pacific Geology, 8, 173-4.

Clifford, T.M., Gronow, J, Rex. D.C., and Burger, A.J. (1975). Geochronological and petrogenetic studies of high-grade metamorphic rocks and intrusives in Namaqualand, South Africa. J. Petrol. 16, 154-188.

Conolly, H.J.C. (1936). A contour method of revealing some ore structures. Econ. Geol. 31; 259-27.

Coward, M.P. and Potgieter, R., (1983). Thrust zones and shear zones of the margin of the Namaqua and Kheis Mobile belts, Southern Africa - Precambrian Research, v. 21 no. 1-2 p.39-54.

Crocker I.T. (1986). The Zaaiplaats Tinfield, Potgietersrus District in : Annaeusser, C.R., and Maske, S., Eds. Min. Dep. of Southern Afr. II Geol. Soc. S. Afr. 1020pp.

Dunn, P.J., (1977). Uvite, a newly classified gem tourmaline : Journal of Gemonology, V. 15, No. 6 : 300-308.

Eugster H.P. (1984). Granites and hydrothermal ore deposits : a geochemical framework. Min. Mag. 49 : 7-23.

Eugster H.P. and Wilson, G.A. (1986). Transport and deposition of ore-forming elements in hydrothermal systems associated with granites : In High Heat production granites. (HHP). Inst. Min. and Met. 1985.

Garson, M.S. and Mitchell, A.H.G. (1977). Mineralization at destructive plate boundaries : a brief review. In ; Volcanic processes in ore genesis. Spec. Publ., Geol. Soc. London, 7, 81-97.

Geringer, G.J., Pretorius, J.J. and Cilliers, F.H., (1986). Stratabound Copper-iron sulphide mineralization at Boksputs, north-west Cape South Africa - A possible proterozoic besshi-type deposit. Geocongress '86 Extended Abstracts - Geol. Soc. of S. Africa pp 1056.

Hartnady, C., Joubert, P., and Stowe, C. (1985). Proterozoic crustal evolution in southwestern Africa. Episodes, 8, No. 4, 236-244.

Henry D.J. and Guidotti, C.V., (1986). Tourmaline as a petrogenetic indicator mineral : an example from the stourolite - grade metapelites of NW Maine. American Mineralogist V. 70 p1-15.

Hutchinson C.S., (1983). Economic Deposits and their Tectonic Setting. MacMillan pp365.

Jankowitz B. (1986). A petrochemical investigation of the Cnydas Batholith west of Upington. Unpubl. MSc. Thesis U.O.F.S. (in Afrkaans).

Joubert, P. (1974). The gneisses of Namaqualand and their deformation. Trans. geol. Soc. S. Afr., 77, 339-345.

----, (1977). The regional tectonism of the gneisses of part of Namaqualand. Bull. Precambrian Res. Unit, Univ. Cape Town 10, 220pp.

----, (1981). The Namaqualand Metamorphic Complex. In : Hunter, D.R. (ed.), Precambrian of the Southern Hemisphere, Developments in Precambrian geology 2, Elsevier, Amsterdam, pp671-705.

Kroner, A. (1981). Precambrian plate tectonics, 57-90. In : Kroner, A., Ed., Developments in Precambrian geology 4, Elsevier, Amsterdam 781pp.

Lombaard, A.F. (1986). The Copper Deposits of the Okiep District, Namaqualand In Anhaesser, C.R, and Maske, S., Eds (1986). Mineral Deposits of Southern Africa. Vols I and II. Geol. Soc. S. Afr., 2376pp.

Lombaard, A.F., and Schreuder, F.J.G., (1978). Distribution pattern and general geological features of steep structures, megabreccias and basic rocks in the Okiep Copper Districts. In : Verwoerd, W.J., Ed., Mineralization in metamorphic terranes, Spec. Publ. geol. Soc. S. Afr., 4, 269-275.

London, D. (1986). Formation of tourmaline-rich gem pockets in miarolitic pegmatites. Amer. Min. 71, 396-405.

---- 1987. Internal differentiation of rare-element pegmatites. Effect of boron, phosphorous and fluorite. Geochimica et Cosmochimica Acta 51; 403-420.

Mallinson, C. (1986). The evolution and metallogeny of the Namaqua Province and environs. Unpublished MSc. report - Rhodes University.

Manning, D.A.C., (1981). The effect of fluorite on liquidus phase relationships in the system Qz-Ab-Or with excess water at 1kb. Contrib. Mineral Petrol. 76 : 206-215.

Manning D.A.C. and Henderson P. (1984). The behaviour of tungsten in granitic melt-vapour systems. Contrib. Mineral Petrol. 86 : 286-293.

Miller C.F. et al., (1981). Composition of plutonic muscovite genetic implications. Can. Min., 19, 25-34.

Minnett, R.C.A. (1986). Porphyry Copper-molybdenum mineralization at Haib River, South West Africa/Namibia. In. Anhaeusser C.R., and Maske S., Eds (1986). Mineral Deposits of Southern Africa. Vols I and II. Geol. Soc. S. Afr., 2376pp.

Mitchell, A.H.G., and Garson M.S., (1981). Mineral Deposits and Global Tectonic Settings. Academic Press. pp405.

Moore, J.M. (1980). A study of certain paragneiss associations and their metallogenic characteristics in Namaqualand and Bushmanland. Ann. Rep. Precambrian Res. Unit., Univ. Cape Town, 17, 65-73.

----, (1984). The regional setting of the Bushmanland paragenesis and their associated stratabound sulphide deposits (Abstr.). Conference on Middle to Late Proterozoic lithosphere evolution Precambr. Res. Unit, Univ. Cape Town.

Mulligan R. (1983). Geology of Canadian Tungsten Occurences Canadian Geological Survey. Econ. Geol. Report 32.

Neiva A.M.R., (1974). Geochemistry of tourmaline (schorlite) from granites, aplites and pegmatites from northern Portugal : Geochim. Cosmochim. Acta, 38 : 1307 - 1317.

Patterson D.J., Ohmoto H. and Solomon M. (1981). Geologic Setting and Genesis of Cassiterite-Sulfide Mineralization at Renison Bell, Western Tasmania. Econ. Geol. v 76 p 393-438.

Pitcher, W.S. (1982). Granite type and tectonic environment In : Hsu, K.J., Ed., Mountain Building Processes. Academic Press, London.

Plimer I.R. (1983). The Association of B and F-rich rocks with stratiform mineralization - Notes to accompany course presented at the Dep. of Geol. Wits. Univ. S. Africa.

---- (1986). Tourmalinites from the Golden Dyke Dome, Northern Australia Mineral. Deposita, v21, pp283-270.

Polard, P.J. Milburn, D., Taylor, R.G., and Cuff, C, (1983). Mineralogical and textural modifications in granites associated with tin mineralization, Herberton-Mount Garnet tinfield, Queensland. In : Permian geology of Queensland. Geol. Soc. of Aust. Queensland Division - 1983.

Poldervaart, A. and von Backstrom, J.W. (1949). A study of an Area at Kakamas. Trans. geol. Soc. S. Afr. Vol. III, pp. 433.

Reid D.L., (1977). Geochemistry of Precambrian igneous rocks in the lower Orange River region. Bull. Precambr. Res. Unit. Univ. Cape Town, 23, 397pp.

Reid, D.L., and Barton E.S., (1983). Geochemical characterization of granitoids in the Namaqualand geotraverse. Geological Society of South Africa Special Publication No. 10, p. 67-82.

Rozendaal, A. (1978). The Gamsberg zinc depoosit, Namaqualand. Spec. Publ. Geol. Soc. S. Afr. 4 p235-262.

----, (1980). The Gamsberg zinc deposit, South Africa : a banded stratifrom base-metal sulphide deposit. Proc. Fifth IAGOD Symp. Vol : 619-633.

Rozendaal A., Toros M.S. and Anderson J.R. (1986). The Rooiberg Tin Deposit, West-Central Transvaal. In : Anhaeusser, C.R. and Maske S., Eds. Min. Dep. of S. Africa, II Geol. Soc. S. Afr. 1020pp.

Ryan, P.J. Lawrence D.L., Lipson R.D., Moore, J.M., Paterson, A, Stedman, D.P., and Van Zyl, D. (1986). The Aggeneys Base Metal Sulphide Deposits, Namaqualand District. In. Anhaeusser, C.R., and Maske, S, Eds. (1986). Mineral Deposits of Southern Africa. Vols. I and II. Geol Soc. S. Afr., 2376pp.

Sawkins F.J., (1984). Metal deposits in relation to plate tectonics. Springer-Verlag. Berlin pp325.

Schwartz M.O. (1986) : Interpretation of the Conolly contour diagram of fault-related veins. Mineral Deposita 21, p1-11.

Sillitoe, R.H. (1976). Andean mineralization : a model for the metallogeny of convergent plate margins In ; D.F. Strong (Ed), Metallogeny and Plate tectonics Geol. Ass. of Canada, Spec. Pap. 14, p59-100.

Slack, J.F., (1982). Tourmaline in Appalachian - Caledonian massive sulphide deposits and its exploration significance : Institution of Mining and Metallurgy, Transactions, V. 91 sec. B (Applied Earth Science), pp1381-1389.

Smith P. and Parsons, I (1974). The alkali-feldspar solvus at 1 kilobar water-vapour pressure. Mineral Mag. London 39 : 747-767.

South African Committee for Stratigraphy (SACS), 1981. Stratigraphy of South Africa, Part 1 (Camp. L.E. Kent). Handb. geol. Surv. S. Afr., 8.

Stemprok M. (1971)., Petrochemical features of tin-bearing granites in the Krusne hory Mts. (Zechoslovakia - Soc. Mining Geol. Japan, Spec Issue 2, 112-118.

Stowe, C.W., (1983). The Upington geotraverse and its implications for craton margin tectonics. Spec. Publ. geol Soc. S. Afr., 10, p147-171.

Stowe, C.W., Hartnady, C.J.H., and Joubert, P. (1984). Proterozoic tectonic provinces of Southern Africa. Precambrian Research, 25, p229-231.

Tankard A.J., Jackson M.P.A., Erickson K.A., Hobday D.K., Hunter D.R. and Minter W.E.L. (1982). Crustal Evolution of Southern Africa. Springer-Verlag, pp523.

Taylor B.E. and Slack J.F. (1984). Tourmalines from Appalachian-Caledonian massive sulfide deposits : Textural, chemical and isotopic relationships. Econ. Geol., 79 : 1703 - 1726.

Taylor R.G. (1979). Geology of tin deposits : Amsterdam, Elsevier, 543p.

Taylor, R.G. and Stevenson, B.G. (1972). An analysis of metal distribution and zoning in the Herberton tinfield of north Queensland, Australia. Econ. Geol. 67 : 1234-1240.

Tischendorf, G. (1977). Geochemical and petrographic characteristics of silicic magmatic rocks associated with rare-element mineralization In ; Metallization Associated with Acid Magmatism Geol. Surv. Prague Vol. 2 p 41 : 98.

Von Backstrom, J.W., (1964). Notes on a tungsten-tin deposit near Upington, Gordonia District. Transactions. Geol. Soc. South Africa, 35-52.

Wheatley, G.J.V. and De Beer, L.J. (1986). The Van Rooi's Vley Tungsten - Tin Deposit, Gordonia, Northern Cape, In : Anhaeusser, C.R., and Maske, S., Eds., Mineral deposits of Southern Africa. Vol. II. Geol. Soc. S. Afr., 2376pp.

Windley, B.F., (1984). The Evolving Continents (2nd Edition). John Wiley & Sons, pp. 399.

APPENDIX 1

List of sample numbers and locations

Sample No.	Thin Section/ Hand Specimen	Rock Type	Location *
DH13	HS	Pink Gneiss	VRD44 (808.5m)
VR15	TS,HS	Sericitized Pink Gneiss	VRD42 (299.14m)
VR20	TS,HS	fluoritized Pink Gneiss	VRD42 (302m)
VR55	TS,HS	fluoritized Pink Gneiss	VRD24/D_2(119.3m)
VR71	TS,HS	Tourmalinized Pink Gneiss	VRD24/D_2(139.8m)
VR74	HS	Ferruginized Pink Gneiss	VRD41/D_1(225.2m)
VR78	TS,HS	Leucogranite	VRD41/D_1(234.9m)
VRD43	TS,HS	Leucogranite	VRD50
VRD72	TS,HS	Ferruginized Pink Gneiss	VRD50 (262.3m)
VRD87	TS,HS	Tourmalinized Dark Gneiss	VRD42 (236.2m)
VRD91	TS,HS	Mineralized Pink Gneiss	VRD42 (287.6m)
VRD122	TS,HS	K-altered Pink Gneiss	VRD45 (322.7m)
VRD131	TS,HS	Fluoritized and silicified Dark Gneiss	VRD27 (149m)

* Location refers to diamond drill core numbers and depths - All core is held by Shell South Africa, Metals Division, at Upington.

The samples quoted above represent only those which have been referenced within this theses. Numerous other samples were used to establish relationships and paragenetic sequences and all are held within the Department of Geology, Rhodes University.

APPENDIX 2

Analytical Techniques

Electron Microprobe.

A Jeol Superprobe 733 wavelength dispersive electron microprobe was used to determine the composition of tourmaline. Accelerating voltage was 15 kv with a current of 25nA. Natural silicate standards were used and data reduction was carried out automatically.